University of Twente

Master Thesis Technical Medicine
Department of pediatrics MST Enschede

Dynamics of lung function and phase diagram

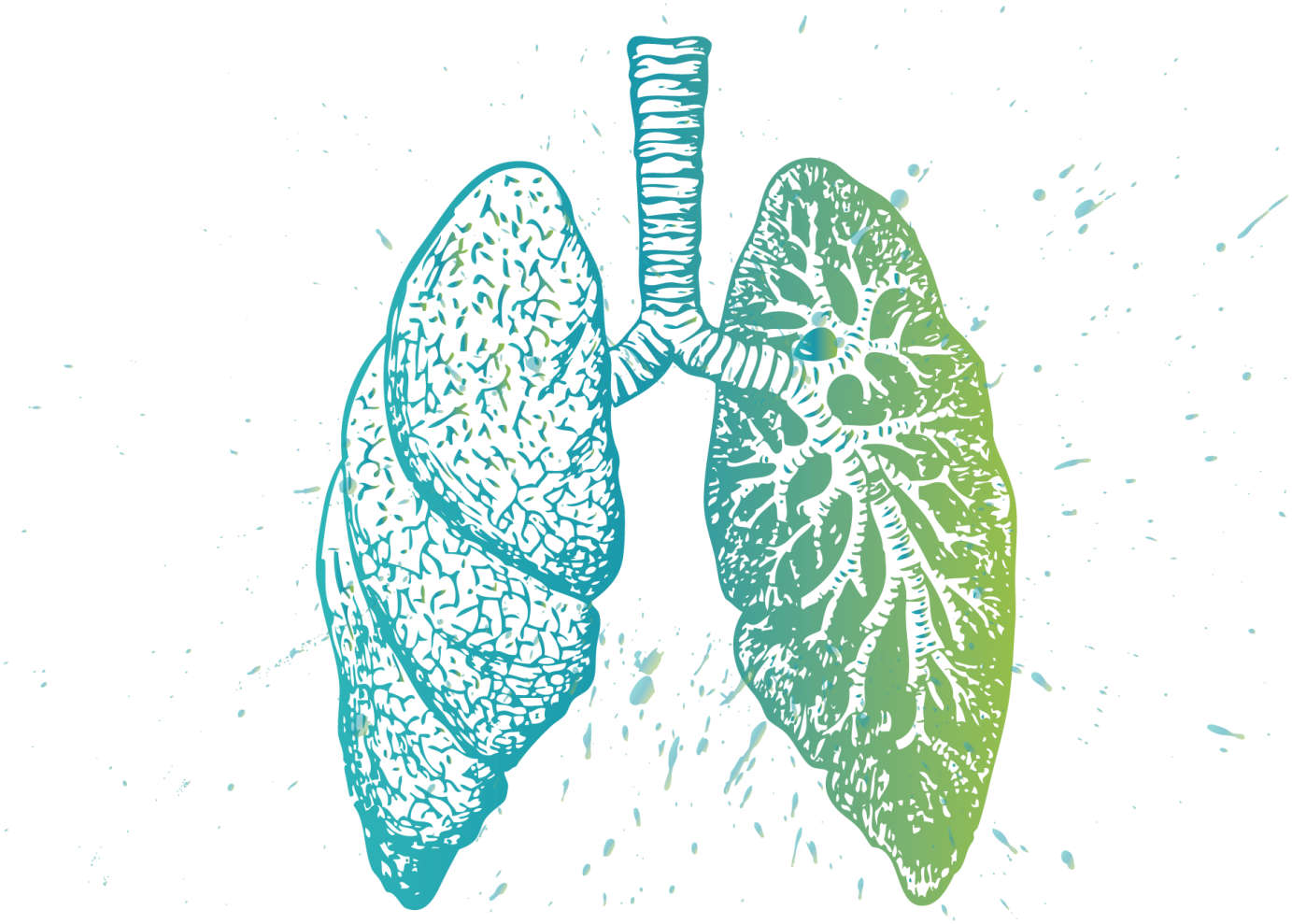

Author

K.A.E. Wijlens, BSc

Supervisors

dr. B.J. Thio
dr. ir. R. Hagmeijer
ir. R.H.J. Hebbink
dr. ir. W.L. van Meurs
drs. B.J.C.C. Hessink-Sweep

Medisch Spectrum Twente
een santeon ziekenhuis

12th August, 2019

UNIVERSITY OF TWENTE.

Preface

Before you lies my thesis, written to obtain the Master's degree of Technical Medicine at the University of Twente and is the result of my work conducted between September 2018 and July 2019.

I started writing my plan of action and afterwards my measurement setup had to be built with the help of technician of the University of Twente. This measurement setup had to be approved by infection prevention and medical technology of the MST. In between, four healthy student volunteers participated in pilot measurement to investigate the effect of manipulations on the data. Finally, the measurement protocol was approved by the Medical Ethics Committee Twente on the 21th of March. Fortunately, all 25 subjects were included between March and May 2019.

After performing all measurement, the challenge of data preprocessing and analysis started. The written script to remove the artefacts helped greatly to preprocess the data, unfortunately the amount of data was huge. Besides, finding a discriminative parameter still keeps me occupied. Nevertheless, I am motivated to obtain such a parameters as differences were seen by naked eye. Concluding, I learned a lot this past year from writing a research protocol, including and measuring subjects, conducting exercise challenge tests, and the processing and analysis of the data.

I would like to gratefully acknowledge various people as this work could not have been established without their help.

I want to thank all the children that participated in my study. Without you this work would not have been possible. Despite the fact that you personally may not have benefited from these measurements, many others in the future may!

Dr. Boony Thio, you welcomed me with open arms despite the fact that I had never been under your supervision before. I enjoyed our conversations and how your door is always open, even though your work schedule is completely filled. You were able to relate the appearance of the phase diagrams to their physics despite the mathematical approaches.

I would like to thank dr. ir. Rob Hagmeijer for his advice when I needed it the most. You guided me through the data analysis and always had ideas to further improve my data analysis.

I want to thank dr. Bregje Hessink-Sweep for guiding me through my internships.

Ir. Rutger Hebbink, I would like to thank you for building the LabVIEW interface to be able to conduct the measurements. Unfortunately, I had to use another application as LabVIEW crashed to frequently without knowing why. However, you also greatly supported me with writing the Matlab scripts and solving the problems.

Dr. ir. Willem van Meurs, I would like to thank you for visiting the Netherland to be the external supervisor of my graduation committee.

Dr. Jean Driessen, thank you for the opportunity to learn how to properly conduct an exercise challenge test, interpret them and to communicate with children of different ages. You made Wednesdays feel like a day off, by always making the day interesting and fun. In addition, I want to thank you for the ability to include and measure the subjects during your outpatient clinic.

I thank my fellow Technical Medicine students for their help and advice in carrying out this study. Other than the serious discussions about our studies, we had a lot of fun and I enjoyed the market on Tuesdays.

Finally, I want to thank my family and boyfriend for providing me with unfailing support and continuous encouragement throughout the process of researching and writing this thesis. This accomplishment would not have been possible without them. Thank you.

I hope you enjoy reading this thesis.

Kim Wijlens

Abstract

Rationale Clinical observations of respiratory distress resulting in imposed work of breathing, respiratory rate, heart rate, and oxygen saturation are currently used to provide feedback whether high flow nasal cannula (HFNC) therapy is effective for the subject. However, these parameters are biased by medication and oxygen supply and vulnerable to misinterpretation. Feedback using pressure to obtain a phase diagram reflecting changes in therapy could, besides clinical parameters, provide valuable information for the clinician to guide optimal therapeutic choices.

Objective To compare the exercise induced changes in lung function to the changes in the phase diagram assessed with the squared perimeter divided by the area (Aex_1), sphericity, and triangularity. The changes in lung function were measured with spirometry, forced expiration volume in 1 second (FEV_1), and forced oscillatory technique (FOT) with the respiratory reactance (R_{RS}) and resistance (X_{RS}). In order to evoke a variation in lung function of subjects, a standard exercise challenge test (ECT) will be performed.

Methods In this observational study 25 children were included and performed an ECT. The pressure was measured with an OMEGA pressure sensor and an Optiflow^{TM} nasal cannula. Lung function was measured with spirometry and FOT. Preprocessing was performed with Matlab version R2018b, several parameters were determined, and data analysis methods were investigated.

Results The mean decrease in FEV_1 was 16.2% with a standard deviation of 8.6%. For the determination of the dot product, 21 Fourier terms should be taken into consideration. The parameters Aex_1, sphericity and triangularity stabilize after 51 Fourier terms. Scaling the Fourier vector had no influence on the appearance of the phase diagram. The dispersion of the dot product values during the total measurement, influences the phase diagrams which should be included for the calculation of the mean phase diagram. A similar link between the FEV_1 changes and the parameters has not been found yet for all subjects. 10 selected healthy and unhealthy phase diagrams were visual distinguishable, however, this was not found for the dot product or parameters.

Discussion Further investigation is needed to determine a parameter that is able to distinguish healthy from unhealthy but also is able to indicate the therapy efficacy or lung function changes over time. As the parameters showed a greater discrimination between healthy and unhealthy when the mean of 10 phase diagrams was taken, the number of phase diagrams for average the parameter should be determined. To further improve the number of representative breaths, criteria can be added to prevent manipulations or unrepresentative breaths to result in phase diagrams.

Conclusion A discrimination between healthy and unhealthy phase diagram is not yet assessed by a parameter. Further work is needed to determine a parameter that is able to indicate a correlate lung function changes to the appearance of the phase diagram.

List of abbreviations

Aex	Area under the expiratory curve
Aex_1	Squared perimeter divided by the area of the expiratory curve
ATS	American Thoracic Society
Ca	Capacitance
CO_2	Carbon dioxide
Diff	Differences between adjacent elements
ECT	Exercise challenge test
EELV	End-expiratory lung volume
EIB	Exercise induced bronchoconstriction
EILV	End-inspiratory lung volume
FEV_1	Maximal volume of air exhaled in the first second of a forced expiration from a position of full inspiration
FOT	Forced oscillatory technique
F_{RES}	Resonance frequency
Fs	Sampling frequency
FVC	Forced vital capacity
HFNC	High flow nasal cannula
HR	Heart rate
L	Tube length
ICU	Intensive care unit
METC	Medical Ethics Committee
η	Viscosity
O_2	Oxygen
ρ	Density
ΔP	Pressure difference
P_{ALV}	Alveolar pressure
P_{ATM}	Atmospheric pressure
P_{AW}	Airway pressure
R	Resistance
r	radius
R_{AW}	Airway resistance
Re	Reynolds number
RR	Respiratory rate
R_{RS}	Respiratory resistance
SpO_2	Oxygen saturation
TBFV	Tidal breathing flow volume
TE	Expiratory time
t_{PTEF}/t_E	Time to peak flow to total expiratory time
V_{PTEF}/V_E	Volume to peak flow to expired volume
$\dot{V}$	Airflow
$\bar{v}$	Velocity
WOB	Work of breathing
X_{RS}	Respiratory reactance
Z_{RS}	Total respiratory impedance

Contents

1. Introduction

High flow nasal cannula (HFNC) therapy is a relatively new non-invasive ventilation therapy which is increasingly used. HFNC therapy consists of two jets of heated, humidified, and oxygen-enriched air which are injected into the patient's nares through relatively small but loosely fitted prongs [1]. The proposed mechanisms of HFNC are an increased washout of nasopharyngeal dead space, improved upper and lower airway mucociliary clearance, and increased airway pressure [2]. HFNC is used in hospitals to treat critically ill patients with acute, severe respiratory disorders, but limited high-quality evidence exists of its efficacy in settings other than intensive care units (ICU). Recently, two clinical trials by Franklin et al.[3] and Kepreotes et al.[4] have been published. Franklin et al.[3] compared HFNC to standard oxygen therapy in a large multicentre, randomized, controlled trial with infants younger than 12 months of age with bronchiolitis and in need of supplemental oxygen therapy. This study showed that patients receiving HFNC had a significantly lower rate of escalation of cure due to treatment failure compared to standard therapy. Kepreotes et al.[4] compared HFNC with standard therapy consisting of low flow therapy, in a single-centre, open, randomised controlled trial with infants younger than 24 months of age suffering from moderate bronchiolitis. Their study indicated a significant difference in survival distributions for time to treatment failure favouring HFNC. Also, the number of children who experienced treatment failure was reduced. 63% of the children who deteriorated on standard therapy avoided transfer to ICU by using HFNC as rescue therapy. The effective working mechanisms of HFNC are, however, not fully understood and there is a lack of evidence-based guidelines to assist clinicians who work with HFNC for therapeutic purpose [5–7]. Clinical observations of respiratory distress resulting in imposed work of breathing (WOB), respiration rate (RR), heart rate (HR), and oxygen saturation (SpO_2) are currently used to provide feedback whether HFNC is effective for the patient. However, these clinical parameters are biased by medication and oxygen supply and vulnerable to misinterpretation. The HFNC does not like most respiratory support devices provide information about therapeutic intensity. There is a safety issue concerning HFNC, namely the actual pressure delivered by HFNC is dependent on the flow but also nasal cannula size and which can have a marked effect on the deliver pressure. Feedback using pressure to obtain a phase diagram reflecting changes in therapy could, besides clinical parameters, provide valuable information for the clinician to guide optimal therapeutic choices. However, these variables cannot be monitored yet [8,9].

Regarding using pressure to obtain a phase diagram as feedback method of therapy efficacy, previous in-vitro experiments indicate that the influence of breathing can be observed in the pressure signal which is a reflection of the airway pressure [10]. The tracheal tree of an infant is relatively small, resulting in a close to maximal WOB of infants during tidal breathing [11]. Therefore, tidal breathing may be a sufficiently discriminating tool to diagnose various pathologies.

In order to determine the phase diagram changes reflecting the efficacy of HFNC therapy, it is essential to investigate whether changes due to lung pathophysiology are also observable in the patient's pressure signal during tidal breathing. During an exercise challenge test (ECT), there is a controlled fall and recovery in lung function in patients with asthma. This patient population can be examined to investigate whether changes in lung function result in change in the pressure signal and therefore in the phase diagram.

Exercise induced bronchoconstriction (EIB) is highly specific for asthma in children and occurs in 80-90% of pediatric asthma patients [12–15]. Asthma is characterized by inflammation of the bronchial walls which can result in bronchospasm, mucus secretion and airway narrowing [16]. During an asthma attack, a variety of alterations in the respiratory system mechanics occur which lead to an increase in the breathing impedance caused by bronchoconstriction. In patients with asthma, exercise (an indirect stimuli) may cause transient narrowing of the lower airways resulting in an expiratory flow limitation [17].

The magnitude of the airway response to stimuli (direct or indirect) is primarily dependent on the degree of bronchial inflammation and the trigger [18]. Lung epithelium condition inhaled air, therefore cold and dry weather conditions induce and increase heat and water loss of the lungs. Nowadays, the osmotic theory is widely accepted as the established underlying mechanism of EIB [19]. The osmotic theory proposes an increased osmolarity of the airway surface liquid as the primary effect of airway water loss [20]. This increased osmolarity extends to include the airway epithelial cells and submucosa. Cellular mechanisms to release various mediators are activated by the hyperosmolar environment. These mediators cause contraction of the airway smooth muscle and subsequent airway narrowing. The osmotic theory can be observed in figure 1.

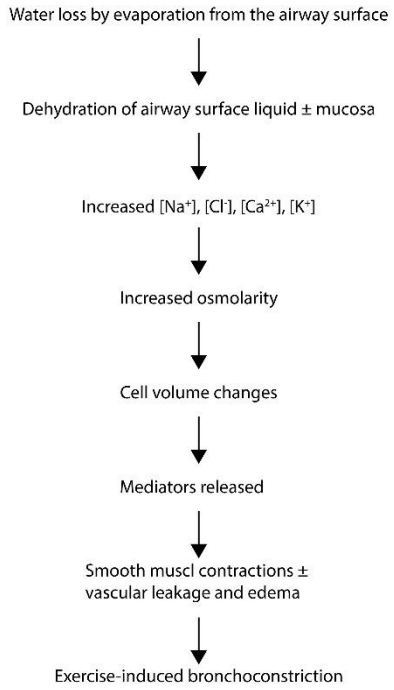

Figure 1: The osmotic theory describing the pathogenesis of exercise induced bronchoconstriction [20].

Spirometry is the golden standard for diagnosis of any condition affecting the lungs of patients who are not critically ill [21]. During spirometry, the patient first needs to inhale maximal and then exhale rapidly. The measured forced expiratory volume in 1 second (FEV_1) is dependent on the effort of the patient. As spirometry requires maximal cooperation and performance, it can be performed from an age of 5 years [22]. Obstructive airflow disorders, e.g. asthma, are characterized by the typical concave shape of the expiratory flow volume curve [23]. Another method which can be used to determine the characteristics of the lung is forced oscillation technique (FOT) [24]. FOT superimposes a multi-frequency airwave on top of the patient's spontaneous breathing and can therefore be used from the early age of 2 years [24,25]. The respiratory reactance (X_{RS}) and the respiratory resistance (R_{RS}) at a frequency of 5 Hz have been used as a primary efficacy variable to investigate asthma due to the heterogeneous peripheral airway obstruction [25,26].

1.1. Rationale

High flow nasal cannula (HFNC) therapy is widely used. There is a lack of guidance for high care professionals to optimize its use as there is no feedback of therapy intensity. Measurements of pressure over time and integration to phase diagrams could provide objective feedback on therapy efficacy.

1.2. Research objective

The primary objective is to compare the exercise induced changes in lung function to the changes in the phase diagram. The changes in lung function will be measured with spirometry as the golden standard, and FOT. In order to evoke a variation in lung function of patients, a standard exercise challenge in a cold chamber and a bronchodilator (salbutamol) will be utilized to induce respectively bronchoconstriction and bronchodilatation in asthmatic patients.

1.2.1. Parameters

To investigate the primary objective, the FEV_1 measured using spirometry and the X_{RS} and R_{RS} measured with FOT will be compared to the changes in the phase diagram. Regarding the changes in the phase diagram, the sphericity and triangularity of the expiratoire curve will be used to assess concavity due to asthma. In addition, instead of the area under the curve, which is dependent on the unit, the squared perimeter divided by the area of the phase diagram will also be assessed. These parameters will be determined at the lowest lung function, before and after a bronchodilator, and the change of every parameter will be compared individually to the change of lung function measurements of spirometry and FOT.

2. Background

2.1. Respiratory physiology

During ventilation, gas exchange occurs between the atmosphere and the alveoli in order to supply the body with oxygen (O_2) and to release the body of carbon dioxide (CO_2) [27]. In a respiratory cycle, 30% of the total ventilation is wasted due to anatomical dead space which consist of the conducting airways [27]. Children have proportionally larger dead space, which can be proportionally two or three times greater compared to adults. The dead space may measure up to 3 mL/kg in new-borns and declines to 0.8 mL/kg after the age of 6 which is similar to the adult volume [5]. Alveolar ventilation is influenced by the body temperature, pressure, and saturation of air with water [27].

The lungs have a tendency to collapse due to their elastic recoil, whereas the rigidity of the chest wall prevents this. In dynamic conditions, when there is flow, one must also exert an extra force to overcome the resistance and inertia of the lung tissues and air molecules [27]. The airflow ($\dot{V}$), if laminar, is dependent on the difference between alveolar pressure (P_{ALV}) and the atmospheric pressure (P_{ATM}) and inversely proportional to airway resistance (R_{AW}), given with equation (1).

$$\dot{V} = \frac{\Delta P}{R_{AW}} = \frac{P_{ALV} - P_{ATM}}{R_{AW}} \tag{1}$$

The flow of a fluid down a tube is laminar when particles passing any particular point, always have the same speed and direction. Due to viscosity, real fluids have the highest velocity down the midline of a tube and the velocity decreases the farther the fluid is located to from the midline. Poiseuille's law states that the resistance (R) of a tube is proportional to the viscosity of the gas (η) and the tube length (l), and inversely proportional to the fourth power of the radius (r) given with equation (2).

$$R = \frac{8}{\pi} \cdot \frac{\eta l}{r^4} \tag{2}$$

Poiseuille's law is only applicable to laminar flow. When using this law, the airflow is extremely sensitive to changes in the airway radius (r) due to the fourth-power dependence. Airflow is transitional when the flow switches between laminar and turbulent. Airflow is transitional through most of the tracheobronchial tree due to the bifurcation of the pulmonary airways which create small eddies resulting in transitional flow. The Reynolds number (Re) can be used to determine if the flow is laminar (Re<2000), transitional (2000<Re<3000) or turbulent (Re>3000), given in equation (3).

$$Re = \frac{2r\bar{v}\rho}{\eta} \tag{3}$$

with r the radius of the tube, $\bar{v}$ the velocity of the gas averaged over the cross section of the tube, ρ the density of the gas, and η its viscosity. As the geometry of the pulmonary airways is complex, the critical Re in the lungs is far lower than the ideal value of 2000. As a result, Re must be less than 1 instead of 2000 to have a laminar airflow. Therefore, airflow is transitional throughout most of the tracheobronchial tree.

The flow pattern influences the amount of energy needed to produce airflow. Laminar flow is proportional to ΔP and therefore requires a relatively low amount of energy. Turbulent airflow, however, is proportional to $\sqrt{\Delta P}$ resulting in lower flow compared to laminar flow when ΔP is similar. The airway resistance (R_{AW}) can be calculated by rearranging equation (1) into (4).

$$R_{AW} = \frac{\Delta P}{\dot{V}} = \frac{P_{ALV} - P_{ATM}}{\dot{V}} \quad (4)$$

2.2. Pathophysiology

In accordance with the GINA guidelines of 2018, asthma is a heterogeneous disease, usually characterized by chronic airway inflammation [28]. Asthma is characterised by a history of episodic respiratory symptoms such as cough, shortness of breath, wheeze and chest tightness, together with variable expiratory airflow limitation [28]. Both symptoms and airflow limitation characteristically vary in intensity and over time. Symptoms are often triggered by factors as allergen or exposure to non-allergic inhaled irritants, change in weather, viral respiratory infections or exercise.

Inflammation of the bronchial walls results in mucus secretion, increased mucosa thickness and bronchospasm, as can be seen in figure 2 [16,29]. The bronchial wall appears thickened in all asthma patients regardless of disease severity. The degree of wall thickening is related to disease duration, severity, and the degree of airflow obstruction [18,30–32]. Furthermore, the smooth muscle cells lining the bronchial wall contract, resulting in bronchospasm, which decreases the lumen size even further [29]. Taking Poiseuille's law (equation 2 and 4) into consideration, a narrowed airway (decreased r) results in an increased R_{AW} and consequently decreased $\dot{V}$.

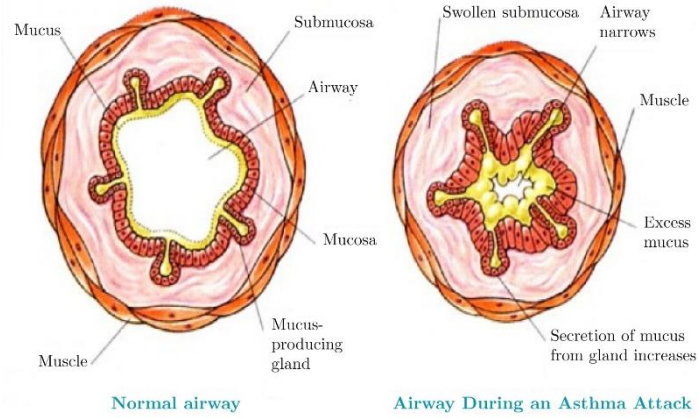

Figure 2: Pathological changes in asthma.

Asthma is an episodic obstructive pulmonary disease [27]. In most asthmatic patients, the lung function is normal or close to normal between attacks [33]. During an asthma attack, however, a variety of alterations in the respiratory system mechanics occur leading to an increase in the breathing impedance caused by bronchoconstriction. In patients with asthma, exercise (an indirect stimulus) may cause transient narrowing of the lower airways which results in an expiratory flow limitation [17]. Cold air aggravates the trigger of exercise for bronchoconstriction in patients with asthma [9].

2.3. Spirometry

Spirometry is the golden standard for assessment of lung function in children with asthma [34]. Spirometry determines the change in lung volume by measuring the volume of inspired and expired air during a forced breathing manoeuvre [27]. The patient first needs to inhale maximally through a spirometer and then exhale rapidly through the same device. During spirometry, the maximal volume of air exhaled in 1 second during a forced expiratory volume (FEV_1) is measured. Another spirometry measure is the forced vital capacity (FVC), which is the maximum amount of air that can be exhaled when blowing out as fast as possible. If the patient

has an airflow limitation, the FEV_1 and the FEV_1/FVC ratio are reduced [22,35]. The flow volume curves of a healthy and asthmatic subject are observable in figure 3 [21]. Concerning the ECT, in accordance to the GINA guidelines this test is positive if there is a decrease in FEV_1 of at least 12%. Regarding the reversibility induced with a β_2-agonist (salbutamol), this indicates a positive test if FEV_1 increases with at least 12% in children [28]. A reduced ratio of FEV_1 to FVC indicates airflow limitation with normal values of FEV_1/FVC, usually exceeding 0.90 in children.

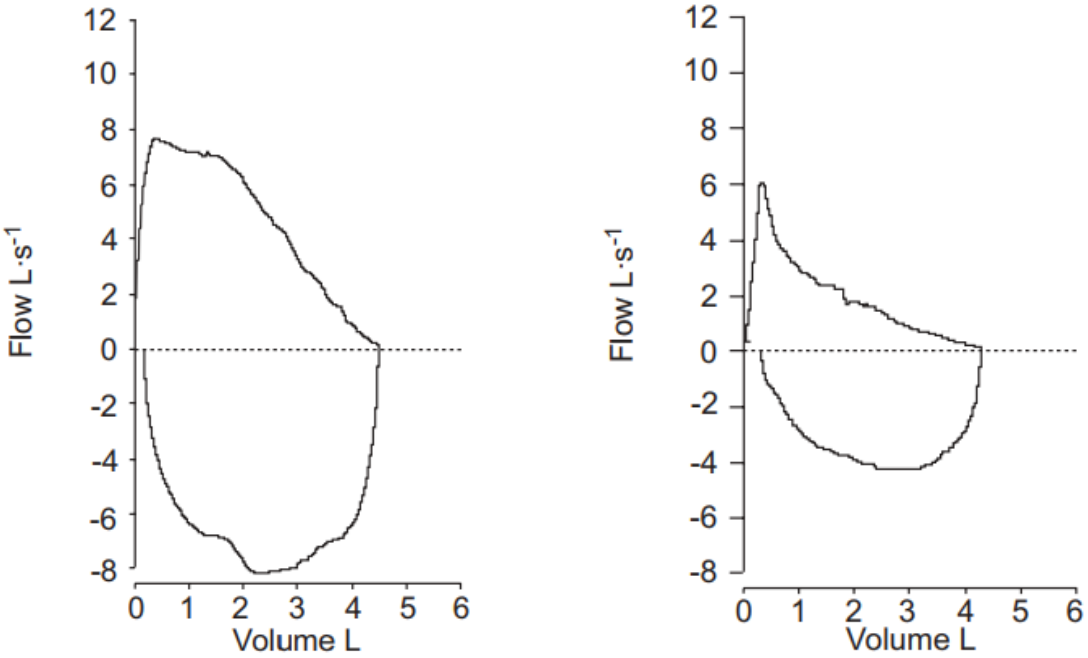

Figure 3: Flow volume curves of a healthy subject on the left and an asthmatic subject with a moderate airflow limitation on the right [21].

Jubran et al.[36], recorded flow volume curves in 50 ventilator-dependent patients over 1 min of spontaneous breathing and observed a saw tooth pattern if secretions was present, see figure 4. This phenomenon can be observed after the use of a bronchodilator as it can improve coughing by increasing bronchial patency and thus expiratory flow. As a result, coughing becomes more effective as there must be sufficient airflow to detach sputum and to mobilize secretions so that they can be expectorated [37].

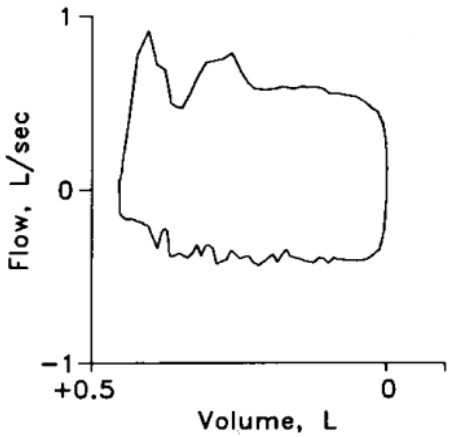

Figure 4: The flow volume curve characteristic for the presence of secretion [36].

2.4. Forced oscillation technique

FOT superimposes a multi-frequency airwave on top of the patient's spontaneous breathing which can assess lung mechanical parameters. This is achieved by measuring the total respiratory impedance (Z_{RS}) [24]. Z_{RS} is a function of the respiratory resistance (R_{RS}) and the respiratory reactance (X_{RS}) at one oscillation frequency, see equation (5).

$$Z_{RS}(f) = R_{RS}(f) + jX_{RS}(f) \qquad \{0 < f < f_{MAX}\} \tag{5}$$

with f the frequency, j the imaginary component, and X_{RS} and R_{RS} the respiratory reactance and resistance. X_{RS} consists of the mass-inertive forces of the moving air column in the conducting airways (I) and the elastic properties of lung periphery (capacitance, Ca), see equation (6).

$$X_{RS}(f) = \omega \cdot I - \frac{1}{\omega \cdot Ca}, \qquad \omega = 2 \cdot \pi \cdot f \qquad \{0 < f < f_{MAX}\} \tag{6}$$

The effect of Ca is most prominent at low frequencies and its effect on X is opposing. In contrast, the effect of I always has positive contribution to X and dominates at higher frequencies. The resonant frequency (f_{RES}) is the frequency with equal and opposite contributions of C and I to X. As a result, X is zero at f_{RES}. R is normally expected to be frequency-independent [25]. In figure 5, the effect of heterogeneous peripheral obstruction on the X_{RS} and R_{RS} can be observed. Asthma results in a heterogeneous peripheral obstruction due to the heterogeneous character of the inflammation [26]. The obstruction results in a frequency-dependent increased R_{RS} due to a larger increase of R_{RS} in lower frequencies compared to higher frequencies. In addition, it results in a shift of X_{RS} in downward-and-right direction [25].

The most commonly utilized oscillation frequency range for multi-frequency oscillations includes frequencies between 5 and 30 Hz [24]. Peripheral airway obstruction results in an increase in magnitude of low frequency $|X_{RS}|$ and a higher resonance frequency (f_{RES}). X_{RS5} (X_{RS} at 5 Hz) has been used as primary efficacy variable to assess asthma. In asthmatic patients, R_{RS} drops rapidly with increasing oscillation frequencies from 5 up to 18 Hz caused by abnormal peripheral airway function. Small changes in X_{RS} at 5 Hz, and f_{RES} occur between the situations pre- and post-bronchodilator. Both high and low-frequency R_{RS} may decrease with a relatively larger decrease in low-frequency R_{RS}. The frequency dependency of resistance between 5 and 20 Hz (R_{5-20}) provides information on the heterogeneity of airway obstruction [25].

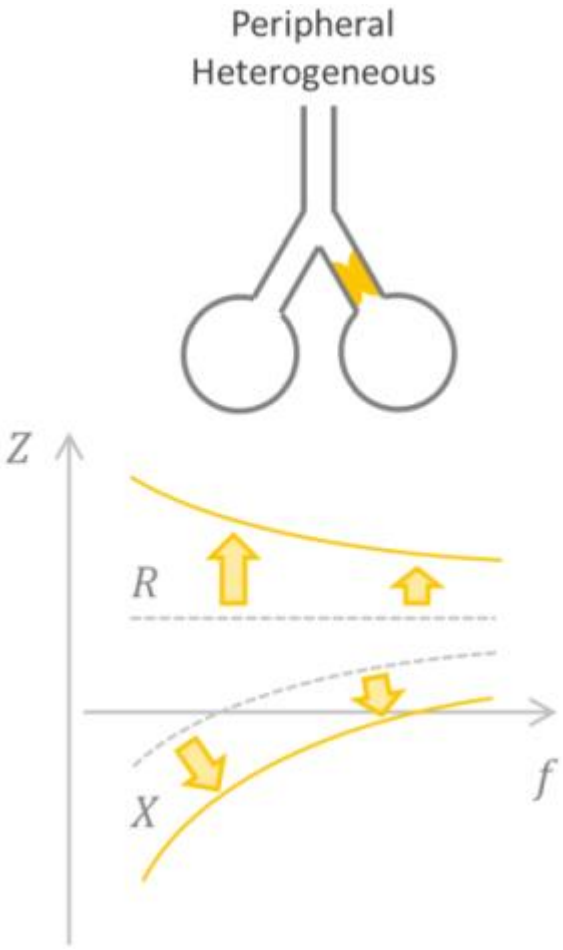

Figure 5: The influence of heterogeneous peripheral obstruction on the reactance (X) and resistance (R) [25].

Bronchoconstriction results in a frequency dependent R_{RS}, where changes become more evident in the lower frequencies. Reactance also decreases due to bronchoconstriction, resulting in a prominent increase in f_{RES} [38].

It has been shown that an increased R_{RS} at 8 Hz is significantly correlated with a decrease in FEV_1. Furthermore, an increase in f_{RES} is correlated with a decrease in FEV_1 as well [38]. The change in Z_{RS} reflects inhomogeneity in peripheral part of the bronchial tree.

2.5. HFNC

The proposed mechanisms of HFNC are the washout of nasopharyngeal dead space, reduction of the inspiratory and expiratory resistance, improved ventilation mechanics and reduction in the metabolic cost of gas conditioning [2,39]. The high flow provided by HFNC causes flushing of the nasopharynx and therefore leads to a reduction in dead space. The flow rate of HFNC is equal or higher than the inspiratory flow, which results in an attenuation of the inspiratory resistance exerted by the nasopharynx. The warmed humidified gas improves the conductance, compliance, and reduces the metabolic work associated with the conditioning of gas. In addition, the gas decreases resistance by making the mucus less tenacious and reducing the amount of mucus by easier mobilization and evacuation [39]. High flow can also generate positive distending pressure which is believed to improve breathing mechanics. This is achieved by optimizing lung compliance, recruitment of the lung, decrease in ventilation-perfusion mismatch, and improvement of patency of the alveoli [2,40]. All the proposed mechanisms of HFNC may relieve effects of induced bronchoconstriction. However, the exact moment at which therapeutic effects occur is unknown.

Within five minutes of respiration, pulmonary compliance and conductance significantly decreases with use of warmed humidified ambient gas in ventilated infants [2]. Therefore, making use of warmed humidified gas limits the bronchoconstriction induced by for instance cold dry gas [5].

Previously performed measurements with the HFNC showed that the pressure could vary greatly depending on the gap between the cannula and the wall of the nostrils. Pressure increases with lager cannula sizes and elevated ratios of cannula diameter compared to nostril diameter [41]. The insertion angle and insertion height had negligible effect on the pressure. However, the pressure increases with an increasing insertion length [42,43]. In order to achieve reproducible phase diagrams, it is necessary to normalize the pressure signal before analyzation of the phase diagrams to eliminate the influence of the insertion length. Nasal cannula size is a critical factor resulting in an advised occlusion of maximal 50% by the nostrils [44]. This is due to the relation between air leak around the cannula prongs and the generated pressure, and the effects of size on the maximum amount of flow.

2.6. Phase diagram – parameters

In order to be able to measure the breathing pressure during ECTs, a pressure sensor will be added to the measurement setup. This is shown in figure 8 of chapter 3. The breathing pressure will be integrated to obtain tidal breathing phase diagrams [39].

In patients with asthma, the expiratory part of the phase diagram provided with spirometry can have a concave or triangular shape [11,23]. In contrast, the inspiratory part usually appears normal in asthmatic patients. Peak flows tend to be higher and occur earlier in the expiration of patients with obstructive lung disease [45,46]. In addition, there is a slow decline in flow over most of the expiration followed by an abrupt drop of flow to zero due to the trigger for the next inspiration. These typical shapes in the phase diagram of a forced manoeuvre, caused by obstructive lung diseases, can be used to evaluate the phase diagram.

Tidal breathing flow volume (TBFV) curves can be evaluated by the shape of the air flow signal [11]. Normalization of these curves is essential to avoid bias due to size or bodyweight of the various subjects. Furthermore, normalization can also be used to eliminate the influence of the insertion length of the prongs. Leonhardt et al.[11] used a sphericit and triangular approach to quantify the expiration. In addition, quantifying the expiration is also possible by approximation with polynomials. The sphericity and triangularity were assessed using equations (7) and (8) respectively

$$O_{exp} = \frac{r_{inscribed,exp}}{r_{circumscribed,exp}} \tag{7}$$

$$\nabla_{exp} = \frac{\int_{\Delta V_{lung}=0}^{VE} \dot{V}_{breath} dV}{0.5 \cdot PTEF \cdot VE} - 1 \tag{8}$$

In figure 6, the difference in sphericity between a healthy and an asthmatic subject can be observed with expiration values of O_{exp}=0.71 and O_{exp}=0.32, respectively. A O_{exp} value of 1 corresponds to a perfectly shaped sphere. Regarding equation (8), a concave shape is indicated with a $\nabla < 0$, and if very triangular, $\nabla \approx 0$. In figure 7, the triangular approximation of the TBFV curve is shown for an asthmatic subject with ∇_{exp} being a perfectly shaped triangle as it approaches zero (∇_{exp}=0.07312).

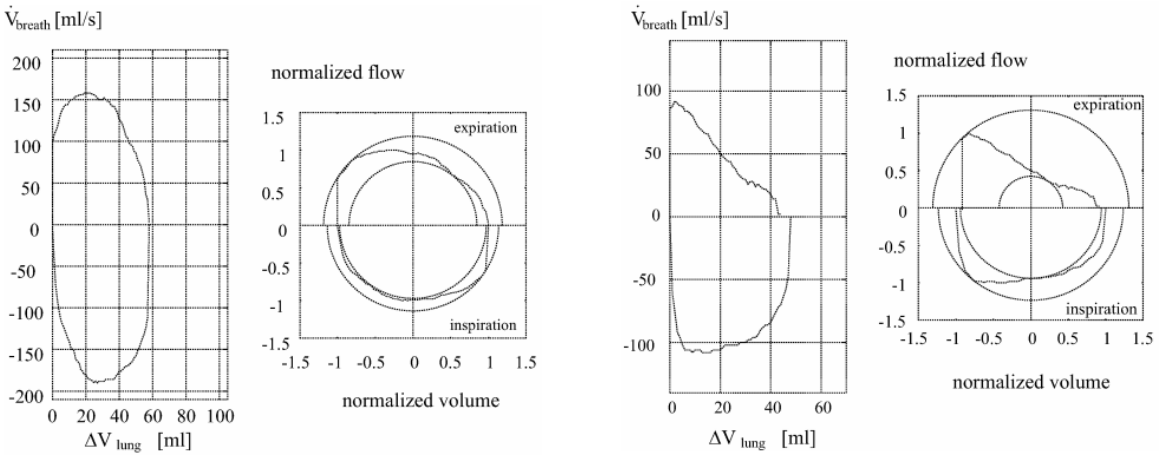

Figure 6: Sphericity for a healthy subject (left two figures). (Left) Original TBFV curve and (right) elucidates roundness after normalization to ±1. The two figures on the right show an asthmatic subject in which expiration does not appear to be particularly 'round' [11].

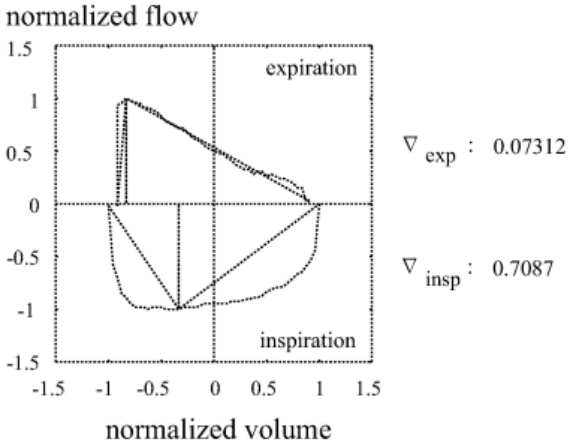

Figure 7: Triangularity for the asthmatic subject. As expected, expiration was classified as being 'very triangular', while inspiration was classified 'not triangular at all' [11].

Regarding the approximation with polynomials, first- and second-order polynomials can be used for the normalized curves with equation (9) and (10) respectively.

$$\textit{First order: } \hat{\dot{V}}_{breath} = a_1 \Delta V_{lung} + b_1 \quad (9)$$

$$\textit{Second order: } \hat{\dot{V}}_{breath} = a_2 (\Delta V_{lung})^2 + b_2 \Delta V_{lung} + c_2 \quad (10)$$

The difficulty regarding approximation by polynomials lies in the interpretation of the coefficients and the quality of the approximation.

Assessing the concavity to quantify airway obstruction, was also studied by Zheng et al.[47]. They used a hyperbolic function using among others the forced vital capacity (FVC). Morris et al.[46] used a time constant of the regression line to fit to the linear part of the expiration. They r^2 value was used to assess the goodness of the fit with a required minimal of 0.85.

Two other parameters that reflect the level of obstruction consisted of the time to peak flow divided by the total expiratory time (t_{PTEF}/t_E) and volume to peak flow divided by the expired volume (V_{PTEF}/V_E) [48–51]. Those measures can also be assessed as a percentage of predicted, resulting in $\Delta V/V$ and $\Delta t/t$ [45,52]. All these parameters showed a significant correlation with FEV_1 [45,48,50,52]. PTEF, however, provides only limited information about the smaller airways as it primarily reflects central airway obstruction [53]. Van der Ent et al.[49] concluded t_{PTEF}/t_E to be a more useful parameter to assess airflow obstruction in epidemiological research than in individual patients due to the limited accuracy and quite large internal variability. Therefore, the clinical usage of these time dependent measures is limited.

The area under the expiratory part of the phase diagram (Aex) provides information on central and peripheral airway obstruction [54]. The magnitude and pattern of Aex changes after bronchodilatation and can therefore be influenced by changes in the lung function. This offers an opportunity to use this parameter to evaluate the efficacy of medication. However, it is desired to obtain dimensionless parameters in order to avoid bias of for example the prong length and therefore be able to assess only the form of the phase diagram. As both the area and perimeter are indicative for the appearance of an object, a dimensionless parameter can be achieved by dividing the squared perimeter by the area. Equation (11) shows the dimensionless parameter, Aex_1,

$$Aex_1 = \frac{perimeter^2}{area} \tag{11}$$

In conclusion, derivation of the parameters sphericity, triangularity, and Aex_1 from the phase diagram are promising measures to assess the lung function variation of asthmatic patients. The correlation between the parameters derived from the phase diagram and the lung function parameters of spirometry and FOT, however, needs to be determined.

3. Method

This study was submitted to the Medical Ethics Committee (METC) Twente as TBFV (Phase diagram in relation to lung function changes during bronchoconstriction and –dilation), and was approved 19-03-2019 with trial number K19-15.

3.1. Study design

This study had an observational cross-sectional design, in which 25 children, aging from 4 to 16 years old, with pediatrician diagnoses asthma or suspicion of asthma, scheduled for an exercise challenge test (ECT), were asked to participate. The measurement setup is observable in figure 8. This measurement setup is used to study the change in the appearance of the phase diagram obtained from tidal breathings to the lung function measurement by performing pilot measurements and the TBFV-curve study.

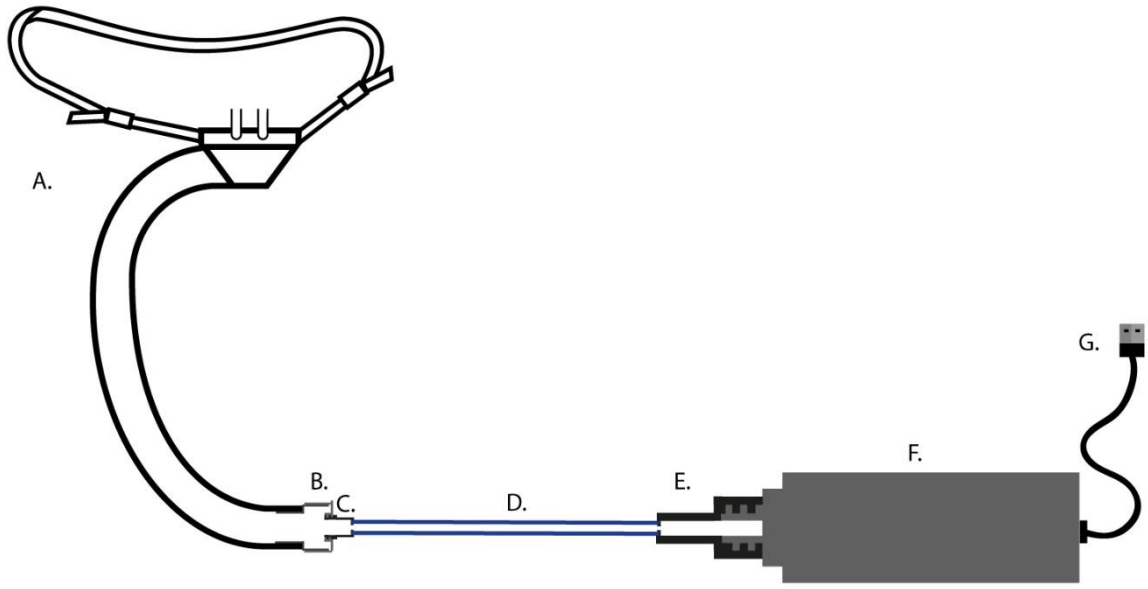

Figure 8: Measurement setup, nasal cannula connected to a pressure sensor.
A. Optiflow^{TM} Nasal High Flow cannula S.
B. Connector of the breathing circuit to the optiflow^{TM}. To this connection part, was handmade and manually attached by the Technician of the University of Twente
C. SNAP fitting
D. Polyurethane tube with adaptable length
E. SNAP fitting
F. Pressure sensor, pxm409-070hcgusbh OMEGA
G. USB connection to extract data using a PC

3.1.1. Inclusion

At first, the children and their parents were informed by telephone 2 weeks prior to the ECT. After verbal agreement, parents received a study information letter (for both themselves and their child) and a (parental) consent form (Appendices A). However, after the first week it became clear that this method was too time consuming and another approach was used. The parents received the information letter one week prior to the appointment. Written informed consent was obtained prior to the start of the measurements, during the appointment at the outpatient clinic. It was signed by either both parents (child under the age of twelve) or parents and child (children between the ages of twelve and sixteen).

3.1.2. Exercise challenge test

During an outpatient visit at the OCON, the ECT was performed according to international guidelines of the American Thoracic Society (ATS) [55]. Children below the age of eight were challenged with six minutes of jumping on a jumping-castle according to van Leeuwen et al. [12]. Children above the age of eight were challenged with six minutes on a treadmill. The slope of the treadmill was set at 10% to reduce running speed and improve safety while maintaining exercise intensity. Each ECT took up to one hour to complete.

A thorough medical history was performed, focusing primarily on any discomforts regarding breathing abnormalities. Furthermore, information was acquired of medication adherence, physical activity and familiar occurrence of asthma, eczema and/or allergies in the first or second degree. During physical examination, attention was paid to the presence of allergic signs, such as Dannie-Morgan lines and Meyers' nasal crease. The clinical research form that was used to capture the medical history, physical examination and other ECT data can be seen in Appendix B.

Baseline measurements were performed using the FOT and spirometry. If the treadmill was used as exercise method, subjects were then equipped with a HR monitor (Polar). The exercise were performed in a climate controlled room at the outpatient clinic. Subjects exercised on a treadmill set at a 10% angle in cold air (10°C) for six minutes with a clip on the nose at submaximal level (80% of maximal predicted HR). These conditions provide the maximal stress for the airways to provoke an asthmatic reaction. Children under the age of eight were not equipped with a HR monitor and exercised on the jumping-castle for six minutes instead. Previous studies state that high intensity exercise is guaranteed in young children when jumping on a bouncy castle [12]. To ensure an appropriate exercise challenge children were encouraged actively to keep jumping for the full six minutes.

Subjects performed double spirometry measurements at one, three, and six minutes after exercise. If FEV_1 was still declining after six minutes, an additional measurement was performed every three minutes until start of recovery of FEV_1 (at for example nine and twelve minutes). A FOT measurement were performed at five minutes after exercise.

After the final spirometry measurements, subjects inhaled 200 µg of salbutamol and five minutes thereafter a final FOT and spirometry measurements were performed to evaluate the effect of medication.

After the ECT, data was acquired from the device and stored anonymously for later data-analysis. A full overview of all actions during an ECT are shown in figure 9.

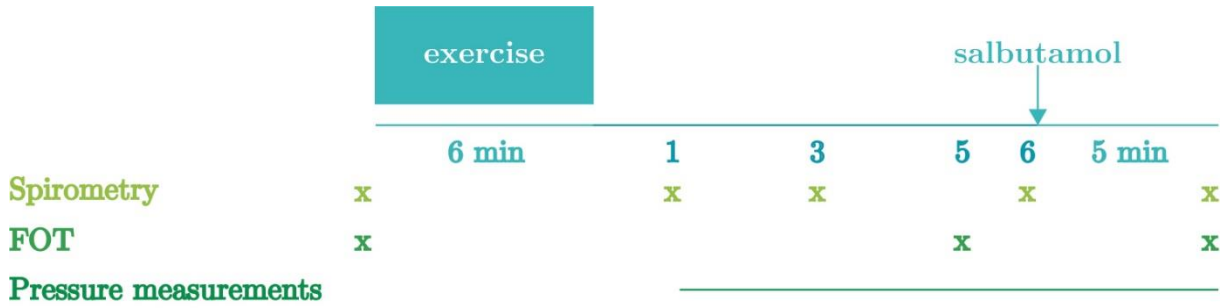

Figure 9: An overview of all actions during an exercise challenge test.

3.1.3. Pressure measurements

All pressure measurements were performed using a PXM409-070HCGUSBH device, see figure 8 part E. The pressor sensor was connected to a laptop via USB and therefore the value pressure data could be observed in real time and extracted as an excel file after each measurement. To analyse TBFV curves, a sampling rate of at least 200 Hz is recommended [56].

During the measurements, only the nasal cannula of the HFNC system was used and connected to a pressure sensor as observable in figure 8. The pressure curves of 25 children were measured from approximately one minute after exercise up to the end of the ECT. These children visited the OCON for an ECT as standardised care to provoke bronchoconstriction by exercise in a cold chamber. The purpose of these measurements is to determine if there is a relation between dynamics of lung function and changes in the phase diagram.

3.2. Population

The population of this study consists of all children with pediatrician diagnosed asthma. One in five girls and one in four boys at the age of two to three years have asthma symptoms. The prevalence decreases to 10% in girls and 15% for boys at the age of six to seven after which it stabilizes [57]. Frequent asthma symptoms are observed in 4-5% and 2-3% of respectively boys and girls five years and older [57]. Children whom are 4 to 16 years of age, who are scheduled for an ECT at OCON were approached to take part of this study.

3.2.1. Inclusion criteria

In order to be eligible to participate in this study, a subject must meet all of the following criteria:

- Children with pediatrician diagnosed asthma.
- Children aged between 4 and 16 years old.
- Children instructable to perform an ECT and repeatable spirometry.

3.2.2. Exclusion criteria

A potential subject who meets any of the following criteria was excluded from participation in this study:

- Children with an unilateral or bilateral obstructed nose
- Children who are unable to speak Dutch, or whose legal guardians are unable to speak Dutch.
- Children for whom it is not possible to wear the Optiflow^{TM} device. For example due to malformations of the nose.
- Children born prematurely <34 weeks.

3.2.3. Withdrawal of subjects

Any subject was allowed to ask for a cessation of measurements at any time without consequences. Subjects were informed of this possibility by means of the patient information letter and also verbally before written consent. Before attachment of the nasal cannula, the child was asked if they still wanted to participate and informed that they could stop at any time. The device would then be detached without further questions and the ECT or spirometry will proceed as it normally would.

3.2.4. Sample size

The largest change in lung function is observed in subjects with uncontrolled asthma. Prior to the ECT in the OCON, the asthma control of the subject is unclear. The effect of the change in lung function on the phase diagram of tidal breathing is also unknown. Taking into consideration the number of patients visiting the outpatient clinic in MST and performing the ECT at the OCON, it was expected that 25 subjects needed to be included at the OCON to measure at least 15 uncontrolled asthma subjects [58]. 25 subjects were included in the period of March to May 2019.

3.3. Data analysis

All data were pre-processed using Matlab (version R2018b). A pilot study was performed to investigate the effect of potential influences on the pressure signal. Performing lung function measurements, swallowing, clearing the throat, coughing, itching the nose, repositioning of the prongs and breathing through the mouth were evaluated. The reason for this is the ability to select only the breaths of which the phase diagram is computed. All previously mentioned influences are distinguishable from breathing and therefore automatic determination of breaths seems possible. These results are observable in Appendix C. The locations of these influences were manually inspected and removed from the raw signal if selected correctly. These scripts can be seen in Appendixes D. The correlation between the change in lung function assessed by spirometry and FOT will be compared to the changes in the phase diagram. As the breathing pattern is variable, a number of consecutive artifact-free breaths should be selected for the determination of the parameters [59]. However, as the setup of the measurements is unique, the number of breaths which should be taken into consideration needs to be investigated.

3.3.1. Pre-processing

The data was first divided into the segments that correspond to the intervals of figure 9. Thereafter, the artefacts for each individual segment were located using the moving standard deviation (movstd) and differences between adjacent elements (diff) functions of Matlab. The reason that those functions have been chosen, is explained in Appendix C. Subsequently, the interval which contains the artefact was removed between two minima that correspond to maximal inspiration. After the removal of non-breathing intervals, the remaining segment was divided into single breaths based in the minimum. These minimum correspond to the maximal pressure obtained during inspiration. Each single breath was expanded into sines and cosines up to the 25^{th} component using Fourier series. This smoothens the pressure signal. 4.1 Number of Fourier coefficients describes why up to 25th components were used.

3.3.2. Fourier terms

The pressure signal during 1 period (one breath from the maximum of the previous inspiration to the next inspiration) was expanded into sines and cosines up to the Nth component. The signal was approached using Fourier to smoothen the signal and to be able to obtain a reliable value for the perimeter of the phase diagram. For three subjects it was determined how many components were needed to stabilize the parameters (Aex_1, sphericity, and triangularity), observable in 4.1 Number of Fourier coefficients. The parameters stabilize after 25 Fourier components, which results in a Fourier vector of 51 terms as it is composed of one constant, 25 sines and 25 cosines.

3.3.3. Phase diagram

In order to determine the TBFV curves (phase diagrams), the minima which is at maximal inspiration were determined. The minima was chosen as it is more difficult to identify the start of an inspiration or expiration correctly. This is mainly needed as errors occur due to the variation around the baseline by the influence of noise and also severely disturbed signals increase the error rate [59]. In order to avoid very short breathing cycles due to noise around zero, the zeros that occur within 40 measurement points or within 0.6 s of the previous zero were removed. The y which resembles the flow was calculated using equation (12). The volume which is represented by x, was determined by integrating the flow over time since the start of the cycle. Equation (13) shows the computation of x.

$$y = \frac{P - P_{mean}}{\max(P - P_{mean})} \tag{12}$$

$$x = \int y \, dt \tag{13}$$

3.3.4. Parameters

It is hypothesized that the sphericity, triangularity and Aex_1 of the phase diagram would be influenced by the level of bronchoconstriction which was induced by exercise in a cold room with dry air and reversed to bronchodilatation by salbutamol. The variation in parameters based on the phase diagram were plotted against the corresponding FEV_1 measured by spirometry. The x-axis of the expiratoire curve on which the sphericity and triangularity was computed were normalized from -1 up to 1. As mentioned before, normalization can also be used to eliminate the influence of the insertion length of the prongs and gap between the prongs and nares. As the trend will be compared between subjects it is also essential to avoid bias due to size or bodyweight of the various subjects.

3.3.5. Number of phase diagrams

As mentioned previously, the procedure for sampling of representative breaths needs to be investigated for standardisation. This can be investigated in two ways. The first methods averages the value of the parameter from the phase diagram which is the closest to the lung function measurements up to the first phase diagrams thereafter. This results in a mean parameter value for the first, first and second, first up to third, etc. of consecutive phase diagram considering breaths. The seconds method uses the factors of the Fourier vector of the phase diagrams for averaging, using the mean of all considered phase diagrams for each factor of the Fourier vector. This results in a mean phase diagram of the phase diagrams taken into consideration. The selection of the phase diagrams is similar to method 1. After the computation of a mean Fourier vector, these factors are used to compute the x_mean and y_mean of the phase diagram averaged at the start and/or end of the segment. Subsequently, as the forced lung function manoeuvre of spirometry influences spontaneous breathing, it is speculated that only the breaths before lung function measurements should be taken into consideration for averaging.

4. Results

Table 1: Subject characteristics. Included subjects in green and excluded subjects in red.

Subject	Age (yr.)	Weight (kg)	Length (cm)	Sex (F/M)	Control medication	Allergy	Nasal cannula type (xl/s)	Lung function change (%)
1	6.5	26	118	M	yes	yes	xl	5.6
2	7.1	28	124	M	yes	yes	xl	14.5
3	8.2	28.7	129	M	no	no	s	9.1
4	9.8	32.5	145	F	yes	no	s	7.3
5	4.3	17	104.5	M	yes	no	xl	13.8
6	14.4	52	162	M	non-adherent	yes	s	11.9
7	8.3	25.8	126.6	M	yes	yes	s	28.5
8	4.3	20.3	107	M	yes	no	xl	16.5
9	7.3	18.6	117	M	no	yes	xl	23.7
10	9.6	38	148.6	M	yes	yes	s	31.8
11	9.8	39.8	150.6	M	no	yes	s	6.1
12	12.3	49	160	M	yes	yes	s	31.6
13	11.4	39.3	147.6	F	no	yes	s	12.0
14	10.8	25.9	131.1	F	non-adherent	no	s	20.5
15	9.6	33.2	143.7	M	yes	yes	s	28.6
16	8.9	46.2	143.8	M	yes	no	s	11.4
17	12.6	55	155.5	M	yes	no	s	16.9
18	13.3	49.5	163	M	yes	yes	s	10.9
19	10.3	37.4	145.6	M	no	no	s	5.0
20	11.5	39.2	147	M	yes	yes	s	23.6
21	9.8	25.8	131.8	F	yes	yes	s	5.5
22	12.8	35	144	M	yes	yes	s	7.5
23	7.5	22.7	122.2	M	yes	yes	s	29.3
24	11.1	38.1	151	M	no	no	s	16.2
25	4.2	17.5	106.5	M	no	no	xl	16.5
Mean (±SD)	9,4 (2,8)	33,6 (10,9)	137,0 (17,3)	84% M	64% (8%)	60%	76% s	16.2% (8.6%)

The characteristics of all subjects are shown in table 1. A few subjects were excluded from the data analyses. The pressure measurements of subjects 1, 11 and 23 were ceased due to discomfort induced by the nasal prongs before the lung function measurement at 6 minutes after exercise. Subjects 4 and 9 were not able to perform reliable lung function measurements and were therefore excluded. The maximal decline in lung function of most children occurred within 6 minutes after exercise, however, subject 20 experienced his minimal lung function between 9 and 12 minutes after exercise and was therefore excluded. The maximal decline in lung function of subject 20 occurred between 9 and 12 minutes, however, most subjects performed lung function measurement up to 6 minutes after exercise. No representative breathing pressures were obtained of subject 8 after the lung function measurement at 3 minutes. This was most likely caused by a fold in the nasal prong due to the nose clip attached to perform the lung function measurements.

The mean Fourier vector of all the phase diagrams of the 18 included subjects was calculated and the dot product of every single phase diagram with this mean Fourier vector was determined. The number of phase diagrams that have a dot product value within a range of 0.01 is indicated on the y-axis of figure 10. The coherence is displayed on the x-axis with a value approaching 1 corresponding to a perfect coherence between the individual phase diagram and the mean of all phase diagrams. The distribution of the dot product value appears log-normal in figure 10. This indicates that the dot product has in general a high coherence with the mean phase diagram.

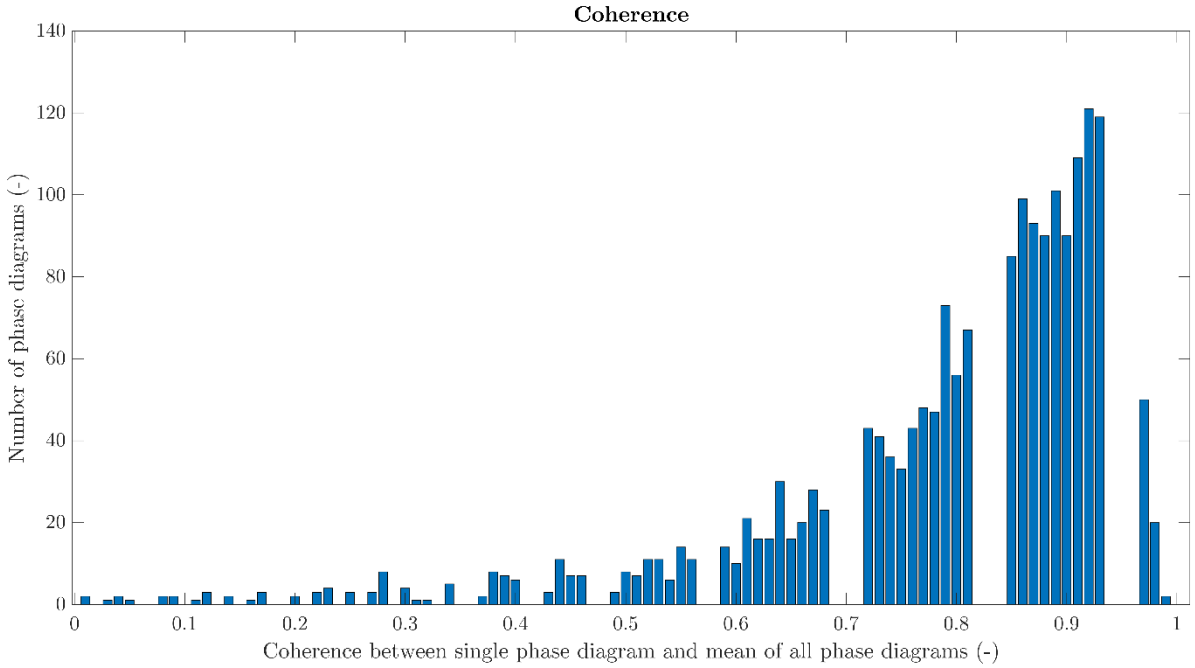

Figure 10: Coherence between single phase diagrams and the mean of all phase diagrams.

Different approaches of data processing have been investigated as they seem to affect the parameter values. These approaches are summarised in 4.1 to 4.7.

4.1. Number of Fourier coefficients

The pressure signal during 1 period (one breath from the maximal pressure obtained during the previous inspiration up to the next inspiration) was expanded into cosines and sines up to the Nth component. The number of components needed for the stabilization of the parameters was determined for one phase diagram of every segment for three subjects. The results of the analysis are shown for one phase diagram of one subject. Figure 11 displays the used phase diagram using the raw data. Stabilization of the parameters seem to occur around 25 Fourier components, see figures 12 to 14. However, stabilization of the parameters of other phase diagrams that were investigated, occurred around 50 components. Therefore, the parameters of subject 2, 3, and 4 were computed for both 25 and 50 Fourier components. These are shown for the triangularity in figures 15 and 16, as this parameters showed more difference between 25 and 50 Fourier components compared to Aex_1 and sphericity. The parameter values differed minimally for 50 compared to 25 Fourier components. This implicates that there is no additional information in the extra 25 Fourier components with regard to the determined parameters. Therefore, for further analysis 25 Fourier components will be used.

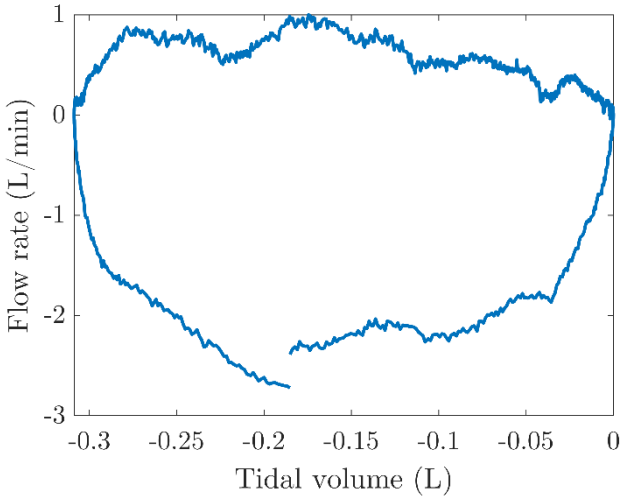

Figure 11: Phase diagram of subject 2 of the segment between bronchodilator administration and lung function measurements.

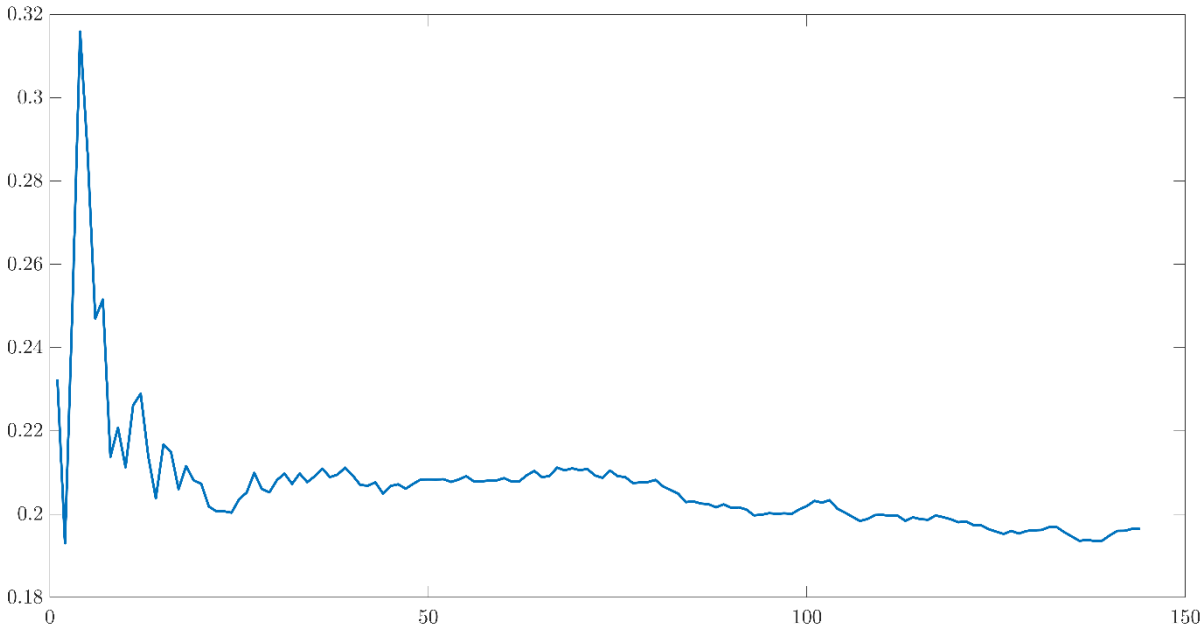

Figure 12: Aex1 of the phase diagram with the number of Fourier components on the x-axis.

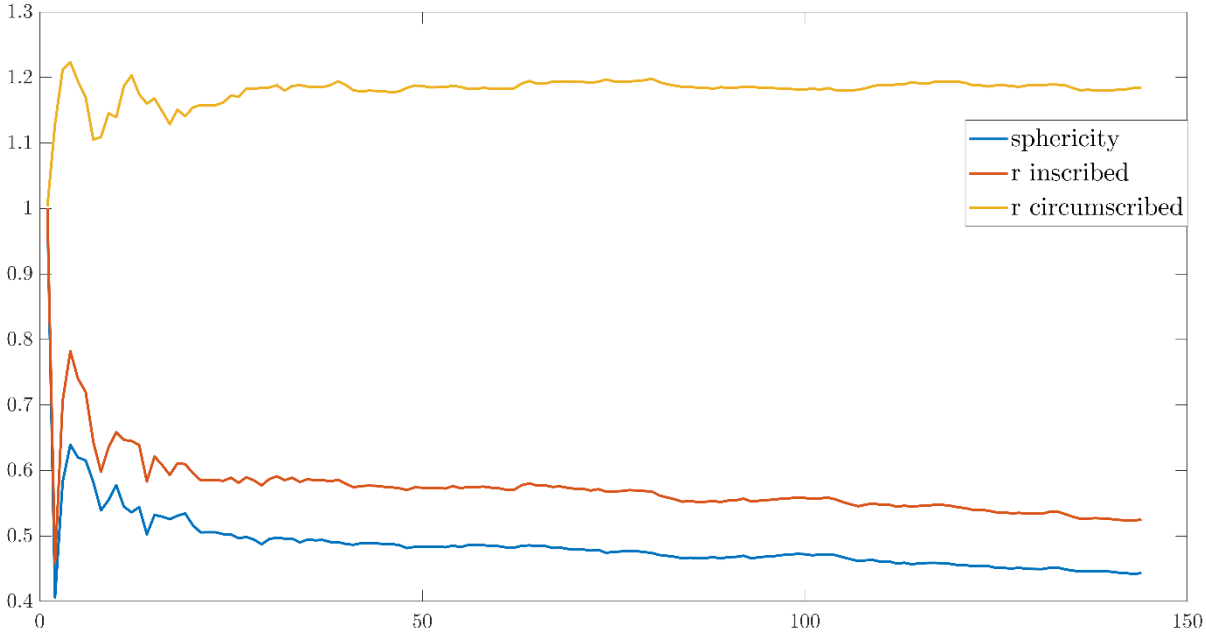

Figure 13: The sphericity (in blue) of the phase diagram with the number of Fourier components on the x-axis. The radius of the inscribed circle and circumscribed circle are observable in respectively the orange and yellow curves.

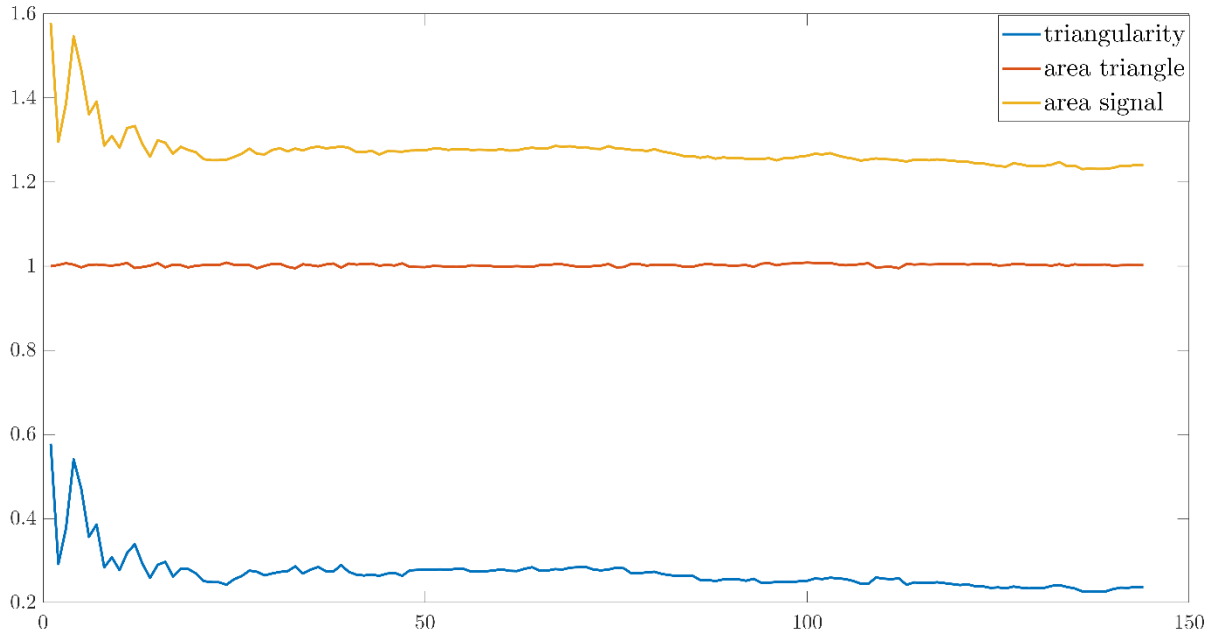

Figure 14: The triangularity (in blue) of the phase diagram with the number of Fourier components on the x-axis. The area of the triangle and area of the signal are observable in respectively the orange and yellow curves.

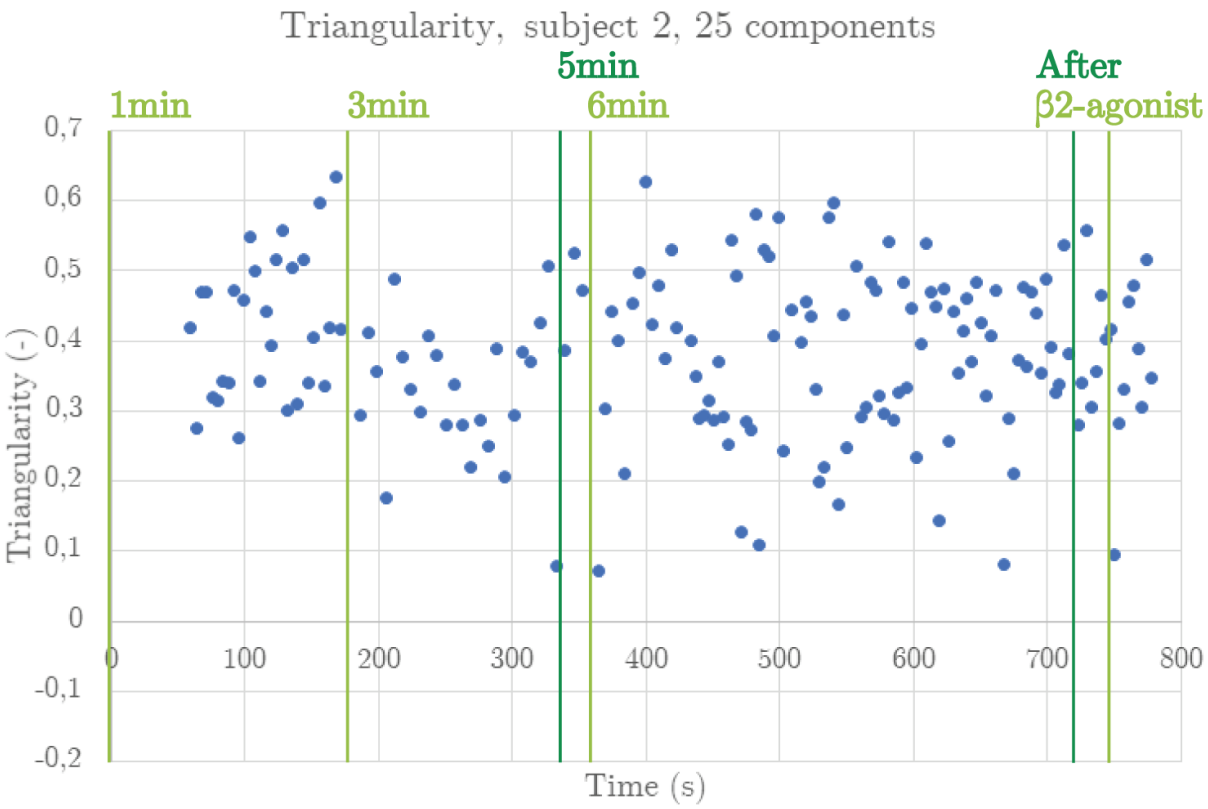

Figure 15: Triangularity of subject 2 with 25 Fourier components. Subject 2 is a 7 years old male with a 14% lung function decline at 3 minutes after exercise.

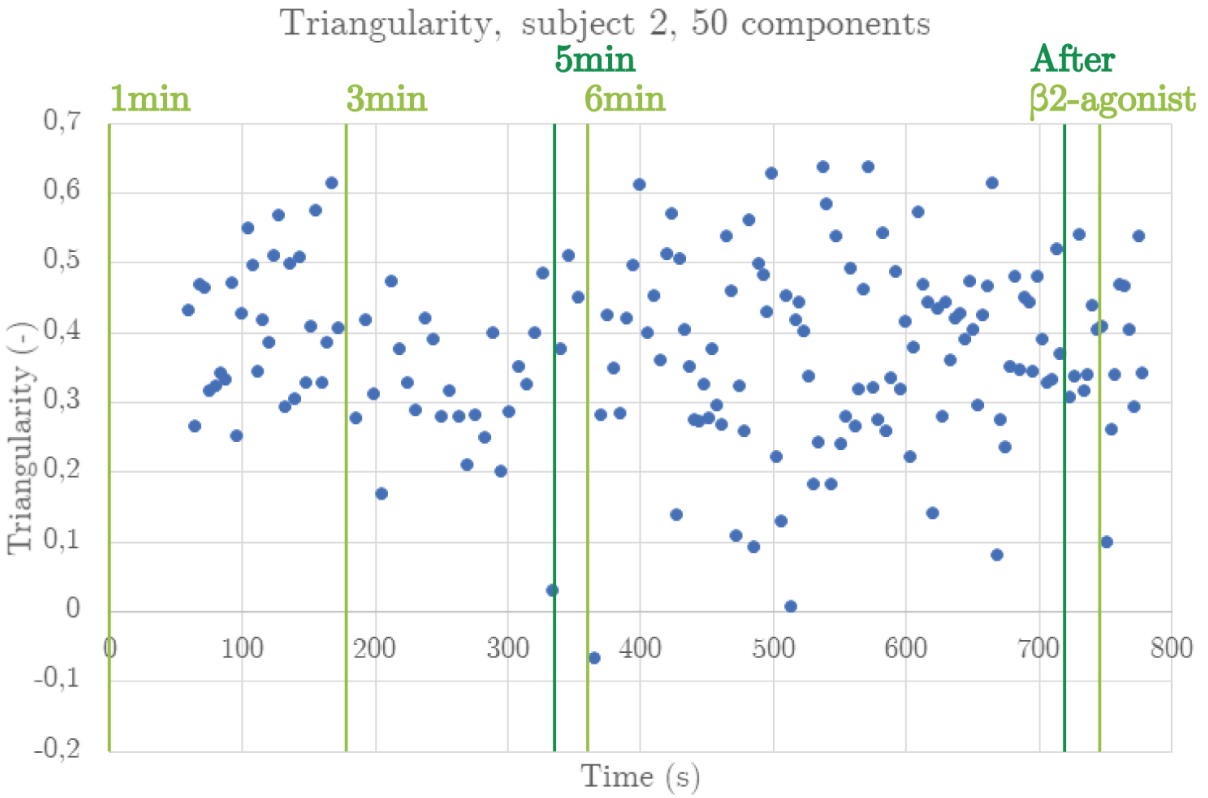

Figure 16: Triangularity of subject 2 with 50 Fourier components. Subject 2 is a 7 years old male with a 14% lung function decline at 3 minutes after exercise.

4.2. Scaling of Fourier vector

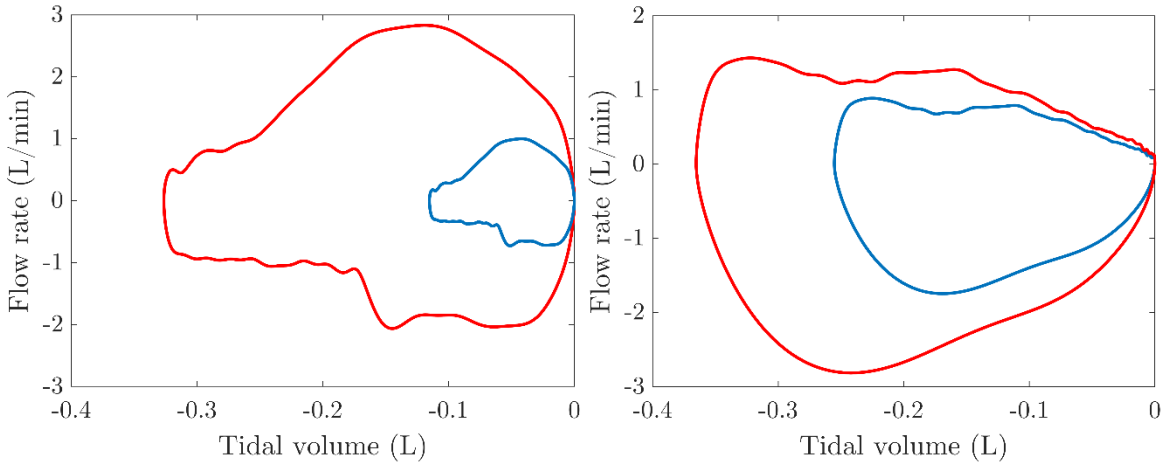

Figure 17: Scaled Fourier vector in blue and unscaled Fourier vector in red.

In figure 17, the influence of scaling the Fourier vector is shown for two phase diagrams. The phase diagrams were aligned to 0,0 which corresponds to the end of expiration, with expiration being positive. Observing figure 17, the appearance of the phase diagram seems similar for the scaled and unscaled Fourier vector. Scaling the Fourier vector results in a proportionally decrease of the total phase diagram. As scaling has no influence on the appearance of phase diagram and the parameters Aex_1, sphericity, and triangularity only dependent on the appearance of the phase diagram, these parameters are not influenced by scaling.

4.3. Influence mean Fourier vector on dot product

It was hypothesized that the phase diagrams close to the final spirometry measurement correspond to normal tidal breathing flow volumes curves as the lung function is nearly maximal at this point due to administration of a bronchodilator. As it is unknown how many phase diagrams should be taken into consideration for the mean Fourier vector, the influence of including additional phase diagrams was investigated. First, all phase diagrams after the final lung function measurement were used to calculate the mean Fourier vector and the dot product between all individual phase diagrams and this mean Fourier vector were determined. Both the dot product values and the lung function values were plotted and a linear and quadratic equation with their norm of residuals were determined. Thereafter, all phase diagrams 15, 30, 45 and 60 seconds prior to the final lung function measurement were taken into consideration for the mean Fourier vector. Subsequently, if the norm of residuals of the equation was still declining, 15 additional seconds concerned for the mean were used up to the moment of increasing norm of residuals.

Figures 18 and 19 show the values of the dot product between the individual phase diagrams and the mean resulting in the minimal norm of residuals for subject 7 and 21. The results of these subjects is shown as subject 7 experienced a lung function change of 28.5% during the total measurement compared to a lung function change of 5.5% of subject 21. Noticeable is the difference in distribution of values between subject 7 and 21. The coherence differs per subject and is higher for subject 21 than 7 which also result in a lower norm of residuals of respectively 1.36 and 2.17 concerning the quadratic functions. There is no consistency observed in the relation between the FEV_1 and the course of dot products during the total measurement for all subjects, as both the same and contradictory trends between FEV_1 and the dot products have been observed.

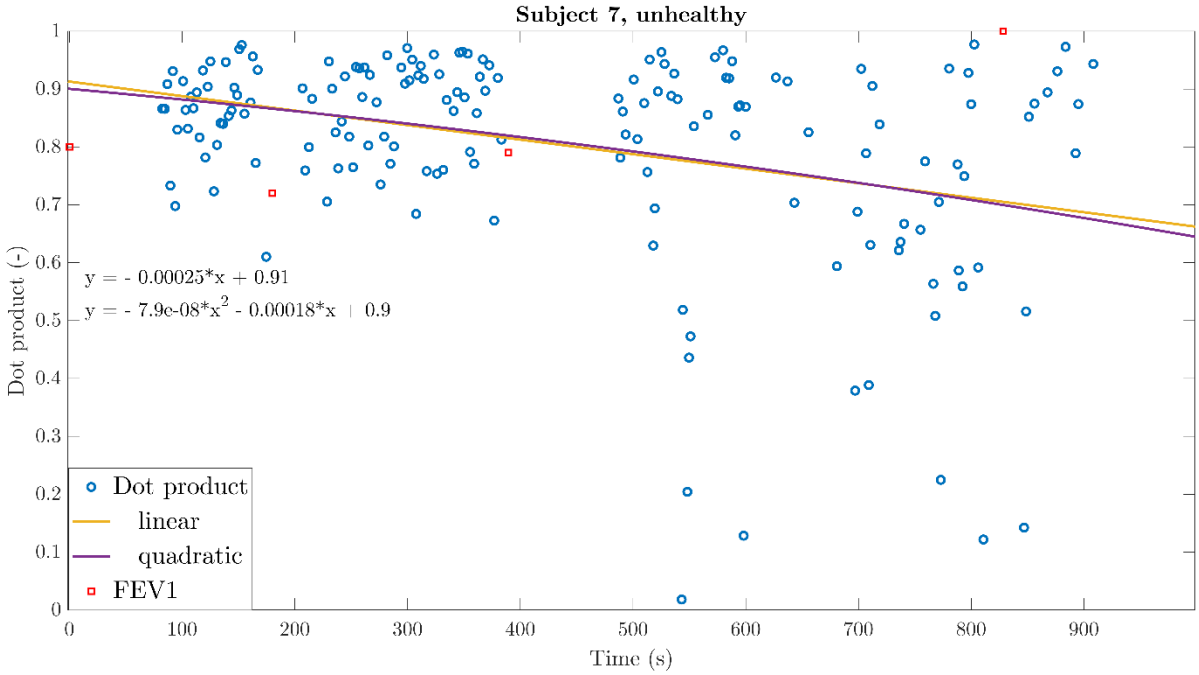

Figure 18: Dot product of the 8.5 years old male subject 7, using up to 75 seconds prior to the final lung function measurement for the mean Fourier vector. Subject 7 had a minimal lung function 3 minutes after exercise which was 28% lower compared to the lung function at the end of the test.

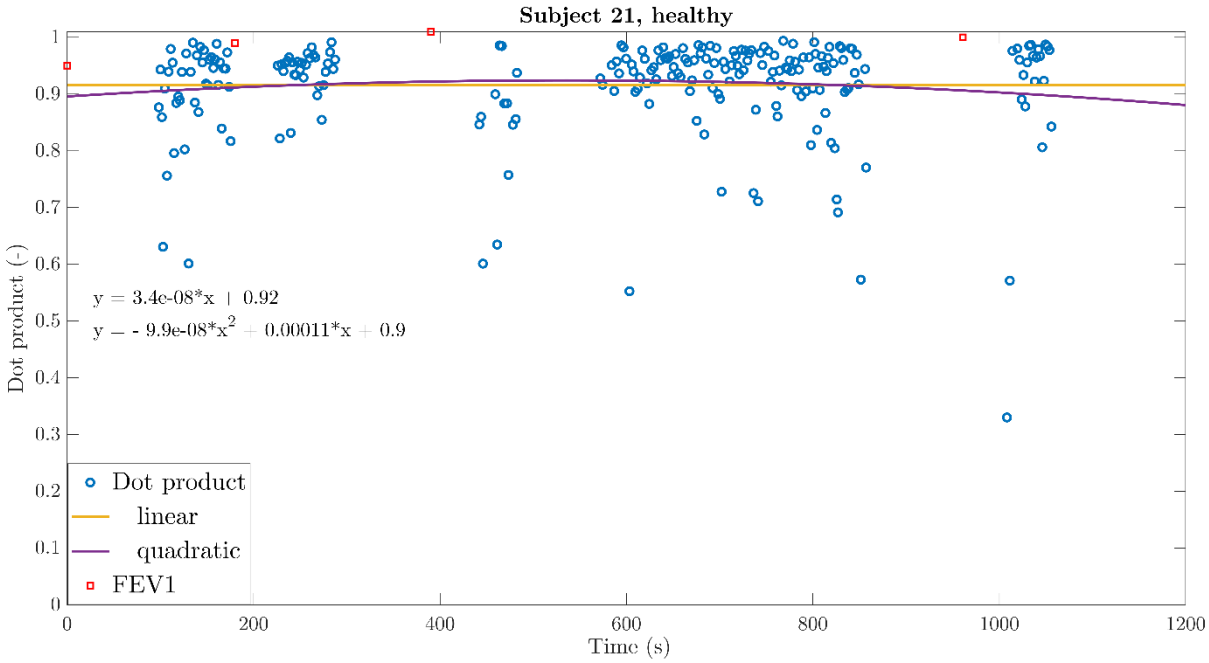

Figure 19: Dot product of the 9.5 years old female subject 21, using up to 60 seconds prior to the final lung function measurement for the mean Fourier vector. Subject 21 had a minimal lung function 1 minutes after exercise which was 5% lower compared to the lung function at the end of the test.

In general, the norm of residuals of the quadratic equation approaching the dot product values was lower compared to the norm of residuals of the linear equation. Besides, using more Fourier vector close to the final spirometry measurement results in a lower norm of residuals and therefore a better approximation of the trend of the dot products during the total measurement of a subject. Nevertheless, every subject has an optimal number of phase diagrams resulting in a minimal norm of residuals. This optimal number was determined using interval of 15 seconds and therefore there is an opportunity to lower the norm of residuals by adding more phase diagrams one by one instead of 15 second intervals. However, this also depends on the coherence of the included phase diagrams for the calculation of the mean Fourier vector. In general, the norm of residuals decreases by including phase diagrams for the mean Fourier vector of which the dot product value is within the range of the already included phase diagrams. So, in order to reduce the norm of residuals the appearance of the phase diagrams must be comparable to previously included phase diagrams. Subsequently, the norm of residuals was, in general, higher if the dot product values during the total pressure measurements were more dispersed. This could be explained as the norm of residuals is an indication of the agreement between the values and the equation. So, if the values are more in line with the equation, the norm of residuals is lower and therefore more dispersed values negatively affect the norm of residuals.

Table 2 gives an overview of the phase diagram used to calculate mean Fourier vector, the corresponding time interval, and the linear and quadratic functions with their norm of residuals. Regarding subject 12, calculation of the mean Fourier vector using all phase diagrams, compared to only those after the final spirometry, results in a lower norm of residuals. Subject 12 had only 37 representative phase diagrams with just 4 phase diagrams after administration of a β_2-agonist. The norm of residuals of the other subjects was minimal by using up to 120 seconds before the final spirometry for the mean Fourier vector with up to 60 seconds for most subjects. As administration of a β_2-agonist results in an increased airflow within 3 to 5 minutes after administration, it is presumed that the appearance of phase diagrams more than 2 minutes before the final should not be taken into consideration for the mean Fourier vector [60].

Table 2: Overview of function with the minimal norm of residuals per subject and the corresponding phase diagrams used for the mean.

Subject	Phase diagrams	Time	Linear	Norm of residuals	Quadratic	Norm of residuals
2	162-171	From spiro	$y=9.90e^{-6}x + 0.85$	1.486	$y=7.82e^{-7}x^2 - 0.00071x + 0.98$	1.407
3	116-136	60 sec before spiro	$y=-9.88e^{-5}x + 0.68$	2.507	$y=5.60e^{-7}x^2 - 0.00062x + 0.80$	2.464
5	92-135	60 sec before FOT	$y=-3.51e^{-5}x + 0.84$	1.410	$y=5.24e^{-7}x^2 - 0.00059x + 0.94$	1.354
6	188-219	60 sec before spiro	$y=9.86e^{-5}x + 0.80$	1.878	$y=-1.23e^{-7}x^2 - 0.00024x + 0.77$	1.873
7	139-167	75 sec before spiro	$y=-0.00025x + 0.91$	2.174	$y=-7.95e^{-7}x^2 - 0.00018x + 0.90$	2.170
10	126-148	90 sec before spiro	$y=0.00019x + 0.81$	1.146	$y=-1.37e^{-7}x^2 + 0.00033x + 0.78$	1.142
12	1-37	Total dataset	$y=-1.10e^{-5}x + 0.83$	0.696	$y=6.03e^{-7}x^2 - 0.00072x + 0.96$	0.653
13	103-116	45 sec before spiro	$y=-0.00013x + 0.87$	1.428	$y=2.72e^{-7}x^2 - 0.00038x + 0.92$	1.424
14	84-126	75 sec before spiro	$y=-8.12e^{-5}x + 0.91$	1.258	$y=-2.17e^{-7}x^2 + 0.00015x + 0.87$	1.251
15	50-59	45 sec before spiro	$y=0.00014x + 0.60$	1.504	$y=-6.31e^{-8}x^2 + 0.00020x + 0.59$	1.503
16	73-79	60 sec before spiro	$y=0.00010x + 0.72$	1.506	$y=5.82e^{-7}x^2 - 0.00044x + 0.81$	1.493
17	92-139	120 sec before spiro	$y=6.87e^{-5}x + 0.73$	2.168	$y=-9.18e^{-7}x^2 + 0.00017x + 0.71$	2.167
18	90-130	30 sec before spiro	$y=-9.31e^{-5}x + 0.84$	1.876	$y=5.67e^{-7}x^2 - 0.00076x + 0.98$	1.808
19	97-104	From spiro	$y=-1.58e^{-5}x + 0.61$	1.663	$y=-4.43e^{-7}x^2 + 0.00043x + 0.53$	1.618
21	179-232	60 sec before spiro	$y=-3.42e^{-8}x + 0.92$	1.366	$y=-9.87e^{-7}x^2 + 0.00011x + 0.90$	1.362
22	207-237	From spiro	$y=9.66e^{-5}x + 0.84$	1.591	$y=-2.66e^{-7}x^2 + 0.00030x + 0.78$	1.567
24	143-171	30 sec before spiro	$y=3.81e^{-5}x + 0.78$	2.653	$y=3.85e^{-7}x^2 - 0.00040x + 0.86$	2.622
25	90-110	45 sec before spiro	$y=-7.64e^{-5}x + 0.84$	1.511	$y=-1.11e^{-7}x^2 + 4.03e^{-5}x + 0.82$	1.510

4.4. Parameter calculation

For the calculation of the sphericity, triangularity and the Aex_1 the equations (7), (8), and (11) were used. These parameters were calculated for every single phase diagram and investigated whether the trend in the values of the parameters was comparable to the FEV_1 and therefore related to lung function changes. The linear and quadratic functions with norm of residuals were determined per parameter per subject. Most quadratic function were parabolic with either a minimum or maximum. Unfortunately, no link between the parabolic appearances of the parameters was observed between the parameter values per subjects. In addition, the lung function change showed no association with the parabola having a minimum of maximum. All parameters of subject 14 showed linearly related values during the total pressure measurement. The linear and quadratic functions with norm of residuals can be observed in tables 3 to 5. As subject 12 only has 37 representative phase diagrams, the subject with the lowest norm of residuals hereafter is subject 16. Figures 20 to 22 display the parameter values of subject 16 during the total measurement.

Table 3: Linear and quadratic functions of Aex_1 per subject.

Subject	Linear	Norm of residuals	Quadratic	Norm of residuals
2	$y=0.23x + 2.1e^2$	7527.7	$y=-0.0032x^2 + 3.2x - 3.1e^2$	7270.3
5	$y=2.4x - 2.5e^2$	57897	$y=0.11x^2 - 9.2x + 1.7e^3$	57298
6	$y=0.62x - 20$	19917	$y=0.003x^2-2.8x+7.2e^2$	19611
7	$y=25x + 1.1e^3$	$1.5409e^6$	$y=-0.23x^2 + 2.4e^2x - 3.6e^4$	$1.5332e^6$
10	$y=-0.067x + 2.4e^2$	1390.1	$y=8.2e^{-5}x^2 - 0.15x + 2.6e^2$	1389.1
12	$y=-0.021x + 3.1e^2$	2552.2	$y=-0.00096x^2 + 1.1x + 99$	2523
13	$y=0.94x + 1.1e^2$	9396.2	$y=0.002x^2 - 0.9x + 4.2e^2$	9357.4
14	$y=0.3x + 0.85$	4191.6	$y=4.2e^{-6}x^2 + 0.3x + 86$	4191.6
15	$y=4.5x + 85$	80782	$y=0.012x^2 - 6.4x + 2e^3$	80681
16	$y=0.079x + 2.9e^2$	1642.9	$y=-0.00013x^2 + 0.2x +2.7e^2$	1642.3
17	$y=0.19x + 2.2e^2$	2412.1	$y=-0.00047x^2 + 0.69x+1.2e^2$	2390.4
18	$y=3e^{11}x - 3.1e^{14}$	$5.0868e^{16}$	$y=1.3e^9x^2 - 1.3e^{12}x + 1.4e^{13}$	$5.0854e^{16}$
19	$y=0.43x + 2.5e^2$	7855.4	$y=0.0041x^2 -3.7x + 9.5e^2$	7004.5
21	$y=-0.029x + 1.5e^2$	2650.9	$y=0.00033x^2 - 0.38x + 2.1e^2$	2625.4
22	$y=0.1x+ 1.5e^2$	2716.1	$y=0.00018x^2 - 0.096x+1.9e^2$	2709.7
24	$y=0.011x + 2.7e^2$	5433.1	$y=-0.00046x^2 + 0.53x+1.7e^2$	5411.7

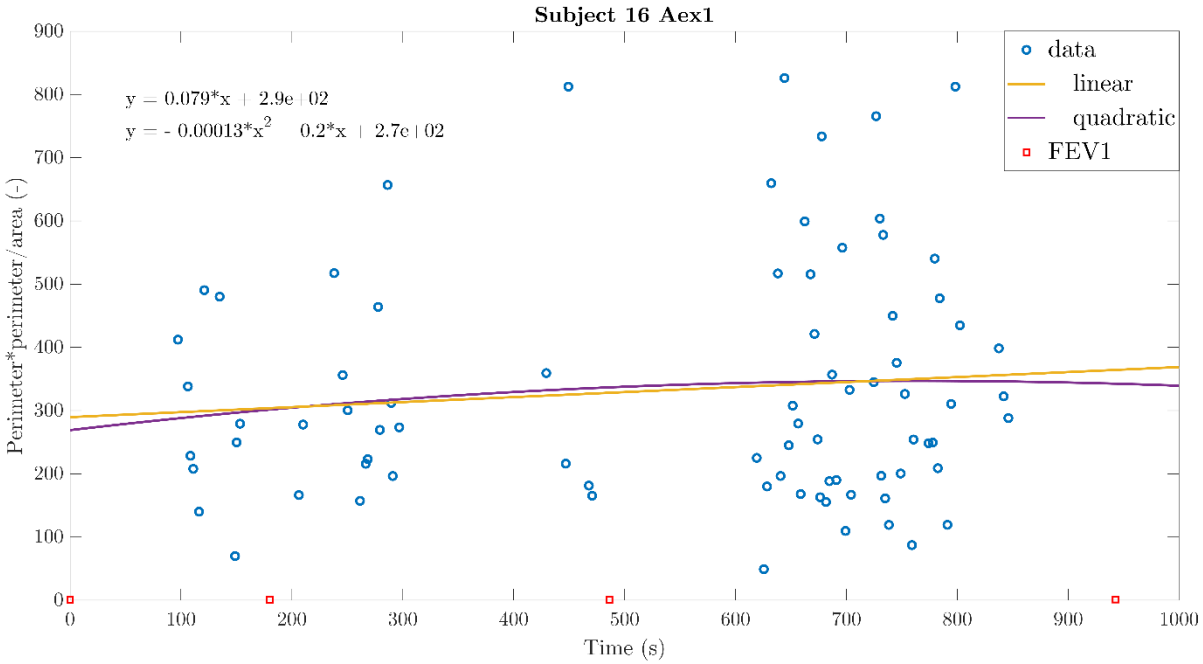

Figure 20: Aex_1 of the 13.5 years old male subject 16 who experienced a minimal lung function at 3 and 6 minutes after exercise which was 11% lowered compared to his maximal lung function during the ECT.

During the determination of the Aex_1 values of the 18 subjects, several subjects displayed a few values which can be interpreted as outliers. Investigation of the phase diagrams of these considered outliers indicated that these phase diagrams displayed artefacts or unrepresentative breaths instead of breaths. In 4.7 different methods for removal of these unrepresentative phase diagrams are proposed.

Table 4: Linear and quadratic functions of sphericity per subject.

Subject	Linear	Norm of residuals	Quadratic	Norm of residuals
2	$y=-8.2e^{-6}x + 0.57$	1.7082	$y=3.7e^{-7}x^2 - 0.00035x + 0.63$	1.6928
3	$y=-2.2e^{-5}x + 0.58$	1.9927	$y=1.5e^{-7}x^2 - 0.00019x + 0.62$	1.9888
5	$y=7.1e^{-5}x + 0.5$	1.743	$y=-2.6e^{-7}x^2 + 0.00035x + 0.45$	1.7318
6	$y=-5.4e^{-5}x + 0.63$	2.1022	$y=-3.7e^{-7}x^2 + 0.00037x + 0.54$	2.0575
7	$y=-0.00016x + 0.66$	1.9233	$y=-3.5^{-7}x^2 + 0.00017x + 0.61$	1.9093
10	$y=0.00021x + 0.4$	0.9978	$y=-1.3e^{-8}x^2 + 0.00022x + 0.4$	0.9978
12	$y=-0.00011x + 0.65$	0.7054	$y=-2.7e^{-7}x^2 + 0.0002x + 0.59$	0.6973
13	$y=-0.00013x + 0.61$	1.5987	$y=2.9e^{-7}x^2 - 0.0004x + 0.66$	1.5937
14	$y=-1.3e^{-5}x + 0.66$	1.4063	$y=-8.2e^{-9}x^2 - 4.9e^{-6}x + 0.66$	1.4063
15	$y=-3.5e^{-5}x + 0.53$	1.1897	$y=-3.2e^{-7}x^2 + 0.00027x + 0.48$	1.1844
16	$y=-1.3e^{-5}x + 0.58$	1.2071	$y=4e^{-7}x^2 - 0.00039x + 0.64$	1.1999
17	$y=-2.5e^{-5}x + 0.53$	1.8158	$y=3e^{-7}x^2 - 0.00035x + 0.6$	1.8038
18	$y=-9.3e^{5}x + 0.62$	2.1286	$y=3.9e^{-7}x^2 - 0.00056x + 0.72$	2.1001
19	$y=-3.4e^{-5}x + 0.57$	1.9229	$y=-8.2e^{7}x^2 + 0.00079x + 0.43$	1.7831
21	$y=9.9e^{-5}x + 0.62$	1.3693	$y=-2.4e^{-7}x^2 + 0.00036x + 0.57$	1.3407
22	$y=-6.5e^{-5}x + 0.57$	2.2536	$y=-3.1e^{-7}x^2 + 0.00027x + 0.5$	2.2314
24	$y=3.8e^{-5}x + 0.62$	1.5045	$y=1.1e^{-7}x^2 - 9e^{-5}x + 0.65$	1.4998
25	$y=1.8e^{-5}x + 0.53$	1.6644	$y=-6.2e^{-9}x^2 + 2.5e^{-5}x + 0.53$	1.6644

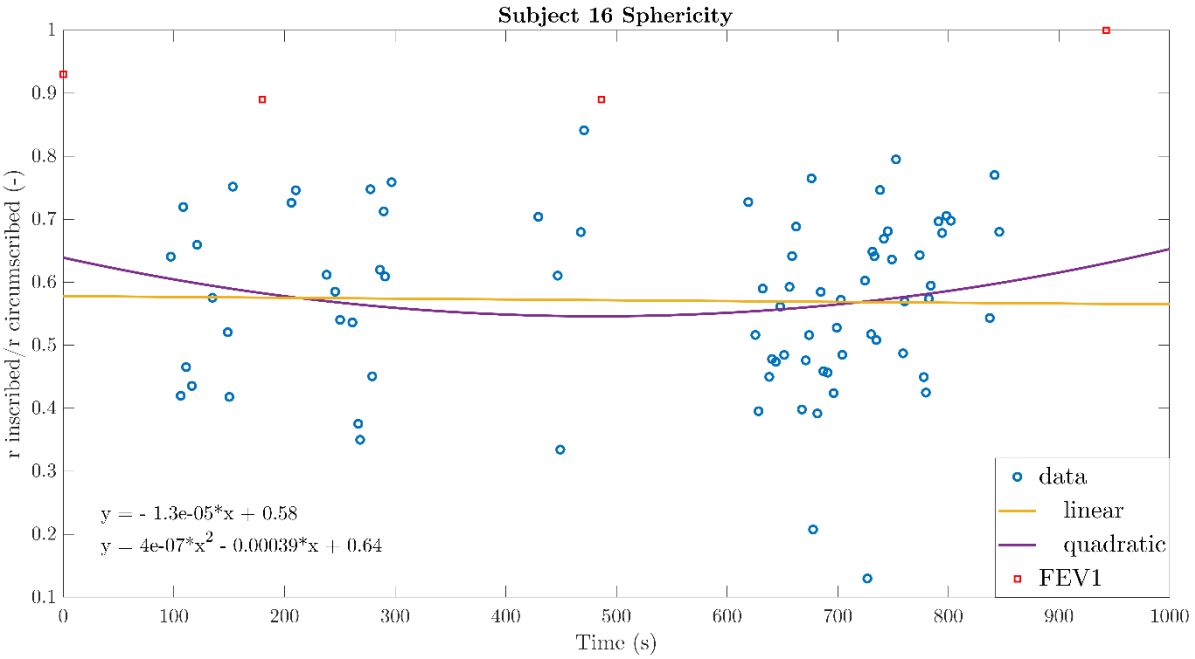

Figure 21: Sphericity of the 13.5 years old male subject 16 who experienced a minimal lung function at 3 and 6 minutes after exercise which was 11% lowered compared to his maximal lung function during the ECT.

Table 5: Linear and quadratic functions of triangularity per subject.

Subject	Linear	Norm of residuals	Quadratic	Norm of residuals
2	$y=-2.15e^{-5}x + 0.37$	1.5712	$y=3e^{-7}x^2 - 0.0003x + 0.42$	1.5604
3	$y=-5.4e^{-5}x + 0.43$	1.3937	$y=-1.3e^{-7}x^2 + 9.2e^{-5}x + 0.4$	1.3906
5	$y=4.5e^{-5}x + 0.27$	1.7449	$y=6.2e^{-8} - 2e^{-5}x + 0.29$	1.7443
6	$y=-0.00011x + 0.46$	1.7887	$y=-3e^{-7}x^2 + 0.00024x + 0.38$	1.7544
7	$y=-0.00014x + 0.45$	1.7711	$y=-6.1e^{-8}x^2 - 8.3e^{-5}x + 0.44$	1.7715
10	$y=0.00022x + 0.15$	1.3951	$y=1e^{-7}x^2 + 0.00012x + 0.17$	1.3937
12	$y=-8.9e^{-5}x + 0.4$	0.7551	$y=-2.1^{-8}x^2 -6.5e^{-5}x + 0.39$	0.7550
13	$y=-0.0001x + 0.36$	1.4882	$y=-3.9e^{-7}x^2 + 0.00025x + 0.3$	1.4789
14	$y=-8.9e^{-5}x + 0.43$	1.5583	$y=3.8e^{-9}x^2 - 9.3e^{-5}x + 0.43$	1.5583
16	$y=-6.1e^{-5}x + 0.37$	1.0799	$y=2.5e^{-7}x^2 - 0.0003x + 0.41$	1.0767
17	$y=2.9e^{-5}x + 0.29$	1.8411	$y=8e^{-7}x^2 - 0.00082x + 0.46$	1.7565
18	$y=-6.5e^{-5}x + 0.36$	1.8997	$y=2.2e^{-7}x^2 - 0.00033x + 0.41$	1.8894
19	$y=-9.7e^{-5}x + 0.37$	1.5511	$y=-5.9e^{-7}x^2 + 0.00049x + 0.27$	1.4631
21	$y=0.00015x + 0.41$	1.8236	$y=-4.2e^{-7}x^2 + 0.0006x + 0.32$	1.7615
22	$y=-0.00015x + 0.42$	2.2111	$y=-8.8e^{-8}x^2 - 5.2e^{-5}x + 0.4$	2.2093
24	$y=7.6e^{-5}x + 0.43$	2.0929	$y=6.8e^{-7}x^2 - 0.0007x + 0.58$	1.9675
25	$y=-7.2e^{-5}x + 0.39$	1.7259	$y=8.9e^{-8}x^2 - 0.00017x + 0.4$	1.725

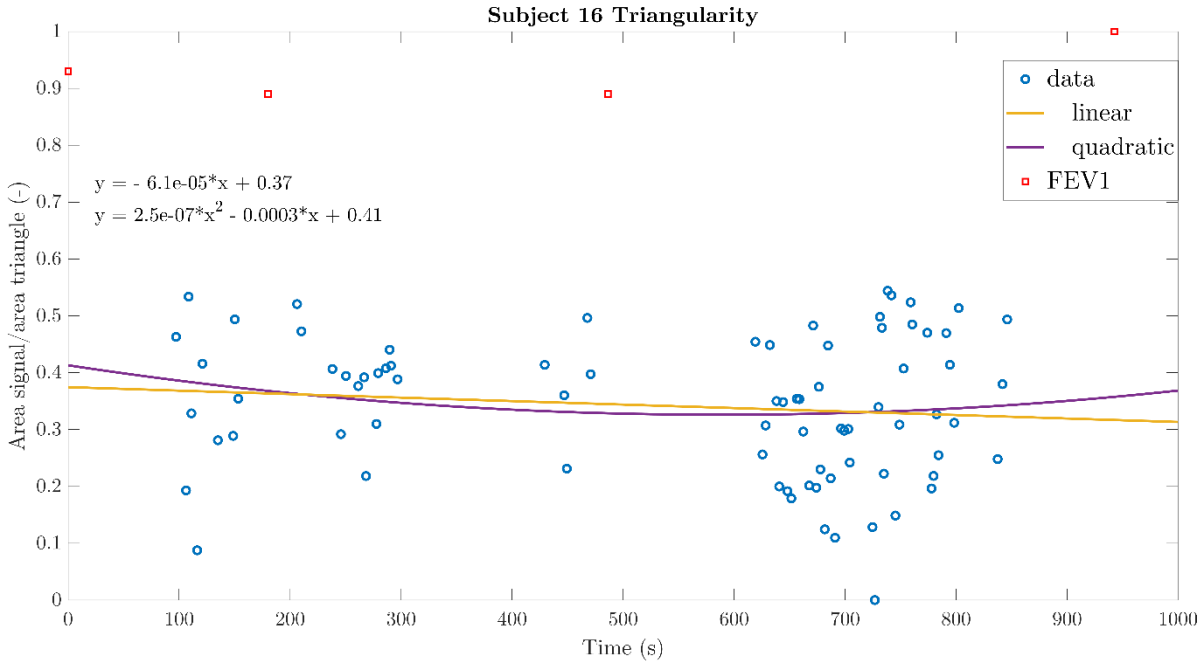

Figure 22: Triangularity of the 13.5 years old male subject 16 who experienced a minimal lung function at 3 and 6 minutes after exercise which was 11% lowered compared to his maximal lung function during the ECT.

4.5. Healthy versus unhealthy

The phase diagrams of subject 21 up to 3 minutes after exercise were investigated to select 10 healthy phase diagrams, see Appendix E.1. Subject 21 had a minimal change of 6% of the lung function during the measurement which occurred at 1 minute after exercise. The phase diagrams of subject 7 between 3 and 6 minutes after exercise were investigated to select 10 unhealthy phase diagrams, see Appendix E.2. Subject 7 was examined as his lung function changes 28% during the measurement, with a minimal value at 3 minutes after exercise.

The dot product between two Fourier vectors provides an indication of the coherence. To investigate if there is a difference between healthy and unhealthy phase diagrams, several dot products were calculated. The dot product between healthy phase diagrams and their mean phase diagram was calculated to check whether the appearance of the healthy phase diagrams was similar. The dot product between unhealthy phase diagrams and their mean phase diagram was calculated to check the variation between the unhealthy phase diagrams. Thereafter, the dot product between unhealthy phase diagrams and the mean of the 10 healthy phase diagrams was calculated to investigate if they differ in appearance, see figure 23 for the results.

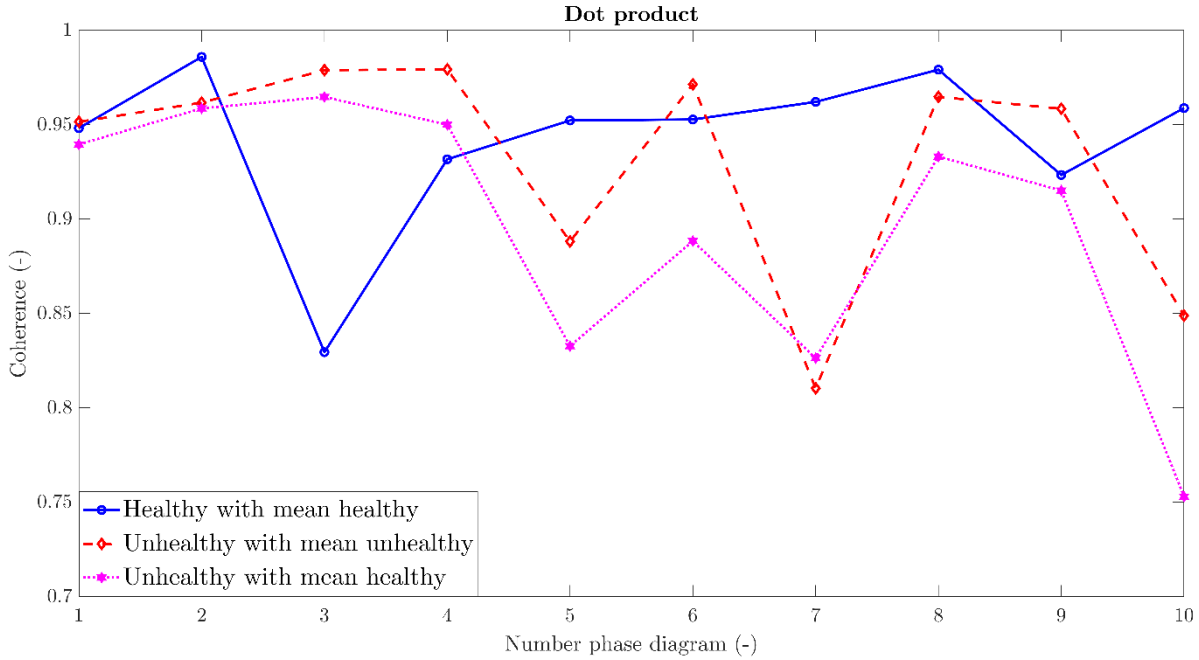

Figure 23: Dot product between a single healthy or unhealthy phase diagram and the mean of 10 selected healthy or unhealthy phase diagrams, see legend. For the 10 selected healthy phase diagrams, subject 21 who is a 9.5 years old experienced a 6% decline at 1 min after exercise. The 10 selected unhealthy phase diagrams were between 3 and 6 minutes after exercise of the 8.5 years old male subject 7 as he experienced a 28% decline at 3 minutes.

The coherence between every healthy phase diagrams and their mean phase diagram is above 0.8, see figure 23. This is comparable to the coherence between unhealthy phase diagrams and their mean phase diagram, observable in figure 24. Regarding figure 25, the range of coherence between the unhealthy phase diagrams and the mean of 10 healthy phase diagrams is unfortunately also above 0.8. This indicates that the dot product between the mean of 10 healthy phase diagrams and a phase diagram is unable to discriminate between a healthy and unhealthy phase diagram. To investigate in more detail if there is a difference between healthy and unhealthy phase diagrams, the Fourier coefficients of both healthy and unhealthy phase diagrams were compared for every single and the mean phase diagrams.

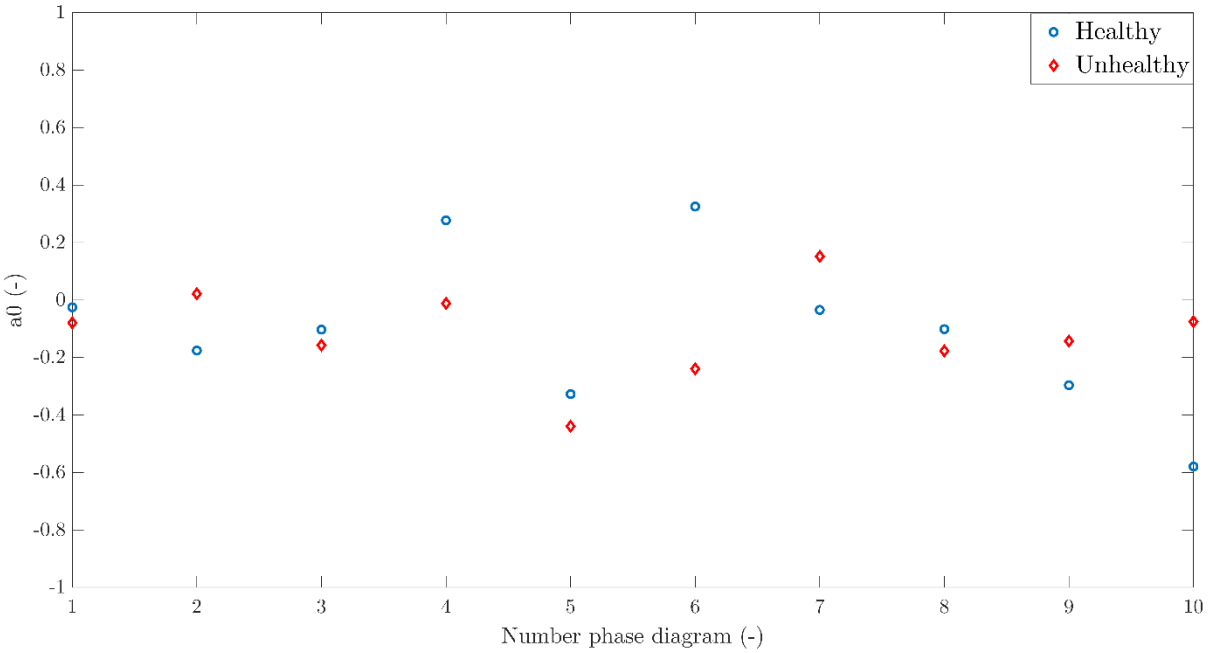

Figure 24: First Fourier coefficient, a0, for the healthy phase diagrams in blue and unhealthy in red. For the 10 selected healthy phase diagrams, subject 21 who is a 9.5 years old experienced a 6% decline at 1 min after exercise. The 10 selected unhealthy phase diagrams were between 3 and 6 minutes after exercise of the 8.5 years old male subject 7 as he experienced a 28% decline at 3 minutes.

In figure 24, the a0 coefficient of the Fourier vector is displayed for both healthy and unhealthy phase diagrams. The range of the healthy and unhealthy a0 values seems comparable and therefore it is assumptive that a0 unsuitable as discriminator between healthy and unhealthy.

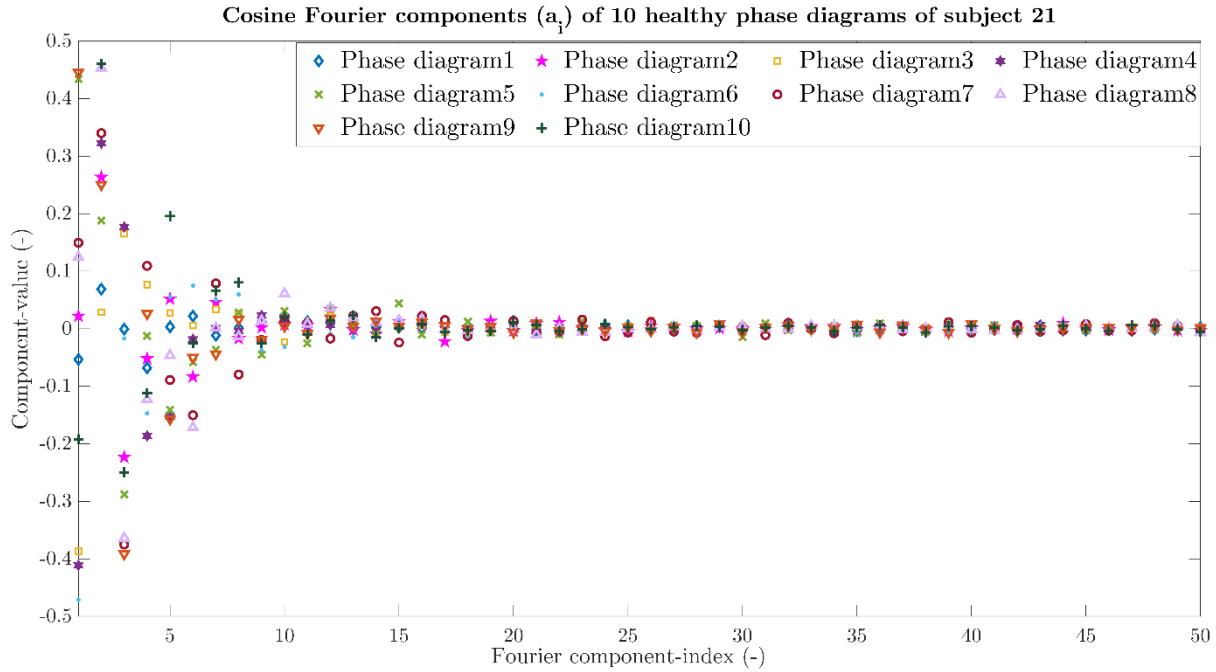

Figure 25: The 50 a's indicating the contribution of the cosine term for the healthy phase diagrams which were selected at the minimal lung function around 1 minute after exercise of subject 2. The number of the Fourier coefficient is indicated on the x-axis and the contribution of the cosine term on the y-axis. Each colour represents one healthy phase diagram.

Figure 25 indicates the contribution of each cosine term for each healthy phase diagram. Noticeable is the decline in contribution of the cosine term as more terms were added. This is also observable for the unhealthy phase diagrams and the sines terms. Therefore, the contribution of the healthy and unhealthy phase diagrams of both sine and cosine components is shown up to 10 components in figures 26 to 29.

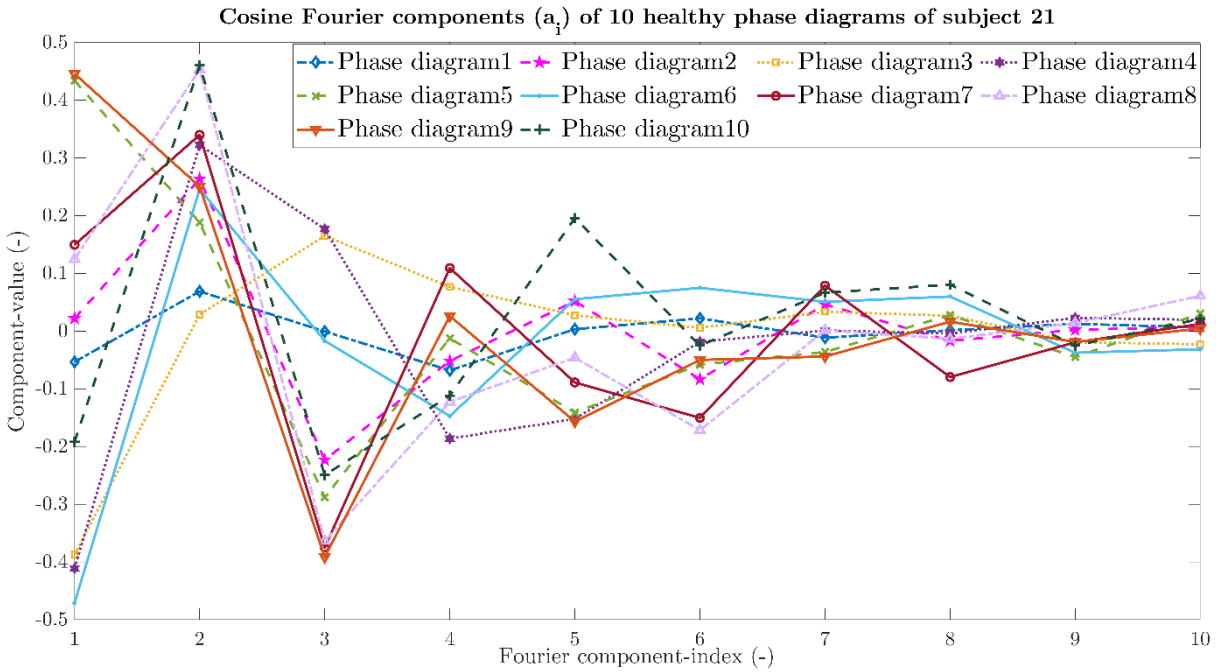

Figure 26: The 10 a's indicating the contribution of the cosine term for the healthy phase diagrams which were selected at the minimal lung function around 1 minute after exercise of subject 21. The number of the Fourier coefficient is indicated on the x-axis and the contribution of the cosine term on the y-axis. Each colour represents one healthy phase diagram.

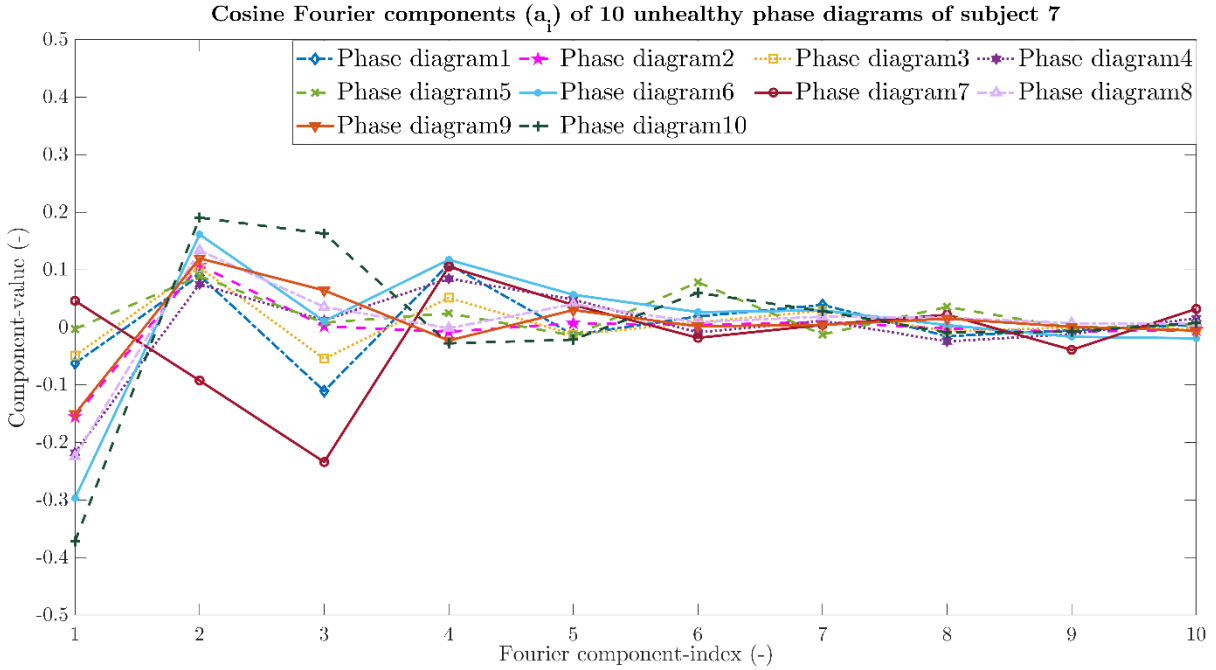

Figure 27: The 10 a's indicating the contribution of the cosine term for the unhealthy phase diagrams which were selected at the minimal lung function around 3 minute after exercise of subject 7. The number of the Fourier coefficient is indicated on the x-axis and the contribution of the sine term on the y-axis. Each colour represents one unhealthy phase diagram.

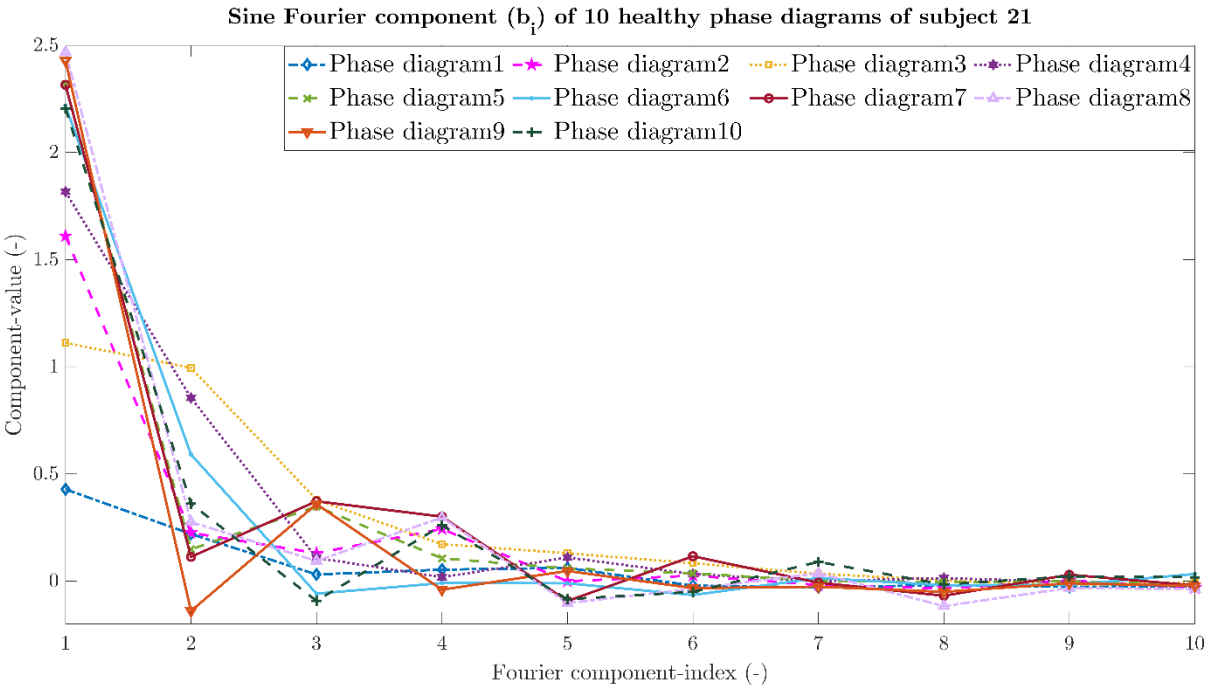

Figure 28: The 10 b's indicating the contribution of the sine term for the healthy phase diagrams which were selected at the minimal lung function around 1 minute after exercise of subject 21. The number of the Fourier coefficient is indicated on the x-axis and the contribution of the sine term on the y-axis. Each colour represents one healthy phase diagram.

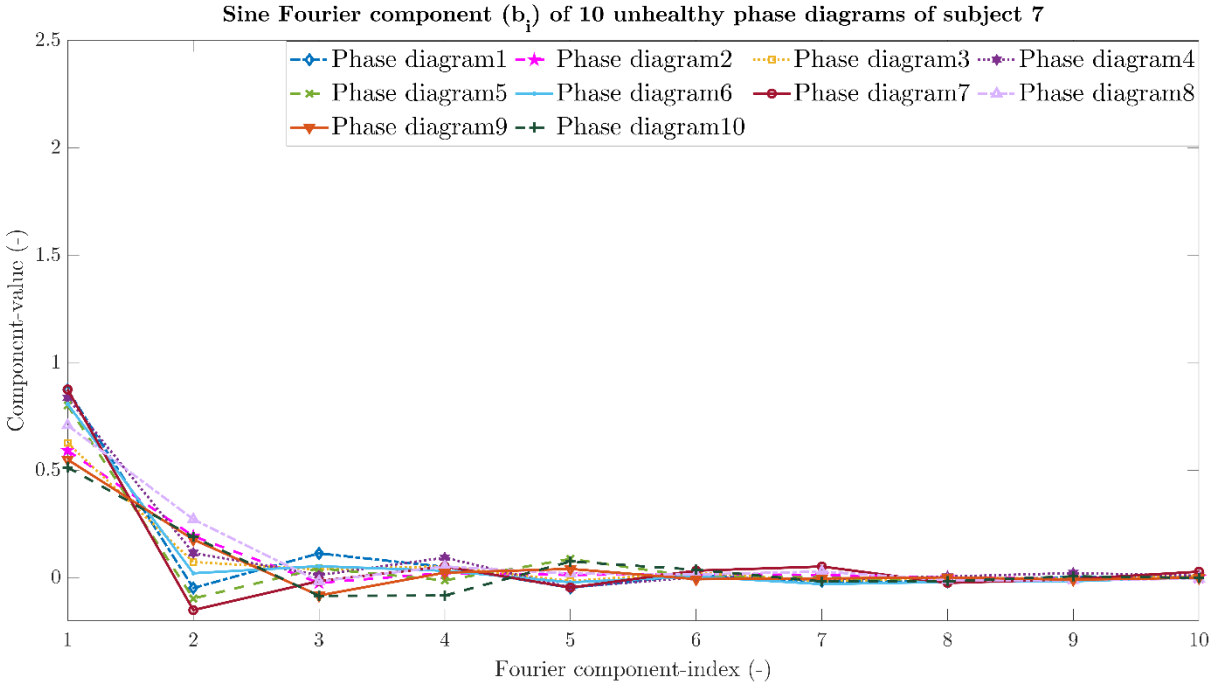

Figure 29: The 10 b's indicating the contribution of the sine term for the unhealthy phase diagrams which were selected at the minimal lung function around 3 minute after exercise of subject 7. The number of the Fourier coefficient is indicated on the x-axis and the contribution of the sine term on the y-axis. Each colour represents one unhealthy phase diagram.

Comparing the value of healthy to unhealthy of figures 26 and 27 regarding the cosines, the range of the first 10 coefficients is wider and higher values were achieved. Subsequently, the contribution of the cosines is, in general, higher for the healthy compared to the unhealthy phase diagrams. Taking into consideration the value of the a's, up to 10 a coefficients might be sufficient in the approach of the raw pressure signal using Fourier analysis.

Figure 28 and 29 indicate the contribution of each sine term for respectively each healthy or unhealthy phase diagram. The decline in contribution of sines started earlier compared to cosines. Comparing the b values of healthy to unhealthy, the range of the first 10 coefficients is wider and higher values were achieved. Subsequently, the contribution of the cosines is, in general, higher for the healthy compared to the unhealthy phase diagrams. Taking into consideration the value of the b's, up to 5 or 10 b coefficients might be sufficient in the approach of the raw pressure signal using Fourier analysis.

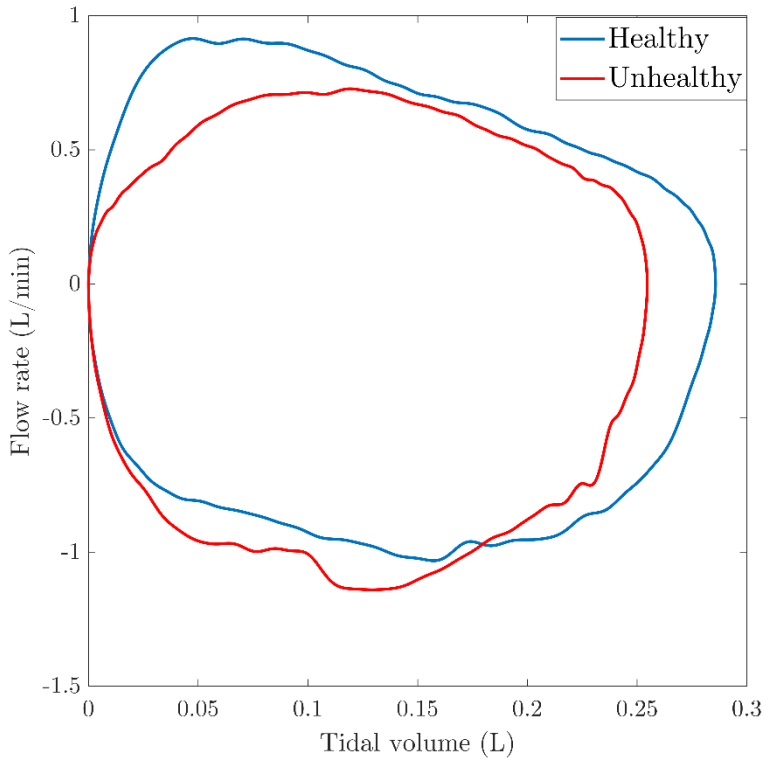

Figure 30: The phase diagram as result of the mean Fourier vector of the healthy phase diagrams in blue and unhealthy in red. For the 10 selected healthy phase diagrams, subject 21 who is a 9.5 years old female experienced a 6% decline at 1 min after exercise. The 10 selected unhealthy phase diagrams were between 3 and 6 minutes after exercise of the 8.5 years old male subject 7 as he experienced a 28% decline at 3 minutes.

In figure 30, the result of calculating the mean Fourier vector separately for the healthy and unhealthy phase diagrams is observable, the breath is aligned to 0,0 with expiration being positive. Appendices E, shows the phase diagrams that were taken into consideration. Comparing the mean phase diagrams, the derived volume during an expiration is higher in the healthy phase diagram. A lower volume during a breath, implicates the need for a higher respiratory rate. Subsequently, a higher derived flow earlier during the expiration is obtained during a healthy phase diagram.

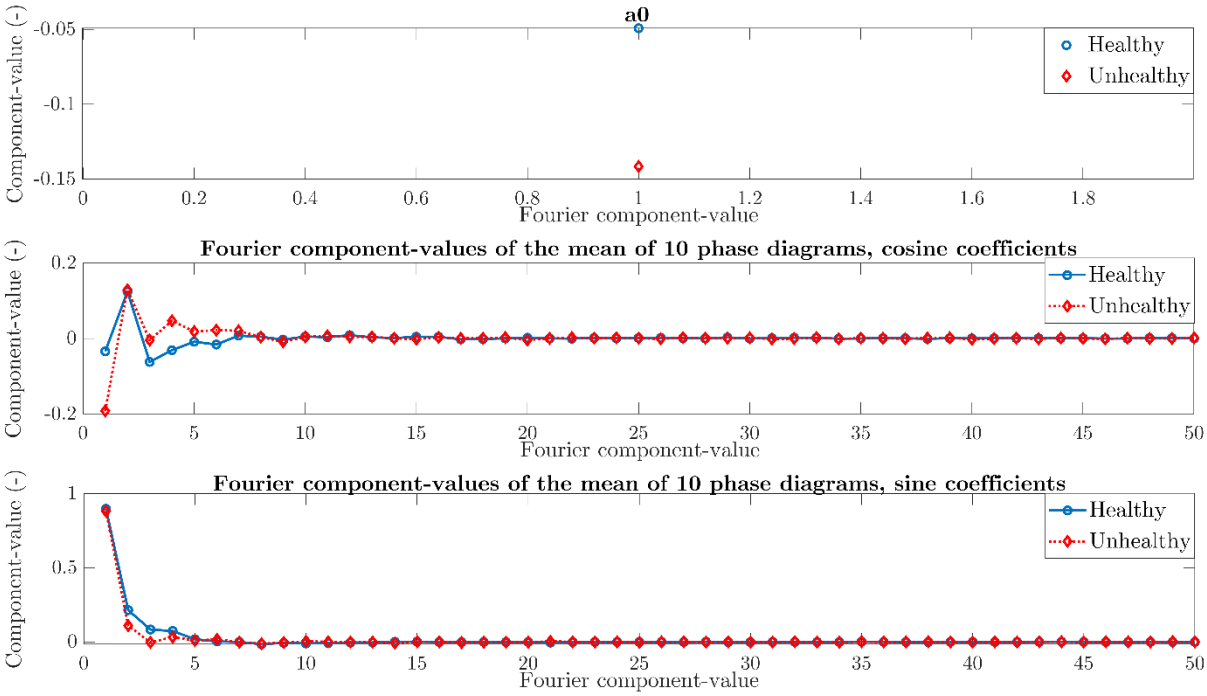

Figure 31: Fourier coefficients of the mean 10 healthy phase diagrams in blue and unhealthy in red. For the 10 selected healthy phase diagrams, subject 21 who is a 9.5 years old female experienced a 6% decline at 1 min after exercise. The 10 selected unhealthy phase diagrams were between 3 and 6 minutes after exercise of the 8.5 years old male subject 7 as he experienced a 28% decline at 3 minutes.

Figure 31 displays the coefficients for the mean healthy and unhealthy phase diagram. There is a difference of 0.1 in the contribution of the a0 coefficient between the healthy and unhealthy mean phase diagram. Regarding the a's, there is a difference in contribution of the coefficients between healthy and unhealthy up to the 7^{th} coefficient. Considering the contribution of the b terms, a difference exist up to the 4^{th} coefficient.

As these result indicate a difference in Fourier coefficient up to maximal 10 coefficients and therefore 21 terms, it is interesting to investigate if the dot product is able to discriminate healthy and unhealthy if only 21 instead of 101 terms are taken into consideration. These results will be discussed in 4.5.1. In addition, as the amplitude of the first 5 sinus (b's) and 10 cosines (a's) is high compared to the other coefficients, these coefficients contribute a lot. To investigate whether higher coefficients could discriminate between healthy and unhealthy phase diagrams, 4.5.2 will describe the results of removing up to the first 10 a and b coefficients.

4.5.1. Dot product, 21 terms

In figure 32, the dot products comparable to figure 23 can be observed. The difference between those figures is the number of Fourier coefficients taken into consideration for the calculation of the dot product. It was expected that the difference between healthy and unhealthy would be more pronounced using 21 Fourier terms instead of 51, as the first 21 terms only showed differences between healthy and unhealthy. Comparing figure 32 to 23 indicate no difference in the dot product using 21 or 51 Fourier terms. Concluding, reducing the number of Fourier terms from 51 to 21 has no effect in discriminating healthy from unhealthy phase diagrams. A possible explanation for this result could be an existing difference between healthy and unhealthy for coefficients above 21 but negligible in their contribution compared to the first 20 coefficient.

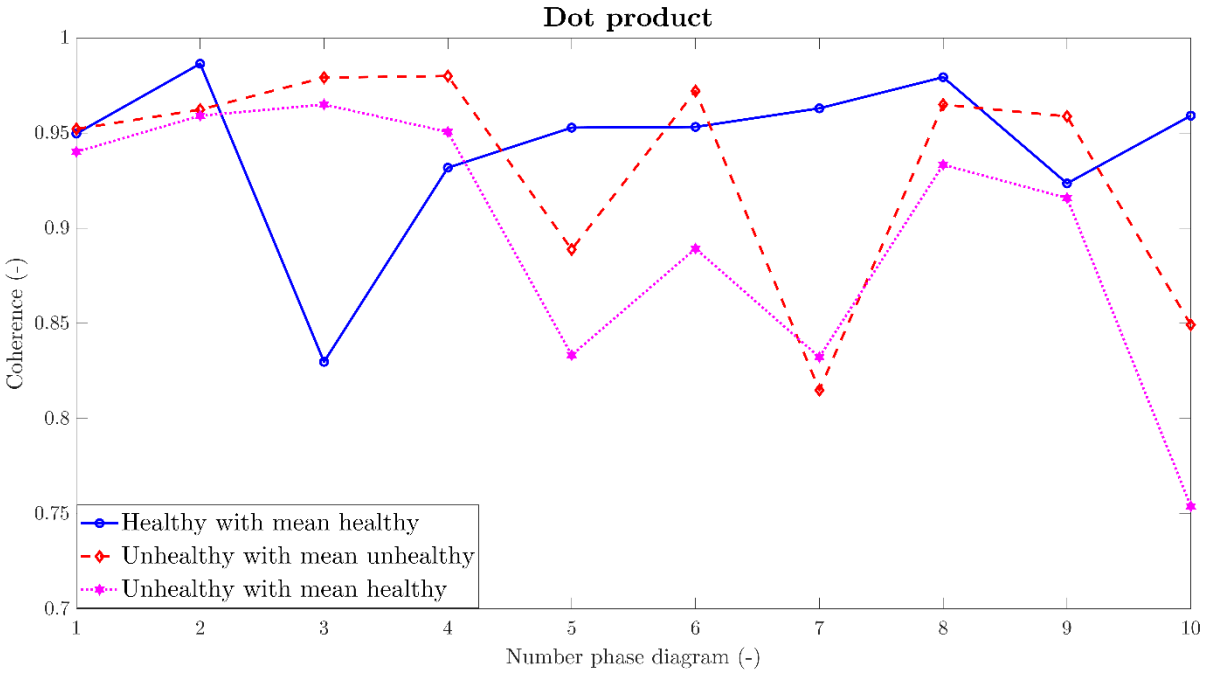

Figure 32: Dot product between single healthy or unhealthy phase diagrams and the mean of 10 selected healthy or unhealthy phase diagrams. Fourier vectors with 21 terms instead of 51 terms were used in the calculation of the dot product.

Figure 33 displays the dot product between every single healthy and unhealthy phase diagram. The mean coherence between a healthy phase diagram and every unhealthy phase diagram is lower if the dot product of this healthy phase diagram was also lower with the mean healthy phase diagrams. The range of coherence between a healthy phase diagram and every unhealthy phase diagram is wider compared to the variation in healthy phase diagrams. This is also observable if the number of the unhealthy phase diagram is indicated on the x-axis. These results could be explained as the dot products seems to be unable to discriminate healthy from unhealthy based on the appearance of the phase diagram and resulting Fourier vector.

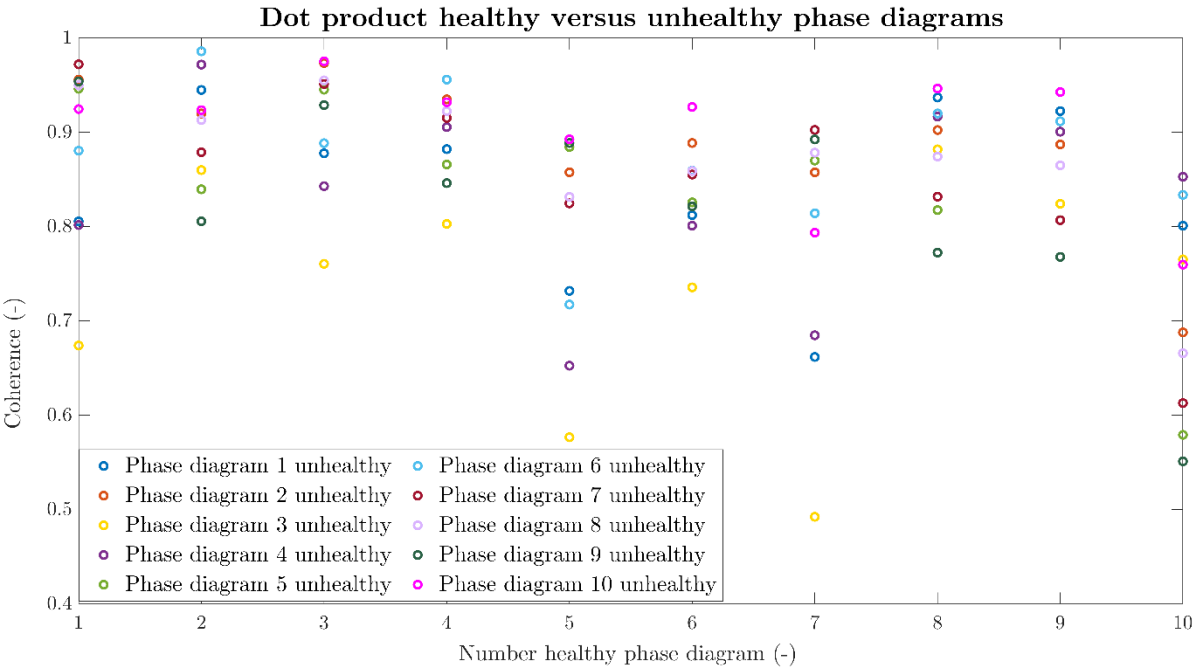

Figure 33: Dot product between every single healthy and unhealthy phase diagram. The number of the healthy phase diagram is indicated on the x-axis and the coherence with every unhealthy phase diagram is indicated per healthy phase diagram on the y-axis. For the 10 selected healthy phase diagrams, subject 21 who is a 9.5 years old female, experienced a 6% decline at 1 min after exercise. The 10 selected unhealthy phase diagrams were between 3 and 6 minutes after exercise of the 8.5 years old male subject 7 as he experienced a 28% decline at 3 minutes.

4.5.2. Removal Fourier terms

In order to investigate whether higher coefficients offer opportunities to discriminate the phase diagrams, the first 10 a and b coefficients were removed. After removal of the a1 and b1 coefficient, all 10 healthy and 10 unhealthy Fourier vectors were scaled again to a length of 1 to be able to calculate the mean Fourier vectors. Thereafter, the dot product between every healthy Fourier vector and the mean of the 10 healthy Fourier vectors were calculated. Regarding the 10 unhealthy Fourier vectors, the dot products were calculated between these vectors and both the mean of the healthy and unhealthy Fourier vectors. Similar calculation have been performed after removing a2, b2 in addition to a1, and b1. This was repeated until the coefficients a1 up to a9 and b1 up to b9 were removed.

The results without removal of any coefficients can be observed in figures 23. Figure 34 shows the effect of removing the Fourier vector coefficients a1, a2, b1, and b2. Of all options of the removed Fourier coefficients, the discrimination between the mean of the different dot products is most prominent after removing a1, a2, b1, and b2. Removing additional coefficients results in less discrimination between the means. In addition, the difference in individual coefficient between the mean healthy and mean unhealthy Fourier vectors remains comparable. The range of dot product values without removal of Fourier coefficients were all above 0.80. Therefore, the disadvantage of removing Fourier coefficient is a wider range of dot product values and also an overlap in the range of values. Apparently, there is a great variation in Fourier vectors coefficients between the 10 healthy, and 10 unhealthy Fourier vectors. However, the discrimination between the mean values improved greatly by removal of a1, a2, b1, and b2.

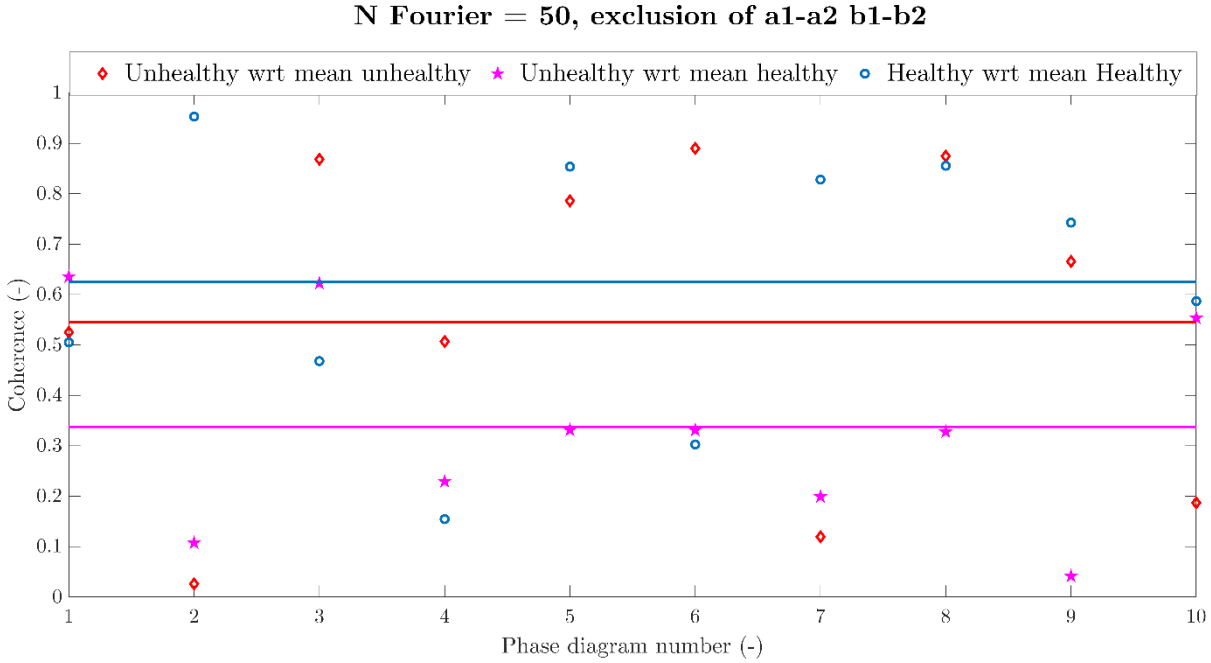

Figure 34: Dot product of the 10 healthy and unhealthy Fourier vectors with different means as indicated in the legend of the figure. The Fourier coefficients a1, a2, b1, and b2 were removed of all Fourier vectors. The mean values of the 10 dot products are indicated with the solid line.

In conclusion, removing Fourier coefficients offers opportunities for discrimination based on the mean value. However, the overlap in range of the dot product values limits the use to determine if an individual phase diagram is healthy or unhealthy based on the dot product.

4.5.3. Parameters

As identification of healthy and unhealthy phase diagrams could not be based on the Fourier coefficients, the parameters Aex_1, sphericity and triangularity were also compared. The sphericity of both healthy and unhealthy phase diagrams is observable in figure 35. The sphericity of the unhealthy phase diagrams varies between 0.68 and 0.85, whereas the range of the sphericity of the healthy phase diagrams is between 0.43 and 0.67. The mean of the 10 healthy phase diagrams compared to the mean of the 10 unhealthy phase diagrams results in a more prominent difference, see figure 35. In conclusion, a sphericity above 0.67 indicate an unhealthy phase diagram whereas a value below 0.67 represents a healthy phase diagram based on the phase diagrams of Appendices E.

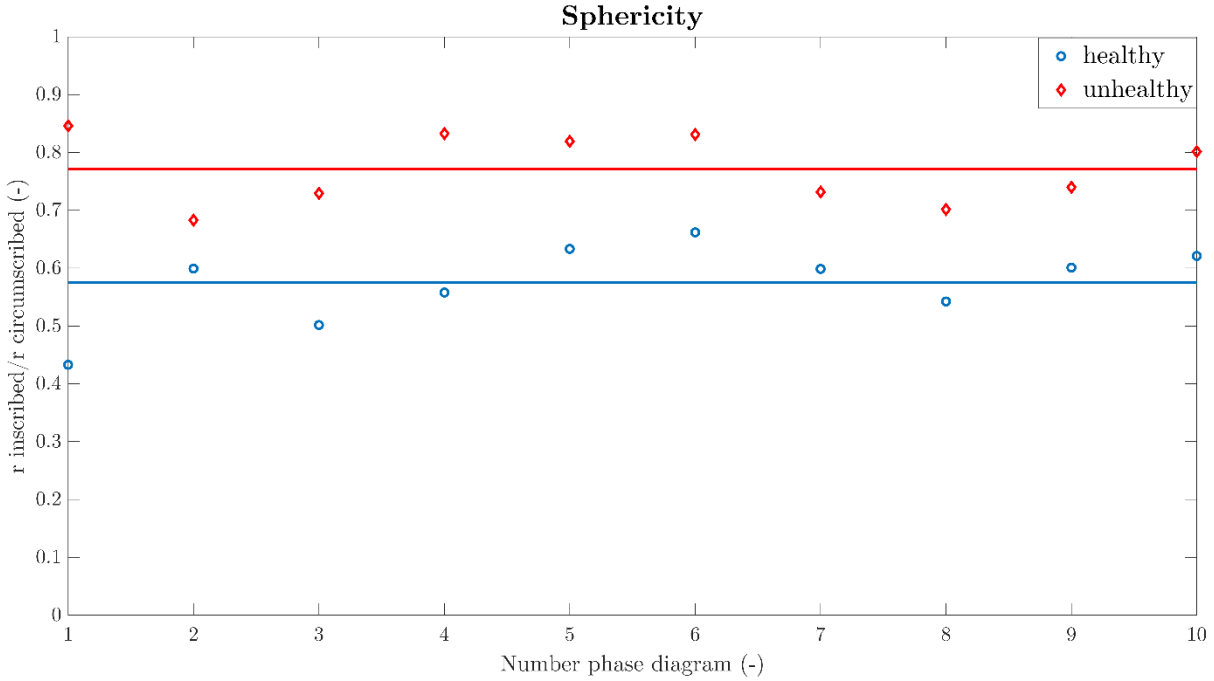

Figure 35: Sphericity of the healthy phase diagrams in blue circles and unhealthy displayed with red diamonds. The mean value is indicated with the line. For the 10 selected healthy phase diagrams, subject 21 who is a 9.5 years old female experienced a 6% decline at 1 min after exercise. The 10 selected unhealthy phase diagrams were between 3 and 6 minutes after exercise of the 8.5 years old male subject 7 as he experienced a 28% decline at 3 minutes.

Concerning the Aex_1 and triangularity in figure 36 and 37, the values of healthy and unhealthy phase diagrams overlap. Despite a difference in the mean value, there is no value of Aex_1 or triangularity that is able to discriminate a healthy phase diagram from an unhealthy phase diagram. However, as a variation in the breathing of a child is likely present, it is presumed that averaging the parameter could result in a discriminative value. For averaging the parameters, the time range around the lung function measurement of which the single breaths, used for the determination of the phase diagram, needs to be determined. It is likely that the time range depend on the stability of the lung function. For example, it is presumed that the time range resulting in a stable parameter is wider 5 minutes after the administration of a β_2-agonist compared to the moment of minimal lung function. In addition, it is speculated that the difference in time range is even bigger for larger change in lung function compared to their maximal lung function.

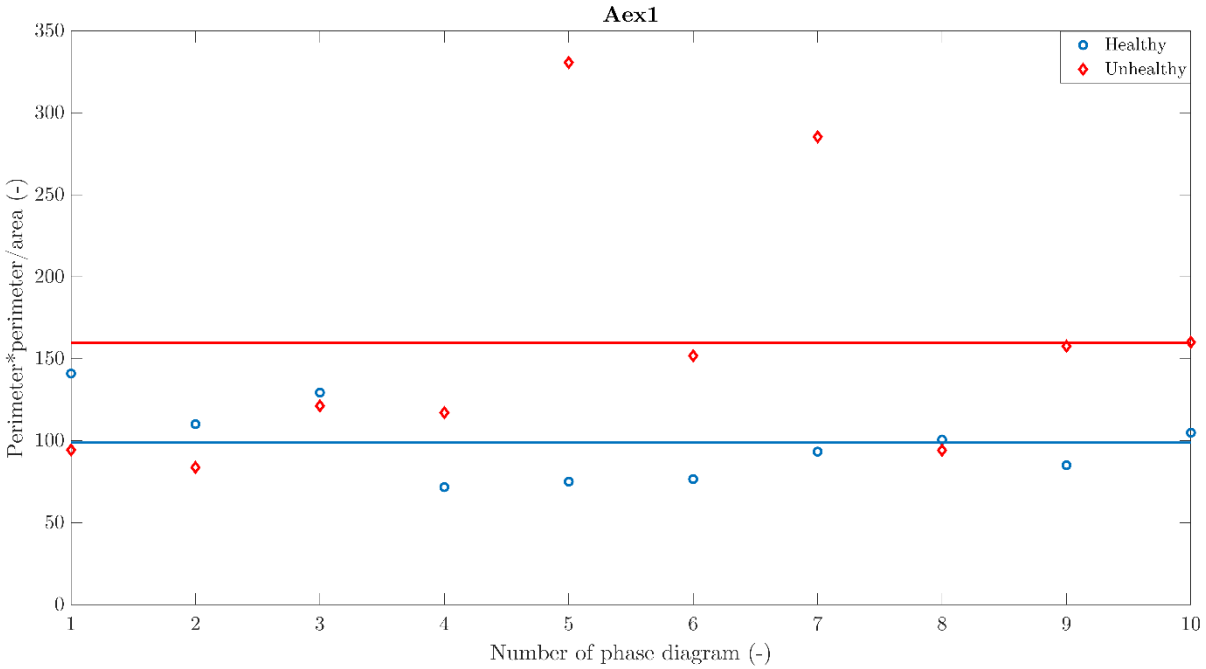

Figure 36: Aex1 of the healthy phase diagrams in blue circles and unhealthy displayed with red diamonds. For the 10 selected healthy phase diagrams, subject 21 who is a 9.5 years old female experienced a 6% decline at 1 min after exercise. The 10 selected unhealthy phase diagrams were between 3 and 6 minutes after exercise of the 8.5 years old male subject 7 as he experienced a 28% decline at 3 minutes.

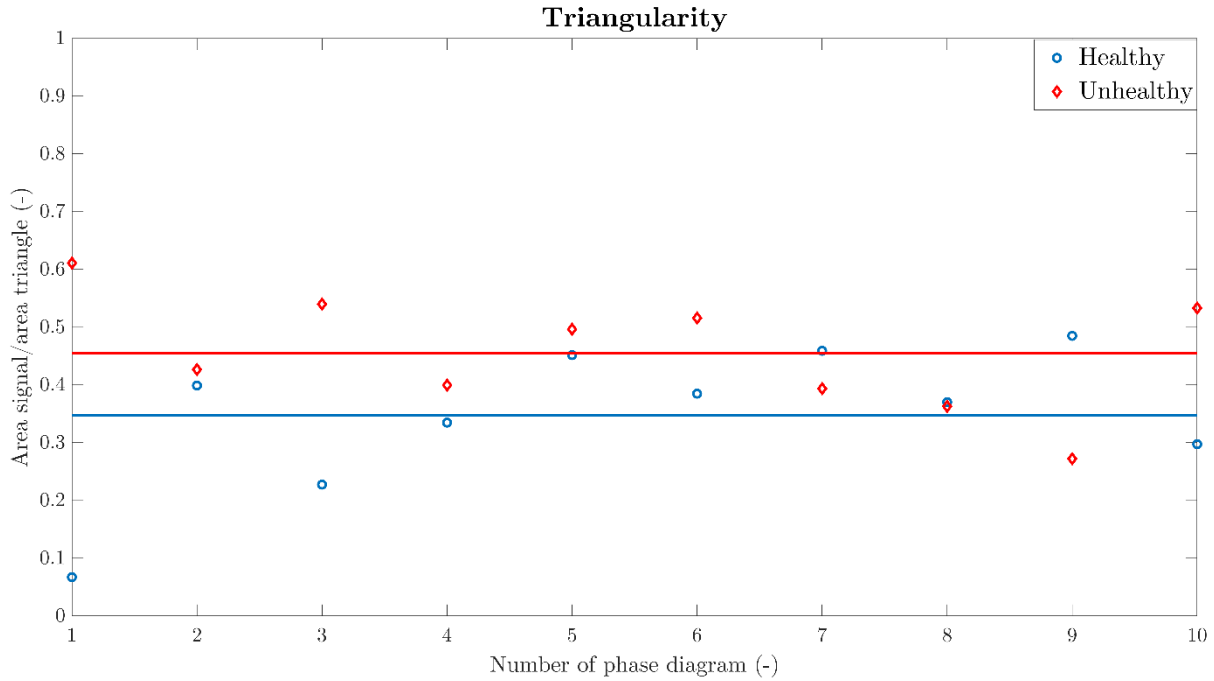

Figure 37: Triangularity of the healthy phase diagrams in blue circles and unhealthy displayed with red diamonds. For the 10 selected healthy phase diagrams, subject 21 who is a 9.5 years old female experienced a 6% decline at 1 min after exercise. The 10 selected unhealthy phase diagrams were between 3 and 6 minutes after exercise of the 8.5 years old male subject 7 as he experienced a 28% decline at 3 minutes.

4.6. Dispersion dot product

To investigate the influence of the number of Fourier components taken into consideration for the calculation of the dot product and the dispersion of the dot product values, two subjects with a large and two subjects with a small dispersion were selected. Subject 3 and 17 had a large dispersion in their dot product values, whereas the dispersion was minimal for subject 10 and 21.

As the Fourier vectors used for calculation of the mean Fourier vector also influences the dot product, the mean Fourier vector of subjects 3, 10, 17 and 21 with a minimal and maximal norm of residuals were selected and compared for 6, 12, 25 and 50 Fourier components. The phase diagrams taken into consideration for the mean Fourier vector resulting in the minimal and maximal norm of residuals were based on the results of 25 Fourier components, see 4.3 Influence mean Fourier vector on dot product.

Subject 3 had a total of 136 phase diagrams. The minimal norm of residuals for both linear and quadratic function was achieved by using the Fourier vectors 116 up to 136 which correspond to the phase diagrams up to 60 seconds before the final lung function measurement. The dot product of every Fourier vector of subject 3 with this mean can be observed in figure 38. The maximal norm of residuals is the result of using the Fourier vectors 126 up to 136 which correspond to the phase diagrams up to 15 seconds before the final lung function measurement. Figure 39 shows the values of the dot product with this mean Fourier vector.

Subject 17 had a total of 139 phase diagrams. The minimal norm of residuals for both linear and quadratic function was achieved by using the Fourier vectors 92 up to 139 consisting of the phase diagrams up to 120 seconds before the final lung function measurement. The dot product of every Fourier vector of subject 17 with this mean can be observed in figure 40. The maximal norm of residuals is the result of using the Fourier vectors 121 up to 139 which correspond to the phase diagrams after the final lung function measurement. Figure 41 shows the values of the dot product with this mean Fourier vector.

Subject 10 had a total of 148 phase diagrams. The minimal norm of residuals for both linear and quadratic function was achieved by using the Fourier vectors 126 up to 148 consisting of the phase diagrams up to 90 seconds before the final lung function measurement. The dot product of every Fourier vector of subject 10 with this mean can be observed in figure 42. The maximal norm of residuals is the result of using all the Fourier vectors for the calculation of the mean Fourier vector. Figure 43 shows the values of the dot product with this mean Fourier vector.

Subject 21 had a total of 232 phase diagrams. The minimal norm of residuals for both linear and quadratic function was achieved by using the Fourier vectors 179 up to 232 consisting of the phase diagrams up to 60 seconds before the final lung function measurement. The dot product of every Fourier vector of subject 21 with this mean can be observed in figure 44. The maximal norm of residuals is the result of using all the Fourier vectors for the calculation of the mean Fourier vector. Figure 45 shows the values of the dot product with this mean Fourier vector.

The figures 38, 40, 42, and 44 display the dot product with the mean of the Fourier vectors resulting in the minimal norm of residuals. More dot product values were changed, between the different numbers of Fourier terms taken into consideration, if there is a greater dispersion of dot product values for the subject. Regarding the figures 39, 41, 43 and 45, which used the mean Fourier vector with the maximal norm of residuals, the subject with less dispersion result in more changed values of the dot product.

Regarding the results of the minimal norm of residuals, the linear and quadratic functions reflecting the trend of the dot products are shown in figures 38, 40, 42, and 44. The norm of residuals increases with increasing number of Fourier components for subjects 10, 21 and 17. Whereas, the norm of residuals decreases with increasing number of Fourier components for subject 3. There is one exception for subject 3, the norm of residuals for 50 components is higher than 25 Fourier components.

Concerning the results of the maximal norm of residuals, the linear and quadratic functions reflecting the trend of the dot products are shown in figures 39, 41, 43 and 45. The norm of residuals increases with increasing number of Fourier components for subjects 10 and 21. Whereas, the norm of residuals decreases with increasing number of Fourier components for subjects 3 and 10. For all subjects, the norm of residuals is equal or higher for 25 Fourier components compared to 50 Fourier components.

In conclusion, the norm of residuals for subjects 10 and 21 were minimal with the use of 6 Fourier components and also for subject 17 regarding the minimal norm of residuals for the mean. Concerning subject 3, the norm of residuals is minimal for 25 or 50 Fourier components and also for subject 17 regarding the maximal norm of residuals for the mean. Besides, taking more Fourier vectors into consideration for the calculation of a mean Fourier vector, negatively influences subjects with great dispersion during the total pressure measurement. Whereas the addition of more Fourier vectors for the mean Fourier vector positively effects subjects with minimal dispersion. This indicate that the Fourier vectors used for calculation of a mean should be determined for every subject individually. However, it should be noted that the improvements in the linear and quadratic equations and norm of residuals could be minimal depending on the dispersion in the Fourier vectors used to calculate the mean Fourier vector. The result may be biased by included unrepresentative phase diagrams which were not removed using the artefact script, see Appendix D.2.

4.6.1. Subject 3, large dispersion, minimal norm of residuals

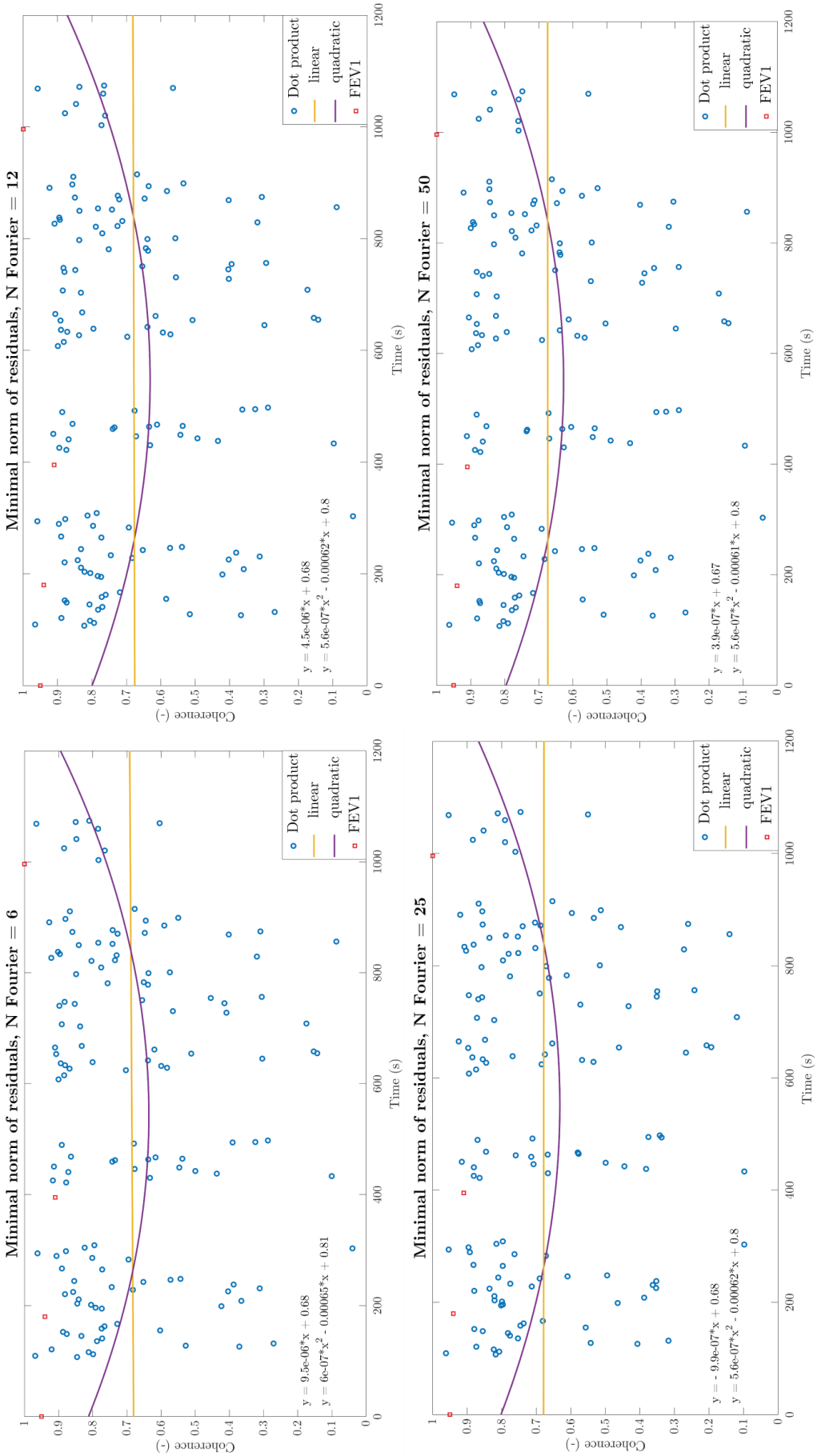

Figure 38: Subject 3, minimal norm of residuals using phase diagram 116 - 136. Number of Fourier components is indicated in the title of every subplot.

4.6.2. Subject 3, large dispersion, maximal norm of residuals

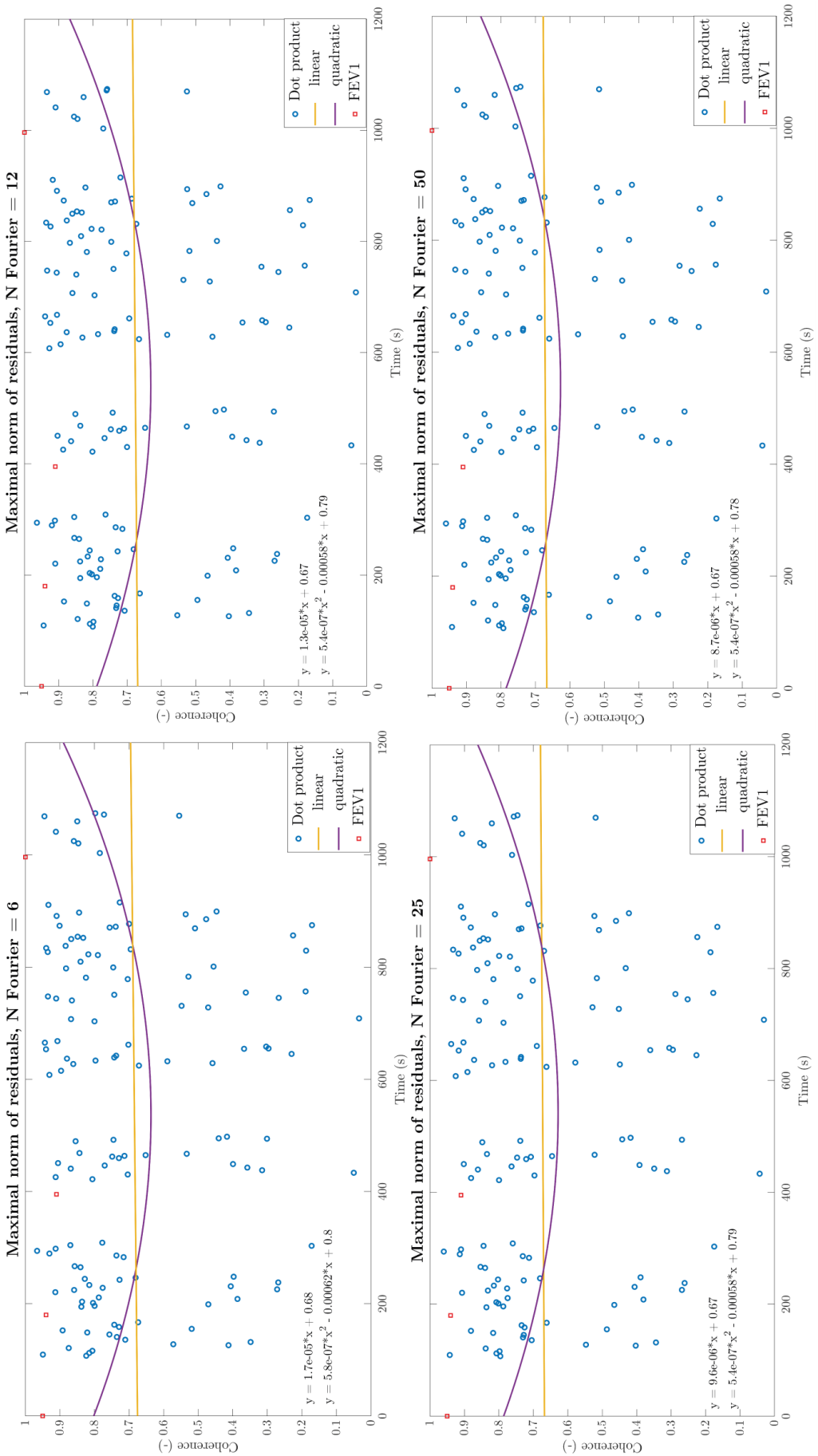

Figure 39: Subject 3, maximal norm of residuals using phase diagram 126 - 136. Number of Fourier components is indicated in the title of every subplot.

4.6.3. Subject 17, large dispersion, minimal norm of residuals

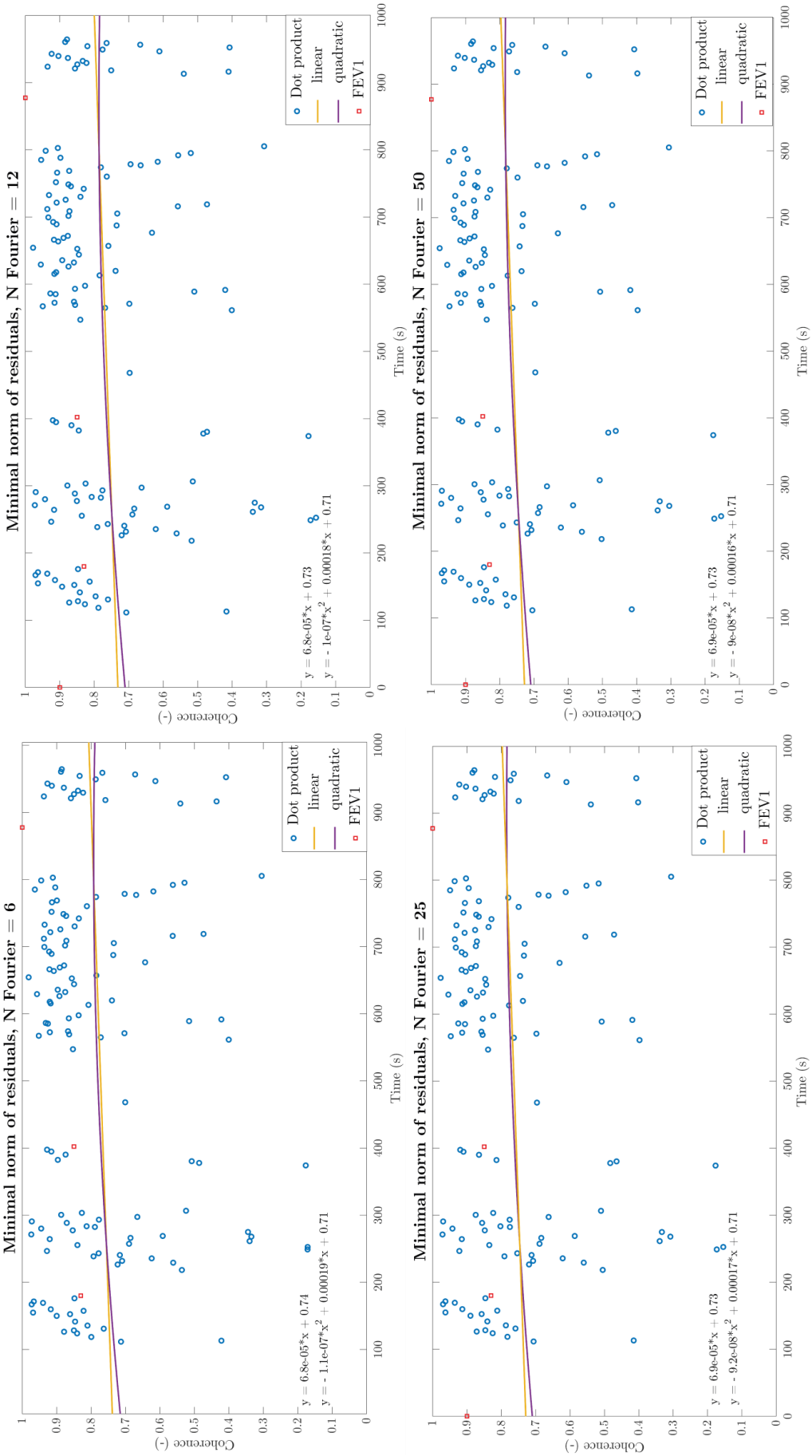

Figure 40: Subject 17, minimal norm of residuals using phase diagram 92 - 139. Number of Fourier components is indicated in the title of every subplot.

4.6.4. Subject 17, large dispersion, maximal norm of residuals

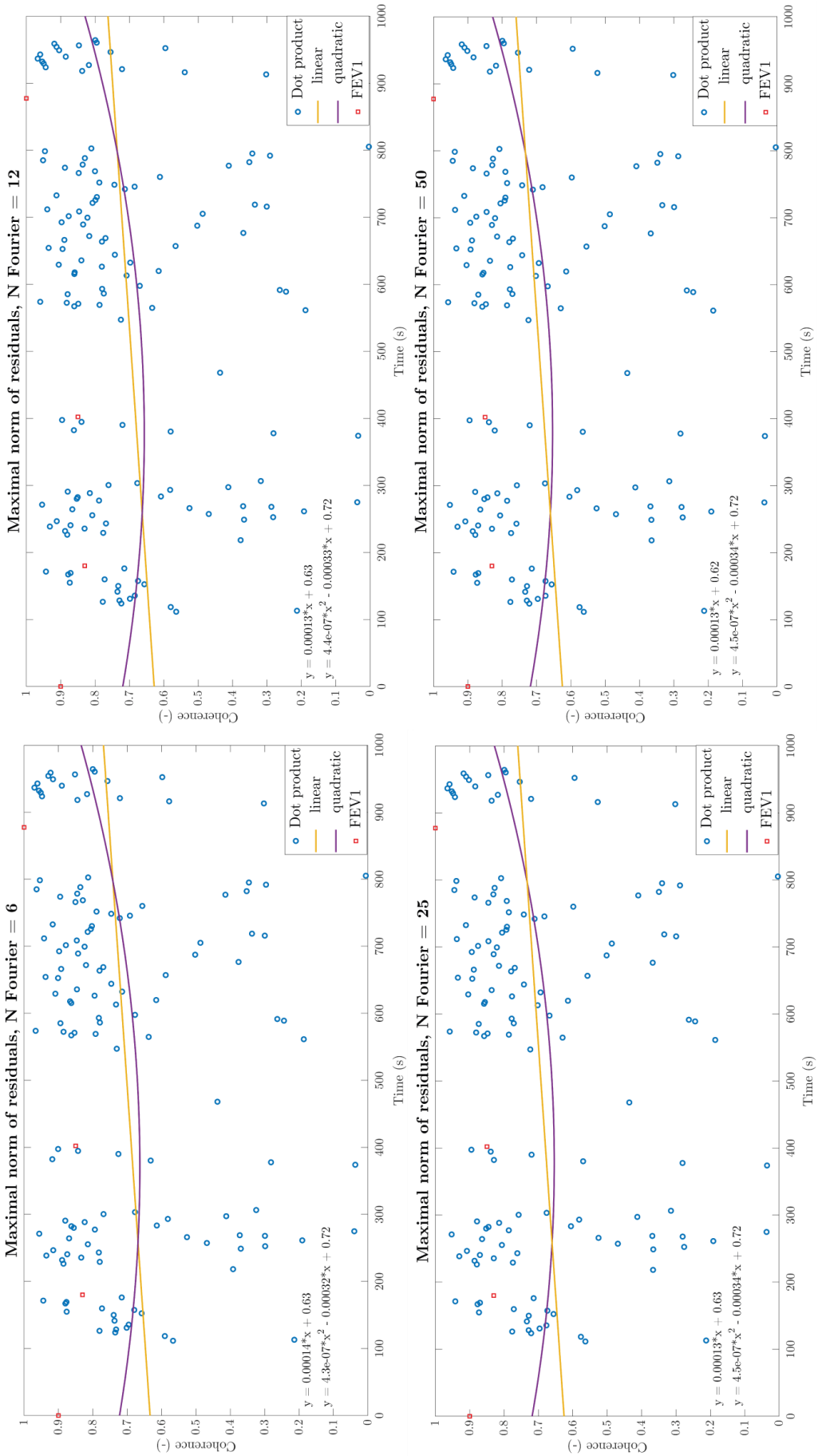

Figure 41: Subject 17, maximal norm of residuals using phase diagram 121 - 139. Number of Fourier components is indicated in the title of every subplot.

4.6.5. Subject 10, minimal dispersion, minimal norm of residuals

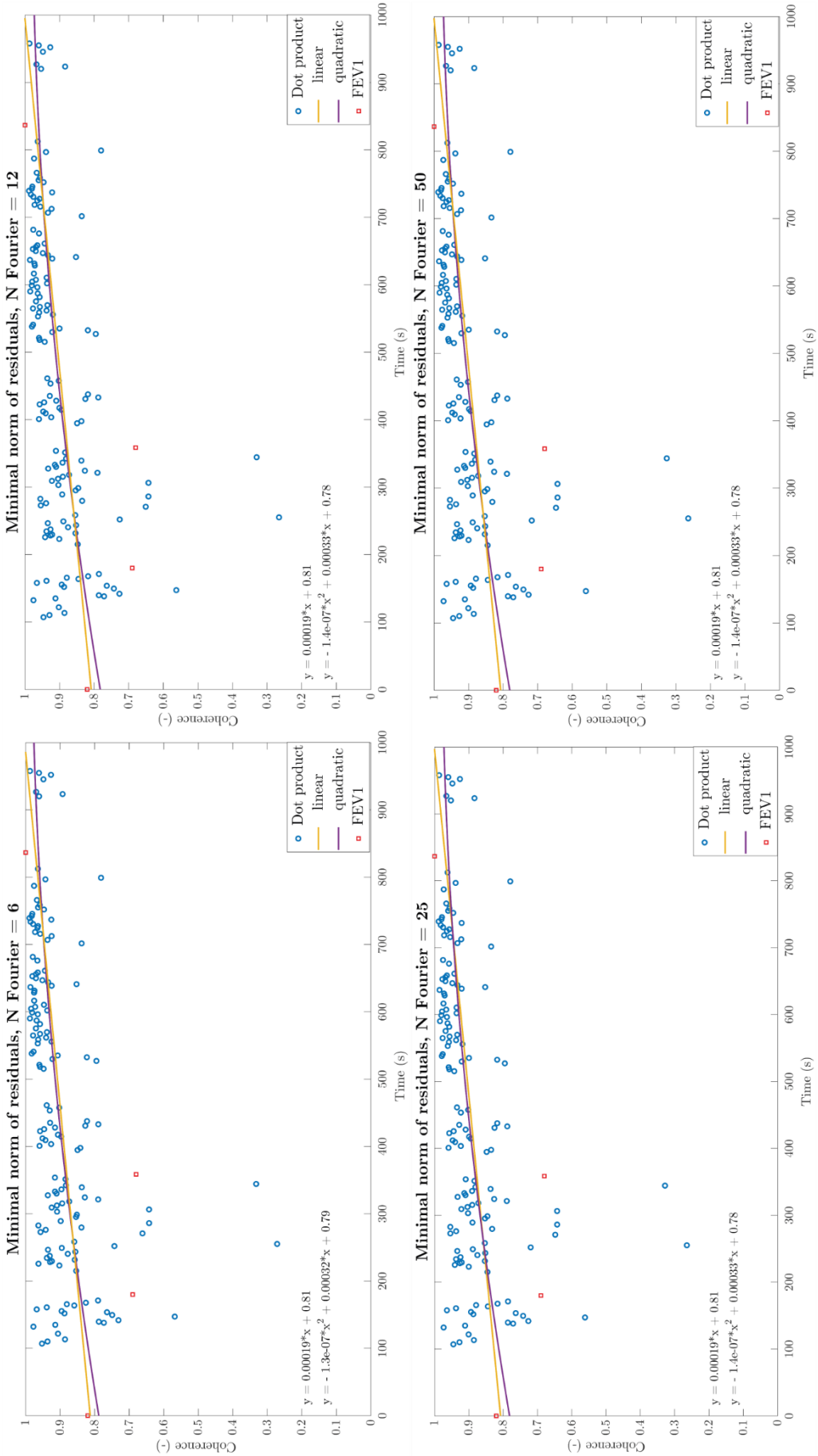

Figure 42: Subject 10, minimal norm of residuals using phase diagram 126 - 148. Number of Fourier components is indicated in the title of every subplot.

4.6.6. Subject 10, minimal dispersion, maximal norm of residuals

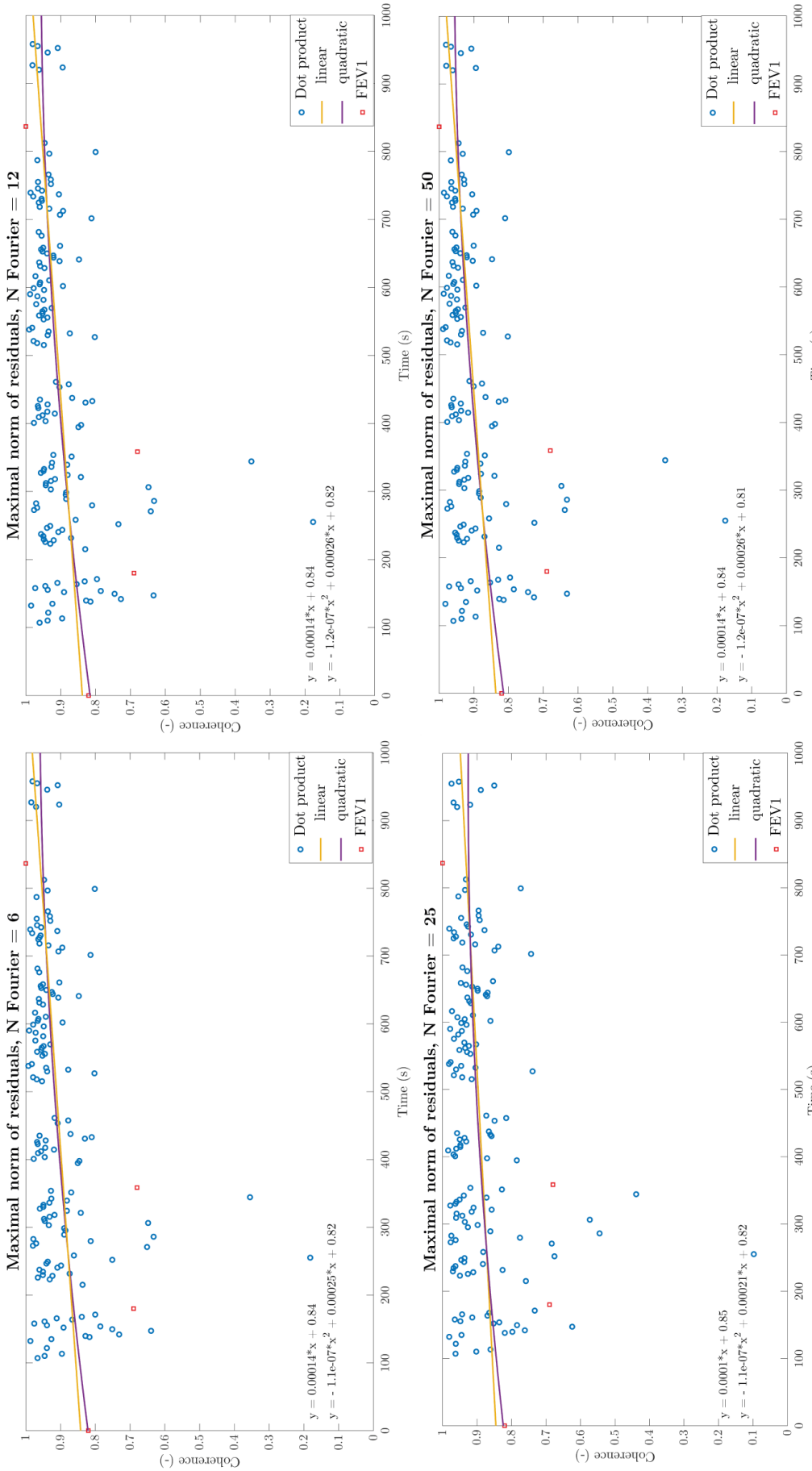

Figure 43: Subject 10, maximal norm of residuals using all phase diagrams. Number of Fourier components is indicated in the title of every subplot.

4.6.7. Subject 21, minimal dispersion, minimal norm of residuals

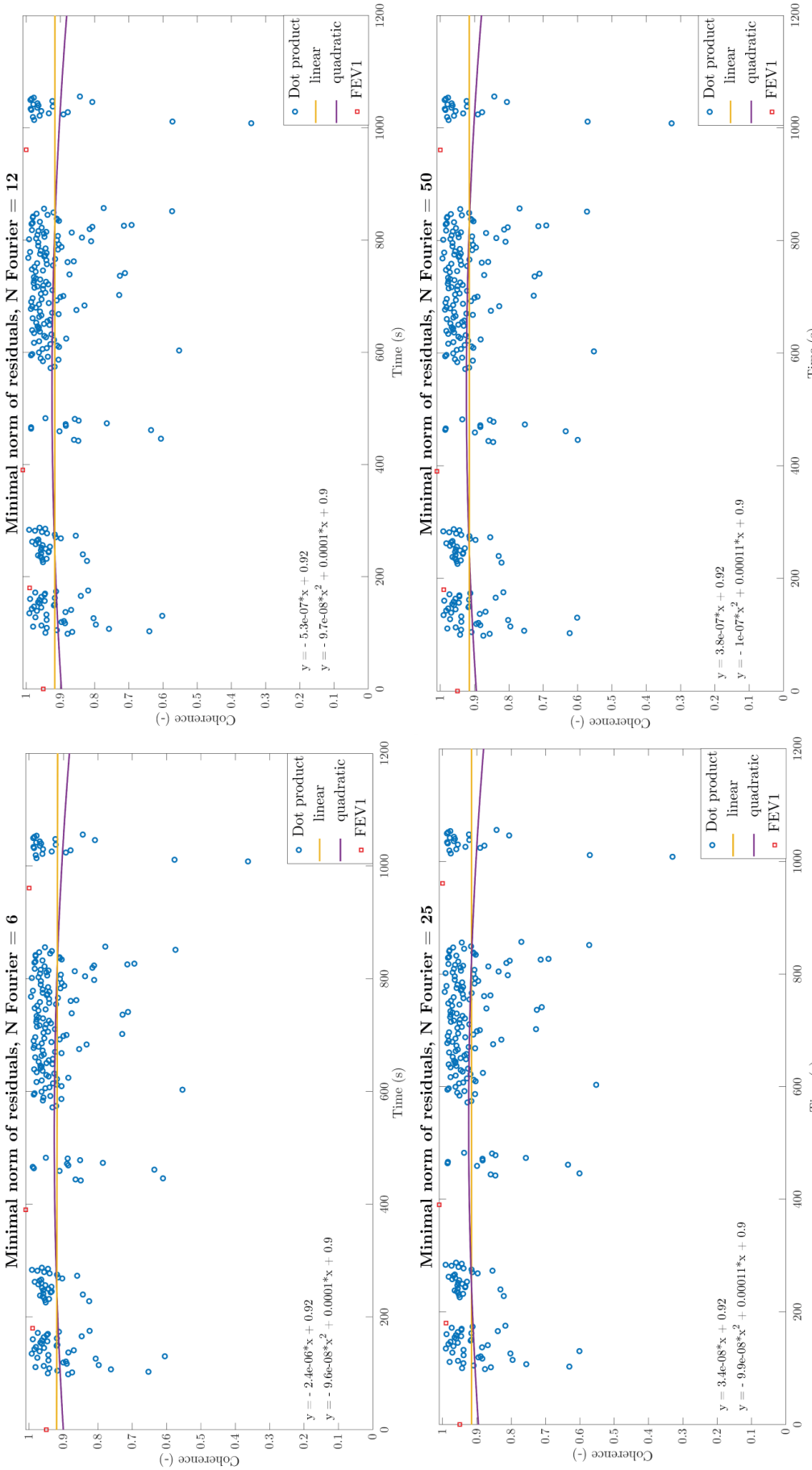

Figure 44: Subject 21, minimal norm of residuals using phase diagram 179 - 232. Number of Fourier components is indicated in the title of every subplot.

4.6.8. Subject 21, minimal dispersion, maximal norm of residuals

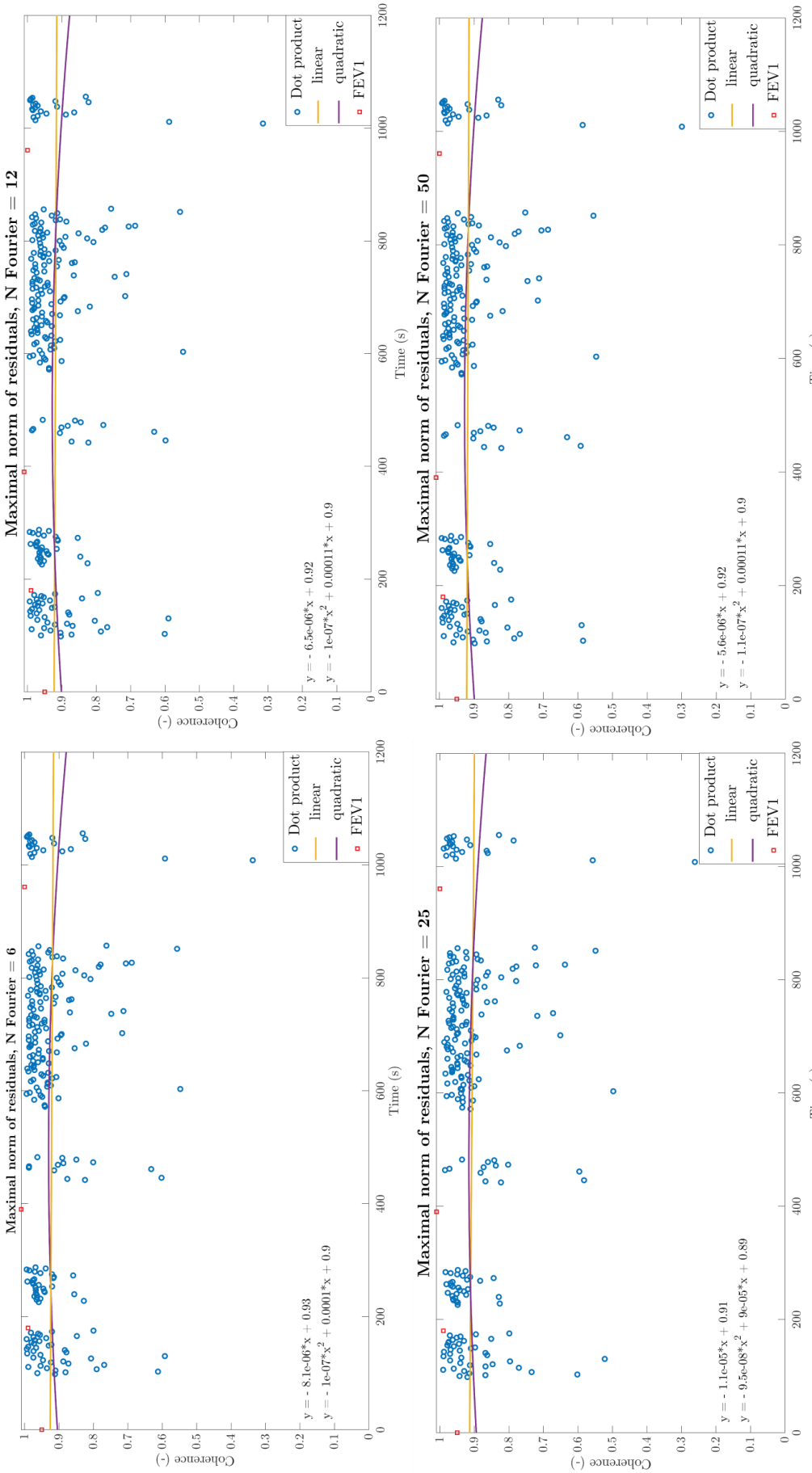

Figure 45: Subject 21, maximal norm of residuals using all phase diagrams. Number of Fourier components is indicated in the title of every subplot.

4.7. Exclusion of phase diagrams

While the parameters were calculated for the first time from the raw data without normalization of the x-axis, a couple of phase diagram had an x-axis range within 0.20 whereas others could be up to 0.60. It therefore seems that not every phase diagram is based on a representative breath. Figure 46 shows an example of a minimal x-axis range. In addition, there were also phase diagram in which the expiratoire breathing was not fully selected, see figure 47.

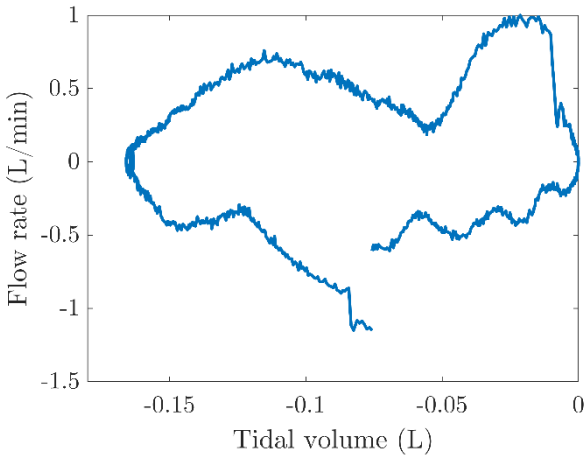

Figure 47: Phase diagram with a minimal x-axis range.

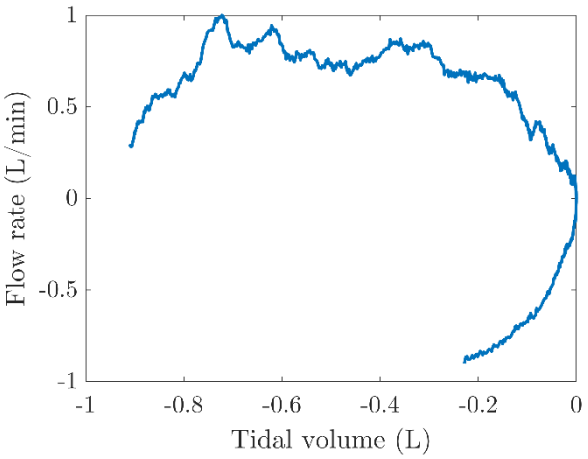

Figure 46: Phase diagram were the expiration is selected incompletely.

Since the dot product between two function provides an indication of their resemblance, it was investigated if the Fourier vectors of above examples had lower coherence to the mean Fourier vector of the subject 22. Subject 22 was chosen as the data contained multiple unrepresentative phase diagrams.

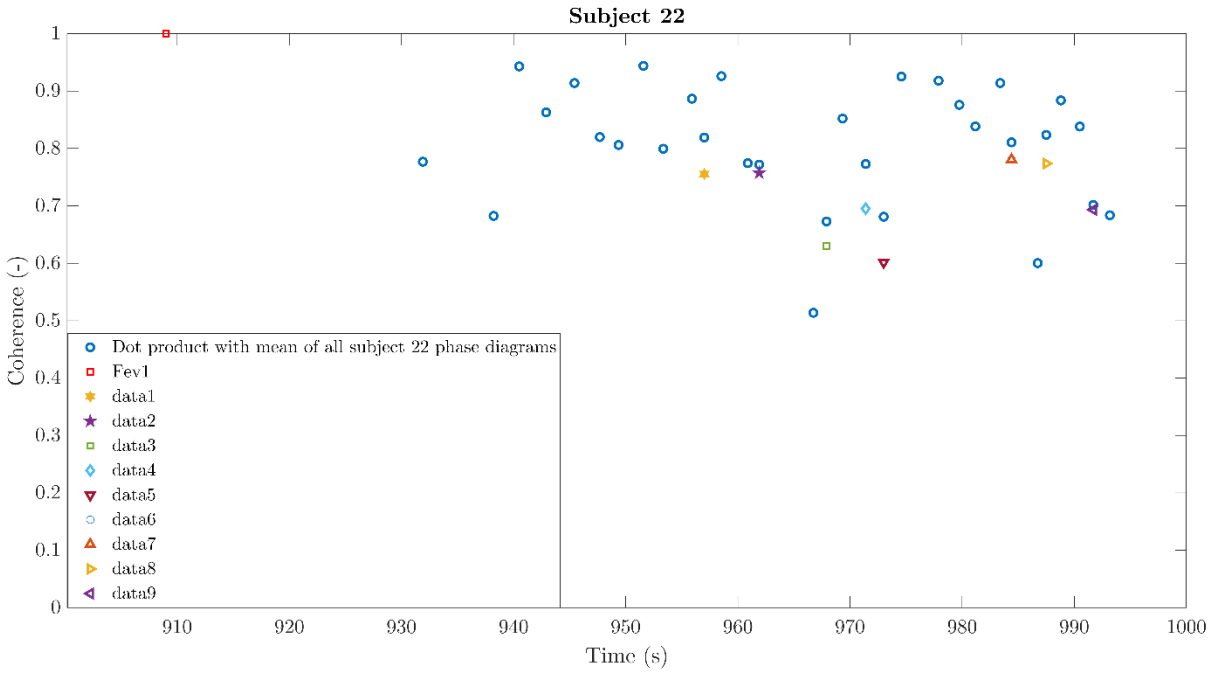

Figure 48: Dot product of phase diagrams in segment spirometry at 5 minutes after salbutamol administration up to end with mean Fourier vector of all subject 22 phase diagrams. The circles observable in the legend with the names 'data' are unrepresentative phase diagrams based on the selection in the raw pressure signal. Subject 22 is a 12.5 years old male with a 8% lung function decline at 3 minutes after exercise.

In figure 48, the dot product between the phase diagrams in the segment from spirometry 5 minutes after a β_2-agonist up to the end of the measurements and the mean of all subject 22 phase diagrams can be observed. 237 phase diagrams were selected out of the raw data. The dot product was first determined between every single phase diagram and the mean of all phase diagrams. The mean of all phase diagrams was chosen as the number of unrepresentative compared to representative phase diagrams is small. Therefore it could be expected that the influence on the mean of all phase diagram will ideally be negligible. The circles indicated in the legend were labelled as unrepresentative based on the raw pressure signal. In order to remove all unrepresentative phase diagrams based on the value of the dot product, the cut-off value should be at least 0.80. This would result in removing at least as many representative as unrepresentative phase diagrams in order to remove all unrepresentative phase diagrams.

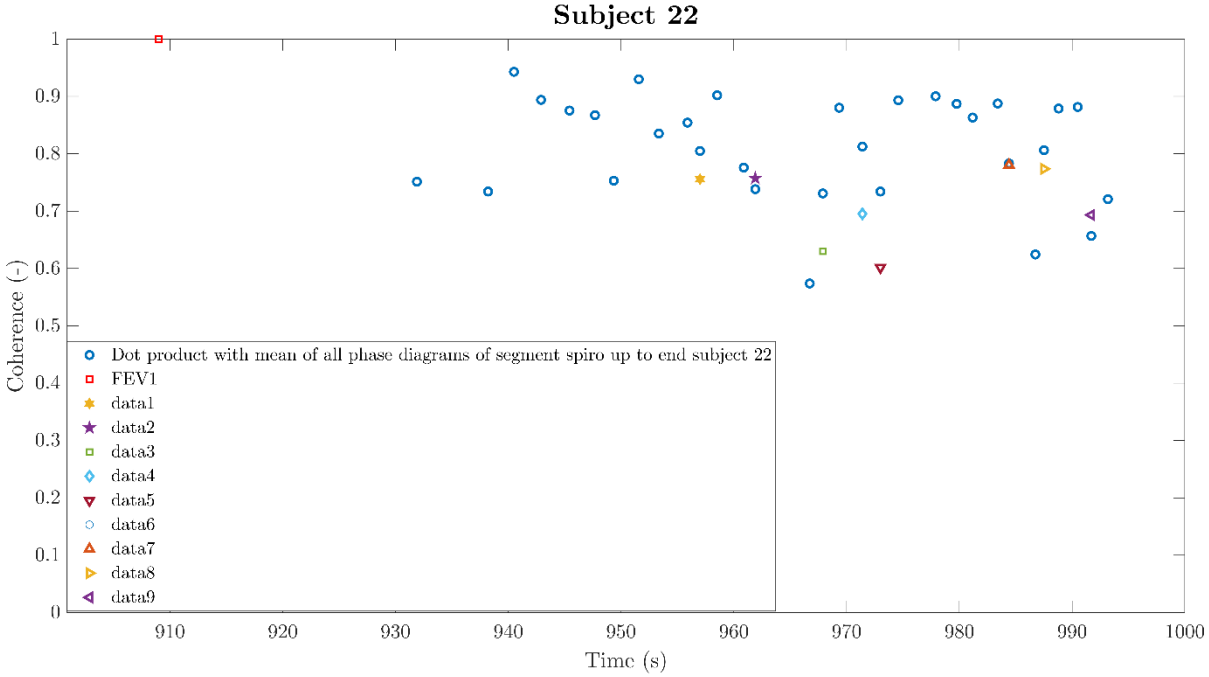

Figure 49: Dot product of phase diagrams after the final lung function measurements up to end with mean Fourier vector of that segment. The circles observable in the legend with the names 'data' are unrepresentative phase diagrams based on the selection in the raw pressure signal. Subject 22 is a 12.5 years old male.

In figure 49, the dot product between the phase diagrams 5 minutes after a β_2-agonist up to the end of the measurements and the mean of these phase diagrams can be observed. This segment was chosen as it is presumed that the appearance of the phase diagram stabilizes as the lung function approaches the maximal value of that subject. However, this may be debatable for this subject as the segment after the maximal lung function measurement contains approximately 30% of unrepresentative breaths. The circles indicated in the legend were labelled as unrepresentative based on the raw pressure signal. In order to remove all unrepresentative phase diagrams based on the value of the dot product, the cut-off value should also be at around 0.80. This would result in removing at least as many representative as unrepresentative phase diagrams in order to remove all unrepresentative phase diagrams.

In conclusion, as inspecting the data manually is time-consuming and the number of unrepresentative phase diagrams is unknown, using a minimal value of the dot product with the mean of certain phase diagrams seems unreliable. Investigating characteristics of the unrepresentative phase diagrams that occur frequently might result in a more accurate selection of phase diagrams in the subject's data that should be removed.

4.7.1. Characteristics unrepresentative phase diagrams

The FUN_periodic_cutter script of Appendix D.3. contains 3 criteria. In order to exclude noise around zero, a minimal half cycle time of 0.6 seconds is demanded. In addition, there must be at least 40 elements between the last minimum or maximum. Lastly, the difference between the starting value and starting minimum / maximum should be at least 1500 Pa.

At first, both minima and maxima were used to divide the pressure signal into single breaths. A drawback of this method is, using maxima for the division results in the expiratory curve consisting of two breaths. As the parameters are based on the appearance of the expiratory curve, it is necessary that the expiration consists of a single breathing manoeuvre. However, the number of elements between the last minimum or maximum and the current was not adapted after using only minima for the division into single breaths. Optimization of this parameter, could result in a reduction of the number of unrepresentative phase diagrams as pressure variations around zero will not result in phase diagrams.

As the breathing frequency is variable, the time at the maxima of expiration were used to plot the parameter of the phase diagram in order to be able to investigate the variation over time. During this selection, the unrepresentative signals selected as single breaths resulting in a phase diagram were observed. Three unrepresentative phase diagrams appeared regularly, these include fluctuations around zero, and division of one expiration into two phase diagrams. The fluctuations around zero appeared in two forms, namely one single positive part but also multiple turns through zero at the beginning or end of the expiratory curve.

There are several options to exclude these unrepresentative phase diagrams. Regarding the selection of two phase diagrams out of one expiration, this could be avoided by adding the condition of a minimal negative pressure or minimal duration of inspiration. The duration of the expiration could also be used as an indication of representative breaths. These criteria should be in the scripts regarding the division into single breaths.

For the turns through zero, this could be corrected by selecting the start of expiration as the last crossing through zero before the maximal positive pressure. Similar for the turns at the end of the expiration, the end of expiration can be selected as the first negative pressure after the maximal positive pressure. However, as the total phase diagram is taken into consideration for the calculation of the Aex_1, phase diagrams with multiple turns through zero should be excluded as this results in a very high Aex_1 value.

In some phase diagrams, the amplitude of the inspiration displayed negative, is proportional larger compared to the amplitude of the expiration. When this phase diagram is approach with Fourier analysis, the approximation of the inspiratory part will be more accurate. Therefore, the Fourier vector is less representative for the expiratory part. These phase diagrams can be excluded using a maximal value of the root mean square between the approximation using Fourier and the original signal. The ideal cut-off value should be investigated.

Concluding, multiple criteria are suggested to exclude or adapt unrepresentative phase diagrams. However, due to limited time, the effectiveness stills needs to be investigated.

5. Discussion

In this study, the relation of pressure measurements to assess lung function changes during an ECT in asthmatic children was investigated. This section will discuss the results and limitations of this study and some further perspectives.

Our hypothesis is that variability of phase diagrams is influenced by a change in lung function. Observing the 10 selected healthy and unhealthy phase diagrams, a possibility to discriminate between those seems possible as it is already observable by eye. However, until this moment a discriminate parameters has not yet been found. The possible bias for the phase diagrams is changing the breathing pattern due to changes in lung function or recovery of exercise induced hyperpnoea. The breathing pattern is determined by the rate and end-expiratory lung volume (EELV) at which a child breaths, which can shift under physiological stress.

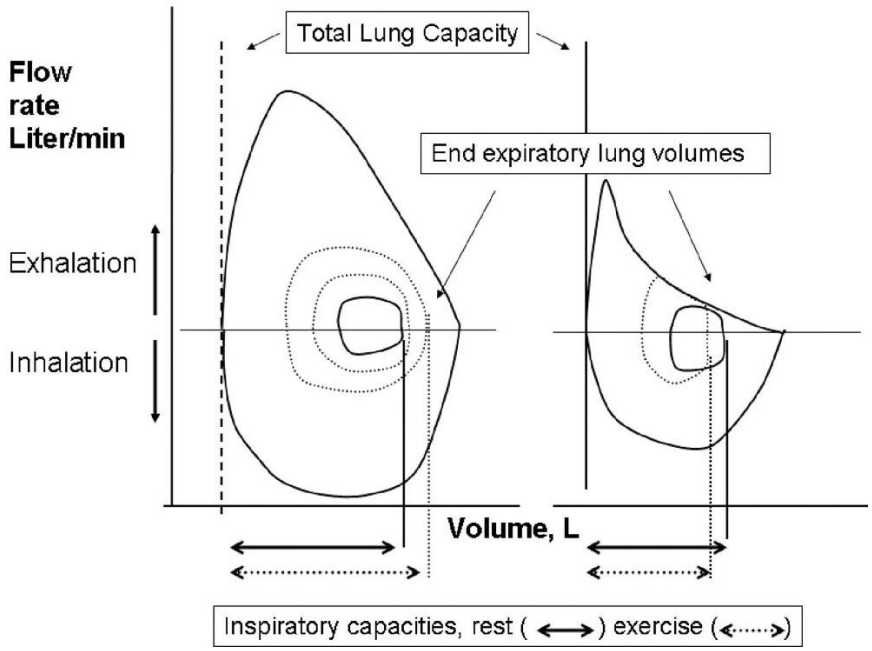

Figure 50: Maximal and tidal flow volume loops of a normal subject on the left and of a subject with an obstructive lung disease on the right. Flow volume loops during exercise are indicated with dotted line and during rest with a solid line [61].

As the breathing strategy seems to affect the pressure measurement, a brief overview is given. Figure 50 shows the difference between subject with an obstructive lung disease and a normal subject of the maximal and tidal flow volumes curve. In addition, the tidal flow volume curves during exercise are shown. The subject with obstructive lung disease is limited by the maximal expiratory flow volume curve during exercise. When breathing occurs at a low lung volume (near residual volume), the available ventilator reserve is limited due to the shape of the expiratory flow volume curve, the reduced chest wall compliance, and the reduced maximal available airflows [62]. Breathing at high lung volumes (near total lung capacity) increase the inspiratory elastic load and therefore the work of breathing (WOB). Regarding the patient with obstructive lung disease, breathing at high lung volumes allows breathing with a higher tidal volume. Pellegrino et al.[63] investigated the influence of airway narrowing by imposing a expiratory threshold load during non-flow and flow limitation. Regarding the non-flow limitation, the imposed load increased the expiratory time (TE) less than the decrease in expiratory flow, and the EELV tended to increase. In contract, during flow limitation, TE

increased more than the expiratory flow decreased, and the subject were not able to achieve maximal expiratory flow until a low volume, and EELV decreased. During exercise, the ventilatory demand increases due to the metabolic acidosis which results in the subject to increase EELV to avoid expiratory flow limitation [62]. To take advantage of the higher available maximal expiratory airflows, end-inspiratory lung volume (EILV) increases to preserve the exercise tidal volume. A breathing strategie where EILV does not increase with increasing exercise intensity usually results in an increase in the RR. A disadvantage of this breathing strategy is the increase in the degree of expiratroy flow limitations due to the higher flow rates as the breathing frequency is increased. As tidal volume, breathing frequency and the expiratory time are influence by the breathing strategy, calculation of these values during the total measurement can be indicative for the breathing strategy used at that moment. A more clear pattern might be observable between subjects in correlation to the lung function changes if tidal volume, breathing frequency, and expiratory time change are shown.

It is speculated that several factor influence the pressure measurements. Due to the variability of the breathing pattern, a number of consecutive artefact-free breaths should be selected to minimize the variability. However, as the setup of this research is never performed in such a way, this number should be determined. It is speculated that the time frame of these breaths is influenced by the rate and value of change in lung function. This means that the time frame can be longer if the change in lung function is minimal. Therefore, the number of breaths likely depends on the variation in lung function over time. Taking figure 9 into consideration, the time frames available for the selection are limited by the lung function measurements. Another variable which should be considered is the breathing frequency which declines with age. Therefore, a greater time frame is needed for older subjects to obtain the same amount of consecutive breaths compared to younger subjects, as their breathing frequency is generally lower.

5.1. Interpretation of results

It is promising that the coherence between the Fourier vector of single phase diagrams and the mean of all phase diagrams is high and therefore a resemblance between phase diagrams of the 18 included subjects exists, see figure 10. However, in order to use the phase diagrams to provide feedback on therapy efficacy, a correlation between the pressure signal and lung function measurements should also be present.

Regarding the number of Fourier coefficients, the Aex_1, sphericity, and triangularity values stabilize after 51 Fourier terms. This indicates that using less Fourier terms results in a too smooth phase diagram to determine these parameters. For the determination of the dot product, up to 21 Fourier terms seem sufficient as the addition of more terms has no effect on the discrimination between healthy and unhealthy classified phase diagrams. This indicates that higher terms have no additional discriminative power compared to the first 21 terms.

The Fourier vectors of the phase diagrams which should be taken into consideration for the calculation of the mean vector differ per subject. The dispersion of the appearance of the phase diagrams seems to influence which phase diagrams have a positive contribution to the mean Fourier vector. It was presumed that the phase diagrams after the final lung function measurement would resemble the healthy situation of the subject and therefore these phase diagrams were certainly taken into consideration for the mean Fourier vector. However, while the Aex_1 and time indication of the phase diagrams of all subject were determined, it was

noticed that not all phase diagrams represent true breaths. If these unrepresentative breaths occur after the final lung function measurement, this mean Fourier vector might not correctly reflect the mean phase diagram of the optimal lung function for that subject.

Regarding the selected healthy and unhealthy phase diagrams, the results of several analysis methods reveal no discriminative parameter. However, figure 30 indicates a clear difference seen by naked eye. This difference consist of a lower maximal amplitude and lower tidal volume regarding the unhealthy phase diagram compared to the healthy phase diagram. In addition, during a breath which results in an unhealthy phase diagram, the subject seems unable to produce a high flow at the start of expiration. Unfortunately, the predetermined parameters and the dot product seem unable to distinguish healthy from unhealthy. The sphericity seems to be the most promising parameters as the sphericity of unhealthy phase diagrams has a value between 0.68 and 0.85, whereas between 0.43 and 0.67 is the range of healthy phase diagrams. So, healthier phase diagrams appear less spherical. In addition, the mean sphericity of the 10 unhealthy phase diagrams has a value of 0.77 compared to 0.57 regarding the mean of the 10 healthy phase diagrams. As the difference between the mean healthy and unhealthy sphericity is greater than between phase diagrams, averaging phase diagrams of parameter outcomes could improve the discriminative power.

The dispersion of the dot product was investigated. Taking more phase diagram into consideration positively affect the norm of residuals if the dispersion of the phase diagrams is little. The dispersion of the phase diagrams during the total measurement was little for the subjects 10 and 21. A possible explanation for the dispersion could be that the pressure measurement consist of comparable breaths and is rarely affected by manipulations.

5.2. Strengths and limitations

As the manipulations seemed easily recognizable and removable, see Appendix C, the performed pressure measurements were simple. The subjects were only instructed to breathe through their nose as much as possible and if mouth breathing was observed during the measurements, the subject was kindly asked to breathe through their nose.

During the inspection of the data afterwards, one subject had to be excluded due to unrepresentative breaths after only two minutes of measurement. This was most likely caused by the folded nasal prong due to the nose clip during the lung function measurement. Unfortunately the folded prong was just noticed when the measurement was completed and the nasal prongs were removed. This could have been prevented if real-time data observance was possible or checking the position of the nasal prongs was performed more often.

Only three subjects removed the nasal prongs themselves due to discomfort as allergic rhinitis induces irritability of the nasal mucosa. This is not a bad result as asthma and allergic rhinitis frequently co-exist. Certainly as the measurement were conducted in the period of March to May which is during the allergic period. Just one subject was not included in the study due to the inability to breathe through his nose.

As the effect of the change in lung function on the phase diagram of tidal breathing is unknown, the sample size could not be calculated and had to be estimated. Therefore it is unknown of 18 included subjects is enough to achieve statistical significance. However, indication of the existence of a possible correlation between pressure measurement and lung function should be possible.

As mentioned earlier, the measured pressure is influenced by the cannula size and the insertion length. Two different cannula sizes were used since the subjects were between 4 and 16 years old and a maximal occlusion of 50% is advised. However, as the pressure and lung function measurements were compared per subject, it is unlikely that there is an influence of the nasal cannula size. Regarding the insertion length, application of the nose clip during the lung function measurement could have influenced the insertion length. However, normalization of the phase diagrams most likely neutralizes this effect if present. As the position of the nasal cannula influence the measured pressure, it was chosen to apply the nasal cannula after the exercise. During the exercise the subject breaths through their mouth, at least after 2 minutes of exercise. As a result, there will be no difference in pressure during the measurement and therefore measurements of the breathing pressure changes during exercise are useless. However, additional information could be obtained by pressure measurement during the baseline measurement of the lung function as the breathing pattern might be more consistent. It was expected that the lung function of the subject at the final lung function measurement were comparable or higher with respect to the baseline measurement. Concerning the 18 included subjects, this is true for 15 subject. Regarding the other 3 subjects, the differences in baseline and final lung function were 1.41 L versus 1.38 L, 1.71 L versus 1.58 L, and 2.21 L versus 2.19 L. Therefore, the maximal difference in were 4.5% instead of 16.3%, 28.5% rather than 33.9%, and 5.0% instead of 5.9%. So, the amount of information which is lost due to starting the measurement after exercise is considered negligible.

5.2.1. General measurement limitations

The pressure measurement of each subject was inspected manually and the Matlab script of Appendix D.2. was used to localise possible manipulations and therefore unrepresentative breaths based on Appendix C. The disadvantage is that representative breaths could have been removed but it is also possible that there is still some influence of the manipulations present in the phase diagrams. Ideally, manipulations should be avoided but this is at the cost of the simplicity of the measurements. However, if pressure measurement are able to objectify therapy efficacy in situations where the subject is unable to perform spirometry measurement, there is still an added value of the pressure measurements.

It is speculated that the effect of the manipulations is less observable if the subject receives flow through the nasal device. Subsequently, a flow at all or increasing the flow, most likely also reduces the variability between breaths induced by the subject. As a result, the pressure measurement will be more coherent and a change in lung function or therapy efficacy can be observed more easily.

5.2.2. Measurement software

At first, the pressure measurement could be viewed in real-time. However, due to the regular failure of the LabVIEW 2017 application during the pilot measurements, the application of OMEGA which only shows the current measurement value was used. Observing the data in real-time offers the opportunity to instruct the subject based on observed mouth breathing or frequent manipulations in the signal. As the OMEGA application was used during the ECT, these instruction could only be based on visual inspection. Besides, for the use in clinical setting, real-time data inspection should be possible. In addition, this also makes it possible to observe the effects of the breathing strategy of the subject on the pressure measurement and also if the subject is breathing regularly.

5.3. Further perspectives

The number of representative breaths can be improved by addition of conditions for the calculation of phase diagrams. However, presumably there are still phase diagrams left which are not interpretable. Therefore, there is a need to check phase diagrams on certain conditions. A condition can be that the flow must increase from the start of expiration to be able to determine the moment of maximal flow compared to the total expiration accurately. In addition, a minimal tidal volume during each expiration can be set. There is less necessity for averaging if the appearance of the phase diagrams is comparable.

For spirometry measurements, the maximal FEV_1 is used as a patient could bias the measurement by less effort but this is limited by the maximal effort the patient can deliver. Therefore, it might be interesting compare the maximal phase diagram during the minimal lung function and maximal lung function. As spontaneous breathing could be influenced by forced breathing manoeuvres as spirometry, it is likely that phase diagrams before spirometry measurements should be used. However, it could also be indicative if the phase diagrams are influenced by a forced breathing manoeuvre. Therefore, comparing phase diagrams before and after spirometry measurements might be interesting.

To further investigate a discriminative parameter, it might be interesting to predefine an ideal healthy and unhealthy phase diagram and calculate the coherence through the measurement using the dot product. It is presumed that the phase diagram will appear less healthy at the moment of minimal lung function and changes to healthy at the maximal lung function. However, as the results of 4.5 indicate that the dot product is not able to discriminate between healthy and unhealthy another parameter will likely perform better.

In order to discriminate phase diagrams based on their appearance, a machine learning could also be applied. To be able to apply machine learning in the clinical setting, the model should be able to classify the phase diagram or pressure measurements and to relate them to therapy efficacy or lung function change of the subject. In addition, the results of the machine learning should contain an indication of the severity of an unhealthy phase diagram or a factor of improvement or decline. This should be observable over time or with respect to a previous chosen phase diagram. Machine learning needs a training set, validation set and testing set. These sets should contain enough data and it needs to be determined if the availability of 2517 phase diagrams are enough and their quality suffices as it is essential that data cleansing is performed.

As tidal volume, breathing frequency, and the expiratory time are influence by the breathing strategy, calculation of these values during the total measurement can be indicative for the breathing strategy used at that moment. These parameters can be plotted relatively easily as the Matlab scripts already determine the actual duration of the selected breath for the phase diagram. This time can be easily converted into a breathing frequency by dividing 60 seconds by this breathing time. In addition, the expiratory time can be calculated by determining the period of positive pressure during this time frame. Concerning the tidal volume, this will be approached by calculation of the x. However, as the phase diagram is aligned to (0,0), the absolute minimal value should approach the tidal volume. It should be investigated whether combination of tidal volume, breathing frequency, expiratory time and the predefined parameters Aex_1, sphericity and triangularity can be combined into a model that correlates to the lung function changes. Subsequently, the ration between inspiration and expiration might also be indicative. However, the determination of the exact moment of the start of an inspiration or expiration is difficult. So, this needs to be automatically determined first in order to be able to calculate the ration between inspiration and expiration.

As the phase diagrams in Appendices E indicate a difference even without flow, applying a flow during an ECT likely magnifies this difference. In order to be able to determine if the lung function measurements were influenced by the use of Optiflow™ therapy, an ECT without and with the use of Optiflow™ should be compared. As bronchial hyperreactivity varies over time, these ECT should be close to each other and it is still possible that the difference in outcomes of the ECT can be explained by the episodic disease. To minimalize the influence of the episodic disease, it is desirable that the ECT without Optiflow™ therapy shows a moderate to severe uncontrolled asthma. Subsequently, the ECT with Optiflow™ should be performed within the next week without change of the medication. Using this research setup, the influence of the Optiflow™ therapy could be investigated with minimal effect of episodic asthma.

6. Conclusion

The report showed and discussed the results of the TBFV-curve study. In this study the correlation between exercise induced changes in lung function were compared to changes in the appearance of the phase diagram. A discrimination between healthy and unhealthy phase diagram is not yet assessed by a parameter although it is seen by naked eye. Further work is needed to determine the parameter that is able to indicate a correlate lung function changes to the appearance of the phase diagram.

7. References

1. Hagmeijer R, Venner CH, Thio BJ. *Towards a Clinical Decision Support System in High-Flow Ventilation Therapy: Integrated Respiration Monitoring*. Enschede
2. Dysart K, Miller TL, Wolfson MR, Shaffer TH. Research in high flow therapy: Mechanisms of action. *Respir Med*. 2009;103(10):1400-1405.
3. Franklin D, Babl FE, Schlapbach LJ, et al. A Randomized Trial of High-Flow Oxygen Therapy in Infants with Bronchiolitis. *N Engl J Med*. 2018;378(12):1121-1131.
4. Kepreotes E, Whitehead B, Attia J, et al. High-flow warm humidified oxygen versus standard low-flow nasal cannula oxygen for moderate bronchiolitis (HFWHO RCT): an open, phase 4, randomised controlled trial. *Lancet*. 2017;389(10072):930-939.
5. Milési C, Boubal M, Jacquot A, et al. High-flow nasal cannula: recommendations for daily practice in pediatrics. *Ann Intensive Care*. 2014;4(1):1-29.
6. Haq I, Gopalakaje S, Fenton AC, McKean MC, J. O'Brien C, Brodlie M. The evidence for high flow nasal cannula devices in infants. *Paediatr Respir Rev*. 2014;15(2):124-134.
7. Mikalsen IB, Davis P, Øymar K. High flow nasal cannula in children: a literature review. *Scand J Trauma Resusc Emerg Med*. 2016;24(1):1-93.
8. Nishimura M. High-flow nasal cannula oxygen therapy in adults. *J Intensive Care*. 2015;3(1):1-8.
9. Nishimura M. High-Flow Nasal Cannula Oxygen Therapy in Adults : Physiological Benefits, Indication, Clinical Benefits, and Adverse Effects. *Respir Care*. 2016;61(4):529-541.
10. Hebbink RHJ. Tidal breathing flow-volume loops in high-flow nasal cannula therapy. 2018.
11. Leonhardt S, Ahrens P, Kecman V. Analysis of Tidal Breathing Flow Volume Loops for Automated Lung-Function Diagnosis in Infants. *IEEE Trans Biomed Eng*. 2010;57(8):1945-1953.
12. van Leeuwen JC, Driessen JMM, de Jongh FHC, Anderson SD, Thio BJ. Measuring breakthrough exercise-induced bronchoconstriction in young asthmatic children using a jumping castle. *J Allergy Clin Immunol*. 2013;131(5):1427-1429.e5.
13. Anderson SD, Daviskas E. The mechanism of exercise-induced asthma is .... *J Allergy Clin Immunol*. 2000;106(3):453-459.
14. Panditi S. Perception of exercise induced asthma by children and their parents. *Arch Dis Child*. 2003;88(9):807-811.
15. Godfrey S, Springer C, Noviski N, Maayan C, Avital A. Exercise but not methacholine differentiates asthma from chronic lung disease in children. *Thorax*. 1991;46(7):488-492.
16. Rubin E, Reisner HM. The respiratory system. In: *Essentials of Rubin's Pathology*. 6th ed. Wolters Kluwer Health; 2013:317-350.
17. Driessen JM, van der Palen J, van Aalderen WM, de Jongh FH, Thio BJ. Inspiratory airflow limitation after exercise challenge in cold air in asthmatic children. *Respir Med*. 2012;106(10):1362-1368.
18. Schweitzer C, Abdelkrim I Ben, Ferry H, Werts F, Varechova S, Marchal F. Airway Response to Exercise by Forced Oscillations in Asthmatic Children. *Pediatr Res*. 2010;68(6):537-541.
19. Aggarwal B, Mulgirigama A, Berend N. Exercise-induced bronchoconstriction: prevalence, pathophysiology, patient impact, diagnosis and management. *npj Prim Care Respir Med*. 2018;28(1):31.
20. Pongdee T, Li JT. Exercise-induced bronchoconstriction. *Ann Allergy, Asthma Immunol*. 2013;110(5):311-315.
21. Miller MR. Standardisation of spirometry. *Eur Respir J*. 2005;26(2):319-338.
22. Moore VC. Spirometry: step by step. *Breathe*. 2012;8(3):232-240.
23. Palange P, Simonds AK. Pulmonary function testing. In: *ERS Handbook of Respiratory Medicine*. 2nd ed. European Respiratory Society; 2013:66-108.
24. Reinhold P, Smith HJ, Goldman MD. Forced oscillation technique and impulse oscillometry. *Eur Respir J*. 2005;31(31):35.

25. Thoracic Medical Systems Inc. *User Manual TremoFlo C-100 Airwave Oscillometry System.*; 2017.
26. Anderson GP. Endotyping asthma: new insights into key pathogenic mechanisms in a complex, heterogeneous disease. *Lancet.* 2008;372(9643):1107-1119.
27. Boron WF, Boulpaep EL. The respiratory system. In: *Medical Physiology.* Updated. GRUNE & STRATTON Incorporated; 2012:927-1142.
28. Global Initiative for Asthma. *Global Strategy for Asthma Management and Prevention - GINA Guidelines.*; 2018.
29. Brusselle GG, Maes T, Bracke KR. Eosinophils in the Spotlight: Eosinophilic airway inflammation in nonallergic asthma. *Nat Med.* 2013;19(8):977-979.
30. Awadh N, Muller NL, Park CS, Abboud RT, FitzGerald JM. Airway wall thickness in patients with near fatal asthma and control groups: assessment with high resolution computed tomographic scanning. *Thorax.* 1998;53(4):248-253.
31. Niimi A, Matsumoto H, Amitani R, et al. Airway Wall Thickness in Asthma Assessed by Computed Tomography. *Am J Respir Crit Care Med.* 2000;162(4):1518-1523.
32. K Kasahara, K Shiba, T Ozawa, K Okuda MA. Correlation between the bronchial subepithelial layer and whole airway wall thickness in patients with asthma. *Thorax.* 2002;57(3):242-246.
33. Hamid Q, Shannon J, Martin J. Breathing strategies in asthma and chronic obstructive pulmonary disease. In: *Physiologic Basis of Respiratory Disease.* Pmph USA Ltd Series. BC Decker, Incorporated; 2005:105-114.
34. Moeller A, Carlsen K-H, Sly PD, et al. Monitoring asthma in childhood: lung function, bronchial responsiveness and inflammation. *Eur Respir Rev.* 2015;24(136):204-215.
35. Kumar PJ, Clark ML. Respiratory disease. In: *Kumar & Clark's Clinical Medicine.* 7th ed. Saunders Elsevier; 2009:811-856.
36. Jubran A, Tobin MJ. Use of flow-volume curves in detecting secretions in ventilator-dependent patients. *Am J Respir Crit Care Med.* 1994;150(3):766-769.
37. Rubin BK. Secretion properties, clearance, and therapy in airway disease. *Transl Respir Med.* 2014;2(1):6.
38. Wesseling J. Forced oscillation technique and spirometry in cold air provocation tests. 1993:254-259.
39. Bors J. Pressure measurements during high flow nasal cannula (HFNC) therapy in infants with a severe airway infection. 2017.
40. Lee JH, Rehder KJ, Williford L, Cheifetz IM, Turner DA. Use of high flow nasal cannula in critically ill infants, children, and adults: a critical review of the literature. *Intensive Care Med.* 2013;39(2):247-257.
41. ter Woord HB. *Effect of Breathing on the Pressures in High Flow Nasal Cannula Therapy.* Enschede
42. Klooster S. Pressure - Flow Rate Relations in High Flow Therapy. Theory and Experiments. 2017;(June).
43. Sivieri EM, Gerdes JS, Abbasi S. Effect of HFNC flow rate, cannula size, and nares diameter on generated airway pressures: An in vitro study. *Pediatr Pulmonol.* 2012;48(5):506-514.
44. Hoppenbrouwer X. Pressure measurements during High Flow Nasal Cannula (HFNC) therapy in infants with a severe airway infection. 2016.
45. Morris MJ, Lane DJ. Tidal expiratory flow patterns in airflow obstruction. *Thorax.* 1981;36(2):135-142.
46. Morris MJ, Madgwick RG, Collyer I, Denby F, Lane DJ. Analysis of expiratory tidal flow patterns as a diagnostic tool in airflow obstruction. *Eur Respir J.* 1998;12(5):1113-1117.
47. Zheng C-J, Adams AB, McGrail MP, Marini JJ, Greaves IA. A proposed curvilinearity index for quantifying airflow obstruction. *Respir Care.* 2006;51(1):40-45.
48. Lødrup Carlsen KC, Stenzler A, Carlsen KH. Determinants of tidal flow volume loop indices in neonates and children with and without asthma. *Pediatr Pulmonol.* 1997;24(6):391-396.

49. van der Ent CK, Brackel HJL, Mulder P, Bogaard JM. Improvement of tidal breathing pattern analysis in children with asthma by on-line automatic data processing. *Eur Respir J.* 1996;9(6):1306-1313.
50. van der Ent CK, Brackel HJ, van der Laag J, Bogaard JM. Tidal breathing analysis as a measure of airway obstruction in children three years of age and older. *Am J Respir Crit Care Med.* 1996;153(4):1253-1258.
51. Seddon PC, Davis GM, Coates AL. Do tidal expiratory flow patterns reflect lung mechanics in infants? *Am J Respir Crit Care Med.* 1996;153(4):1248-1252.
52. Cutrera R, Filtchev SI, Merolla R, Willim G, Haluszka J, Ronchetti R. Analysis of expiratory pattern for monitoring bronchial obstruction in school-age children. *Pediatr Pulmonol.* 1991;10(1):6-10.
53. Zapletal A, Hladíková M, Chalupová J, Svobodová T, Vávrová V. Area under the Maximum Expiratory Flow-Volume Curve – A Sensitive Parameter in the Evaluation of Airway Patency. *Respiration.* 2008;75(1):40-47.
54. Majak P, Cichalewski Ł, Ożarek-Hanc A, Stelmach W, Jerzyńska J, Stelmach I. Airway response to exercise measured by area under the expiratory flow–volume curve in children with asthma. *Ann Allergy, Asthma Immunol.* 2013;111(6):512-515.
55. Crapo RO, Casaburi R, Coates AL, et al. Guidelines for methacholine and exercise challenge testing-1999. This official statement of the American Thoracic Society was adopted by the ATS Board of Directors, July 1999. *Am J Respir Crit Care Med.* 2000;161(1):309-329.
56. Bates JH, Schmalisch G, Filbrun D, Stocks J. Tidal breath analysis for infant pulmonary function testing. ERS/ATS Task Force on Standards for Infant Respiratory Function Testing. European Respiratory Society/American Thoracic Society. *Eur Respir J.* 2000;16(6):1180-1192.
57. Wijga AH, Buul LW van, Blokstra A, Wolse APH. *Astma Bij Kinderen.* Vol 77.; 2009.
58. Green SB. How Many Subjects Does It Take To Do A Regression Analysis. *Multivariate Behav Res.* 1991;26(3):499-510.
59. Schmidt M, Foitzik B, Wauer RR, Winkler F, Schmalisch G. Comparative Investigations of Algorithms for the Detection of Breaths in Newborns with Disturbed Respiratory Signals. *Comput Biomed Res.* 1998;31(6):413-425.
60. Tinitinallis JE. Pediatrics. In: *Tintinalli's Emergency Medicine, 7th Ed, McGraw-Hill, 2011: Tintinalli's Emergency Medicine,*. Tintinalli's Emergency Medicine,. Bukupedia; 2011:805.
61. Balady GJ, Arena R, Sietsema K, et al. Clinician's Guide to cardiopulmonary exercise testing in adults: a scientific statement from the American Heart Association. *Circulation.* 2010;122(2):191-225.
62. Johnson BD, Weisman IM, Zeballos RJ, Beck KC. Emerging Concepts in the Evaluation of Ventilatory Limitation During Exercise. *Chest.* 1999;116(2):488-503.
63. Pellegrino R, Brusasco V, Rodarte JR, Babb TG. Expiratory flow limitation and regulation of end-expiratory lung volume during exercise. *J Appl Physiol.* 1993;74(5):2552-2558.

Appendices

A. Study information letter and consent form

A.1. Parental information letter

de TBFV-curve studie

INFORMATIE OVER DEELNAME AAN EEN WETENSCHAPPELIJK ONDERZOEK

Neusbril en longfunctie,
de TBFV-curve studie

ONDERZOEKERS: *dr. B.J. Thio, Kinderarts / K.A.E. Wijlens, master student Technische Geneeskunde*

Geachte heer/mevrouw,

U heeft aangegeven geïnteresseerd te zijn in deelname van uw kind aan het bovengenoemde medisch-wetenschappelijk onderzoek. Dit onderzoek is opgezet in het MST om bij 25 kinderen te testen of met een neusbril (Optiflow), die gebruikt wordt op de afdeling bij kinderen die ondersteuning nodig hebben bij het ademen, we kunnen meten hoe de longen functioneren.

Voordat u en uw kind de beslissing nemen, is het belangrijk om meer te weten over het onderzoek. Lees deze informatiebrief rustig door. Bespreek het met elkaar, vrienden of familie. Verdere algemene informatie over meedoen aan zo'n onderzoek staat in de bijgevoegde brochure 'Medisch-wetenschappelijk onderzoek'.

Hebben u of uw kind na het lezen van de informatie nog vragen? Dan kunt u terecht bij de onderzoekers. Ook kunt u het bespreken met de onafhankelijke arts, die veel weet van het onderzoek. Op bladzijde 3 vindt u de contactgegevens (vraag 12).

1. Wat is het doel van het onderzoek?

In de winterperiode worden veel kinderen opgenomen met benauwdheid waardoor ze in de problemen kunnen komen met ademen. Om het ademen gemakkelijker te maken kunnen ze een neusbril krijgen, zoals op de afbeelding te zien is. De arts kijkt naar het kind om in te schatten of de neusbril helpt en welke instellingen er nodig zijn om het kind te ondersteunen met ademen. Met dit onderzoek willen we kijken of we kunnen meten hoe de long functioneren tijdens het gebruik van de neusbril.

2. Hoe wordt het onderzoek uitgevoerd?

Uw kind is ingepland voor een inspanningstest die volgens normaal protocol zal verlopen, zoals de kinderarts verteld heeft. De enige toevoeging hierop is dat uw kind na de inspanning de neusbril gaat dragen tot het einde van de test. Uw kind kan normaal door de neusbril ademen. De inspanningstest zal niet langer duren dan normaal.

3. Wat wordt er van je verwacht?

Er wordt van uw kind verwacht dat hij/zij de neusbril draagt tijdens de geplande inspanningstest.

4. Wat zijn mogelijke voor- en nadelen van deelname aan dit onderzoek?
Uw kind heeft zelf geen direct voordeel van deelname aan dit onderzoek. Wel geeft de inspanningstest in de astma van uw kind. Ook is het mogelijk dat het onderzoek tot nieuwe inzichten kan leiden die de behandeling van longproblemen tijdens een opname waarbij beademing nodig is met een neusbril kan verbeteren. Een nadeel van deelname kan zijn dat het uw kind het niet zo prettig vindt om de neusbril te dragen gedurende een gedeelte van de inspanningstest. De belasting van het onderzoek is zo klein mogelijk gehouden en er worden geen extra medicijnen toegediend. Er zijn dan ook geen risico's verbonden aan deelname aan dit onderzoek.

5. Wat gebeurt er als u of uw kind niet wensen deel te nemen aan dit onderzoek?
U en uw kind beslissen zelf of uw kind aan het onderzoek deelneemt. Deelname is vrijwillig. Als u of uw kind besluiten niet mee te doen, hoeft u verder niets te doen. U hoeft niets te tekenen. U hoeft ook niet te zeggen waarom uw kind niet wil meedoen. Als uw kind wel meedoet, kunt u of uw kind zich altijd bedenken en toch stoppen. Zo wordt na de inspanning gevraagd aan uw kind gevraagd of hij/zij nog steeds mee wil doen met het onderzoek. Ook tijdens het onderzoek mag uw kind op elk moment stoppen. Als uw kind zich tijdens het onderzoek verzet – denk hierbij aan sterke angst, verdriet of boosheid – dan wordt het onderzoek gestopt.

6. Wat gebeurt er als het onderzoek is afgelopen?
Na de inspanningstest is het onderzoek afgerond.

7. Is uw kind verzekerd wanneer hij/zij aan het onderzoek meedoet?
Deelname aan dit onderzoek heeft een dermate laag risico dat ontheffing van verzekering is verkregen.

8. Worden u en uw kind geïnformeerd als er tussentijds voor u relevante informatie over de studie bekend wordt?
Als blijkt dat tussendoor relevante informatie bekend wordt, bespreken we dat direct met u. U en uw kind beslissen dan zelf of uw kind met het onderzoek wil stoppen of doorgaan. Als uw kind zijn/haar veiligheid of welbevinden in gevaar is, stoppen we direct met het onderzoek.

9. Wat gebeurt er met de gegevens van uw kind?
Alle gegevens van uw kind zijn vertrouwelijk. De meetresultaten worden gecodeerd opgeslagen, nooit met naam. De sleutel voor de code blijft bij de onderzoekers van de Kindergeneeskunde. Ook in rapporten over het onderzoek wordt alleen die code gebruikt.
Sommige mensen mogen uw medische en persoonsgegevens inzien. Dit is om te controleren of het onderzoek goed en betrouwbaar uitgevoerd is. Algemene informatie hierover vindt u in de brochure 'Medisch-wetenschappelijk onderzoek'.
Mensen die de gecodeerde meetresultaten mogen inzien zijn: De onderzoekers van de kindergeneeskunde, de Medisch Ethische Toetsingscommissie Twente (METC Twente), controleurs vanuit MST en de Inspectie voor de Gezondheidszorg. Zij houden de gegevens van uw kind geheim.
De gecodeerde onderzoeksgegevens worden na afloop van het onderzoek 15 jaar bewaard.
Misschien kunnen we daar later een ander onderzoek mee uitvoeren binnen hetzelfde onderzoeksgebied. Als u of uw kind dat niet willen, kunt u dit aangeven op het Toestemmingsformulier.
Als u of uw kind aan het einde van de studie de resultaten via e-mail willen ontvangen, dan kunt u dat aangeven op het Toestemmingsformulier. Op het Toestemmingsformulier kunt u daarnaast aangeven of u en uw kind in de toekomst opnieuw benadert mogen worden voor deelname aan nieuw onderzoek.
Daarnaast zullen we de behandelend kinderarts van uw kind op de hoogte stellen in het geval van onverwachte bevindingen.

10. Is er een vergoeding wanneer u besluit aan dit onderzoek mee te doen?
Voor deelname aan het onderzoek wordt geen vergoeding uitgekeerd.

11.Welke medisch-ethische toetsingscommissie heeft dit onderzoek goedgekeurd?
Voor dit onderzoek is toestemming verkregen van de Raad van Bestuur van het MST Enschede na een positief oordeel van de Medisch Ethische Toetsingscommissie Twente (METC Twente). Meer informatie over de goedkeuring vindt u in de Algemene brochure (Bijlage 1).

12. Willen u of uw kind verder nog iets weten?
U en uw kind hebben minimaal vijf werkdagen bedenktijd voor deelname aan dit onderzoek. Als u of uw kind nog vragen hebben over het onderzoek, kunt u contact opnemen met uitvoerend onderzoeker mevr. K.A.E. Wijlens (tel. 06-50981962 en mail *k.wijlens@mst.nl)* of de behandelend kinderarts via telefoonnummer 053-4872310.

13. Hoe te handelen bij klachten?
Als u of uw kind klachten hebben kunt u dit melden aan de onderzoeker of aan uw behandelend arts.

14. Wilt u deelnemen aan het onderzoek?
Dan verzoeken wij u om het bijgevoegde toestemmingsformulier mee te nemen naar uw afspraak op het OCON. Indien hierbij 1 van beide ouders en/of voogd niet aanwezig is, verzoeken wij u het toestemmingsformulier van te voren door de afwezige ouder/voogd in te laten vullen. Dit aangezien van beide ouders de handtekening op het toestemmingsformulier behoort te staan.

Met vriendelijke groet,

Dr. Boony Thio, Hoofdonderzoeker en Kinderarts
Kim Wijlens, uitvoerend onderzoeker en master student Technische Geneeskunde

Bijlagen
- Algemene brochure medisch-wetenschappelijk onderzoek met mensen
- Toestemmingsformulier

Toestemmingsformulier

Titel van het onderzoek:

Neusbril en longfunctie,

de TBFV-curve studie

ToetsingOnline nr:

Versie 2, 21-2-2019

Ik ben gevraagd om toestemming te geven voor deelname van mijn kind aan dit medisch-wetenschappelijke onderzoek:

Naam proefpersoon (kind): Geboortedatum: __ / __ / __

Ik heb de informatiebrief (versie 2, datum: 7-6-2019) voor de proefpersoon gelezen. Ik kon aanvullende vragen stellen. Mijn vragen zijn naar tevredenheid beantwoord. Ik had genoeg tijd om te beslissen of mijn kind mag meedoen.

Ik weet dat meedoen helemaal vrijwillig is. Ik weet dat mijn kind of ik op ieder moment kunnen beslissen om toch niet mee te doen. Daarvoor hoeft mijn kind of ik geen reden op te geven.

Ik weet dat sommige mensen de gegevens van mijn kind kunnen zien. Deze personen staan vermeld in de informatiebrief.

Ik geef toestemming om mijn behandelend kinderarts op de hoogte stellen van eventuele onverwachte bevindingen.

Ik geef toestemming om de gegevens van mijn kind te gebruiken, voor de doelen die in de informatiebrief staan.

Ik geef toestemming om de onderzoeksgegevens van mijn kind 15 jaar na afloop van dit onderzoek te bewaren.

Ik geef toestemming voor het gebruiken van de geanonimiseerde onderzoeksgegevens om later een ander onderzoek mee uitvoeren binnen hetzelfde onderzoeksgebied indien relevant.

☐ Ja

☐ Nee

Ik geef toestemming om mij en mijn kind in de toekomst opnieuw te benaderen voor deelname aan nieuw onderzoek.

☐ Ja

☐ Nee

Ik wil de uitslag van het onderzoek via de mail ontvangen:

☐ Ja , graag op het volgende e-mail adres: .....

☐ Nee

Ik wil mijn kind laten meedoen aan dit onderzoek.

Naam ouder/verzorger*:	Naam ouder/verzorger*:
Datum: __ - __ - __	Datum: __ - __ - __
Handtekening:	Handtekening: .....

Ik verklaar hierbij dat ik de ouders van deze proefpersoon volledig heb geïnformeerd over het genoemde onderzoek.

Als er tijdens het onderzoek informatie bekend wordt die de toestemming van de proefpersoon zou kunnen beïnvloeden, dan breng ik hem/haar daarvan tijdig op de hoogte.

Een kopie van de informatiebrief en ondertekende verklaring wordt meegegeven aan de proefpersoon.

Naam onderzoeker:	Aanvullende informatie is gegeven door (indien van toepassing):
Datum: __ - __ - __	Datum: __ - __ - __
Handtekening:	Handtekening: .....

* Doorhalen wat niet van toepassing is.

A.2. Children information letter (4-11 years)

INFORMATIE OVER HET MEEDOEN AAN EEN ONDERZOEK

Neusbril en longfunctie

de TBFV-curve studie

ONDERZOEKERS: *Dokter Thio, kinderarts en Kim Wijlens, student Technische Geneeskunde*

Beste [*naam kind*],

Leuk dat je misschien wilt meedoen aan dit onderzoek. Voordat je definitief de beslissing neemt, is het belangrijk om meer te weten over het onderzoek. Lees deze informatiebrief rustig door en praat erover met je ouders. Heb je na het lezen van de informatie nog vragen? Dan kunnen jij of je ouders altijd contact opnemen met ons.

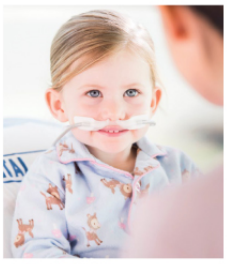

Waarom doen we dit onderzoek?
In de winter periode worden veel kinderen op genomen doordat ze problemen krijgen met ademen. Om de kinderen te helpen met ademen kunnen ze een neusbril krijgen, zoals op het plaatje hier naast te zien is. Dit helpt de kinderen om makkelijker te ademen. De arts kijkt naar het kind om te kijken of de neusbril helpt. Met dit onderzoek willen we kijken of we kunnen meten hoe het met ademen gaat.

Wat houdt het onderzoek in?
Binnenkort kom je samen met je ouders langs voor een inspanningstest. Bij een inspanningstest kijken we voor en na inspanning hoe je adem haalt met een blaastest. Voor dit onderzoek vragen we om de neusbril te dragen bij de inspanningstest nadat je op het springkussen of de loopband bent geweest tot na de laatste blaastest. Je kunt tijdens het dragen van de neusbril normaal door je neus ademen.

Wat als ik niet meer mee wil doen aan dit onderzoek?
Je beslist samen met je ouders of je mee wilt doen aan het onderzoek. Als je niet mee wilt doen hoef je verder niks te doen. Ook kun je op elk moment tijdens het onderzoek zonder reden stoppen met het onderzoek als je dat wilt.

Wil je verder nog iets weten?
Als je nog vragen hebt over het onderzoek, kunnen jij of je ouders altijd contact opnemen met Kim Wijlens (tel. 06-50981962 of via mail *k.wijlens@mst.nl)* of jouw behandelend kinderarts via telefoonnummer 053-4872310.

A.3. Children information letter (12-16 years)

INFORMATIE OVER DEELNAME AAN EEN WETENSCHAPPELIJK ONDERZOEK

Neusbril en longfunctie

de TBFV-curve studie

ONDERZOEKERS: *dr. B.J. Thio, Kinderarts / K.A.E. Wijlens, master student Technische Geneeskunde*

Beste [*naam kind*],

Je hebt aangegeven geïnteresseerd te zijn in deelname aan het bovengenoemde medisch-wetenschappelijk onderzoek. Dit onderzoek is opgezet in het MST om testen of met een neusbril (Optiflow), die gebruikt wordt op de afdeling bij kinderen die ondersteuning nodig hebben bij het ademen, we kunnen meten hoe de longen functioneren.

Voordat je de beslissing neemt, is het belangrijk om meer te weten over het onderzoek. Lees deze informatiebrief rustig door. Bespreek het met je ouders. Verdere algemene informatie over meedoen aan een onderzoek staat in de bijgevoegde brochure 'Medisch-wetenschappelijk onderzoek'.

Hebben je na het lezen van de informatie nog vragen? Dan kunnen jij of je ouders terecht bij de onderzoekers. Ook kan je het bespreken met de onafhankelijke arts, die veel weet van het onderzoek. Op bladzijde 3 vind je de contactgegevens (vraag 12).

1. Wat is het doel van het onderzoek?

In de winterperiode worden veel kinderen opgenomen met benauwdheid waardoor ze in de problemen kunnen komen met ademen. Om het ademen gemakkelijker te maken kunnen ze een neusbril krijgen, zoals op de afbeelding te zien is. De arts kijkt naar het kind om in te schatten of de neusbril helpt en welke instellingen er nodig zijn om het kind te ondersteunen met ademen. Met dit onderzoek willen we kijken of we kunnen meten hoe de long functioneren tijdens het gebruik van de neusbril.

2. Hoe wordt het onderzoek uitgevoerd?

Je bent ingepland voor een inspanningstest die volgens normaal protocol zal verlopen, zoals de kinderarts verteld heeft. De enige toevoeging hierop is dat je na inspanning de neusbril draagt tot het einde van de test. Je kunt gewoon door de neusbril ademen. De inspanningstest zal niet langer duren dan normaal.

3. Wat wordt er van je verwacht?

Er wordt van je verwacht dat je de neusbril draagt tijdens de geplande inspanningstest.

4. Wat zijn mogelijke voor- en nadelen van deelname aan dit onderzoek?
Je zult zelf geen direct voordeel hebben van deelname aan dit onderzoek. Wel geeft de inspanningstest een inzicht in je astma. Ook is het mogelijk dat het onderzoek tot nieuwe inzichten kan leiden die de behandeling van longproblemen met een neusbril kan verbeteren. Een nadeel van deelname kan zijn dat je de neusbril niet zo prettig zit. De belasting van het onderzoek is zo klein mogelijk gehouden en er worden geen extra medicijnen toegediend. Er zijn dan ook geen risico's verbonden aan deelname aan dit onderzoek.

5. Wat gebeurt er als je niet wenst deel te nemen aan dit onderzoek?
Je beslist samen met je ouders of je aan het onderzoek deelneemt. Deelname is vrijwillig. Als je besluit niet mee te doen, hoef je verder niets te doen. Je hoeft niets te tekenen. Je hoeft ook niet te zeggen waarom je niet wilt meedoen. We zullen ook na de inspanning vragen of je nog steeds mee wil doen met het onderzoek. Als je wel meedoet, kun je je altijd bedenken en stoppen. Ook tijdens het onderzoek mag je op elk moment stoppen.

6. Wat gebeurt er als het onderzoek is afgelopen?
Na de inspanningstest is het onderzoek afgerond.

7. Ben je verzekerd wanneer je aan het onderzoek meedoet?
Deelname aan dit onderzoek heeft een dermate laag risico dat ontheffing van verzekering is verkregen. Meer informatie over de algemene verzekering kun je vinden in de Algemene Brochure.

8. Word je geïnformeerd als er tussentijds voor jou relevante informatie bekend wordt?
Als blijkt dat tussendoor relevante informatie over de studie bekend wordt, bespreken we dat direct met jou en je ouders. Jullie beslissen dan zelf of je met het onderzoek wilt stoppen of doorgaan. Als je veiligheid of welbevinden in gevaar is, stoppen we direct met het onderzoek.

9. Wat gebeurt er met jouw gegevens?
Al jouw gegevens blijven vertrouwelijk. De meetresultaten worden gecodeerd opgeslagen, nooit met naam. De sleutel voor de code blijft bij de onderzoekers van de Kindergeneeskunde. Ook in rapporten over het onderzoek wordt alleen die code gebruikt.
Sommige mensen mogen je medische en persoonsgegevens inzien. Dit is om te controleren of het onderzoek goed en betrouwbaar uitgevoerd is. Algemene informatie hierover vind je in de brochure 'Medisch-wetenschappelijk onderzoek'.
Mensen die de gecodeerde meetresultaten mogen inzien zijn: de onderzoekers van de kindergeneeskunde, de Medisch Ethische Toetsingscommissie Twente (METC Twente), controleurs vanuit het MST en de Inspectie voor de Gezondheidszorg. Zij houden jouw gegevens geheim.
De gecodeerde onderzoeksgegevens worden na afloop van het onderzoek 15 jaar bewaard. Misschien kunnen we daar later een ander onderzoek mee uitvoeren binnen hetzelfde onderzoeksgebied. Als je dat niet wilt, kun je dit aangeven op het Toestemmingsformulier. Als je aan het einde van de studie de resultaten via e-mail wilt ontvangen, dan kun je dat aangeven op het Toestemmingsformulier. Daarnaast zullen we jouw behandelend kinderarts op de hoogte stellen in het geval van onverwachte bevindingen.

10. Is er een vergoeding wanneer je besluit aan dit onderzoek mee te doen?
Voor deelname aan het onderzoek wordt geen vergoeding uitgekeerd.

11. Welke medisch-ethische toetsingscommissie heeft dit onderzoek goedgekeurd?
Voor dit onderzoek is toestemming verkregen van de Raad van Bestuur van het MST Enschede na een positief oordeel van de Medisch Ethische Toetsingscommissie Twente (METC Twente). Meer informatie over de goedkeuring vind je in de Algemene brochure (Bijlage 1).

12. Wil je verder nog iets weten?
Je hebt minimaal vijf werkdagen bedenktijd voor deelname aan dit onderzoek. Als je nog vragen hebt over het onderzoek, kun je zelf of je ouders contact opnemen met uitvoerend onderzoeker K.A.E. Wijlens (tel. 06-50981962 en mail *k.wijlens@mst.nl)* of de behandelend kinderarts via telefoonnummer 053-4872310.

13. Hoe te handelen bij klachten?
Als je klachten hebt, kun je zelf of je ouders dit melden aan de onderzoeker of aan je behandelend arts.

Met vriendelijke groet,

Dr. Boony Thio, hoofdonderzoeker, kinderarts
Kim Wijlens, uitvoerend onderzoeker, master student Technische Geneeskunde

Bijlagen
- Algemene brochure medisch-wetenschappelijk onderzoek met mensen
- Toestemmingsformulier

Toestemmingsformulier

Titel van het onderzoek:

Neusbril en longfunctie

de TBFV-curve studie

ToetsingOnline nr:
Versie 1, 11-2-2019

Ik ben gevraagd om toestemming te geven voor deelname aan dit medisch-wetenschappelijke onderzoek: De TBFV-curve studie.

Ik heb de informatiebrief (versie 1, datum: 7-6-2019) voor de proefpersoon gelezen. Ik kon aanvullende vragen stellen. Mijn vragen zijn naar tevredenheid beantwoord. Ik had genoeg tijd om te beslissen of ik meedoe.

Ik weet dat meedoen helemaal vrijwillig is. Ik weet dat ik op ieder moment kan beslissen om toch niet mee te doen. Daarvoor hoef ik geen reden te geven.

Ik weet dat sommige mensen mijn gegevens kunnen zien. Die mensen staan vermeld in de informatiebrief.

Ik geef toestemming om mijn behandelend kinderarts op de hoogte stellen van onverwachte bevindingen.

Ik geef toestemming om mijn gegevens te gebruiken, voor de doelen die in de informatiebrief staan.

Ik geef toestemming om mijn onderzoeksgegevens 15 jaar na afloop van dit onderzoek te bewaren.

Ik geef toestemming om in de toekomst opnieuw gevraagd te worden voor deelname aan nieuw onderzoek.

☐ Ja

☐ Nee

Ik wil de uitslag van het onderzoek via de mail ontvangen:

☐ Ja , graag op het volgende e-mail adres: .....

☐ Nee

Ik wil meedoen aan dit onderzoek.

Naam proefpersoon: .....
Handtekening: ..... Datum : _ / _ / _

Ik verklaar hierbij dat ik deze proefpersoon volledig heb geïnformeerd over het genoemde onderzoek.

Als er tijdens het onderzoek informatie bekend wordt die de toestemming van de proefpersoon zou kunnen beïnvloeden, dan breng ik hem/haar daarvan tijdig op de hoogte.

Een kopie van de informatiebrief en ondertekende verklaring wordt meegegeven aan de proefpersoon.

Naam onderzoeker:	Aanvullende informatie is gegeven door (indien van toepassing):
Datum: __ - __ - __	Datum: __ - __ - __
Handtekening:	Handtekening: .....

B. Clinical research form

Ocon Invullijst – TBFC-curve

Datum: ... / ... / 2019

Anamnese

Klachten: Benauwd / Hoesten / Piepen / Kortademig / ..... / .....

Frequentie klachten: ..... per week 's nachts: Ja / Nee Bij inspanning: Ja / Nee

Sport: ..... Aantal uren per week: .....

Astma medicatie: ..... (...dd...) ..... (...dd...)

..... (...dd...) ..... (...dd...)

Therapie trouw?: Ja / Nee .....

Allergisch?: Ja / Nee / ?? > zoja wat, ... All. Test: Ja / Nee RAST/HPT

Familie?: Ja / Nee / ?? > zoja wat, ...

Prematuur?: Ja/Nee Roken:Rookt zelf/Ouders binnen/Ouders buiten/Niet roken Koffie: Ja/Nee

Probleem gat bij zwemmen?: Ja / Nee

LO

Meyers: Ja / Nee Dennie-Morgan Lines: Ja / Nee

Lengte: ..... cm Gewicht: ..... kg

Longfunctie

Tijdstip	FEV_1	%	FEV0.5	Opmerkingen
Baseline				
T=1				
T=3				
T=6				
(T=9)				
Na Salbutamol				
Referentiewaarde				

FOT

Tijdstip	R_5	X_5	AX	$R_5 - R_{20}$
Baseline				
T=5				
Na Salbutamol				
Referentiewaarde				

Opmerkingen

.....

.....

.....

.....

.....

.....

.....

C. Pilot measurements

Previous experiments, using the pressure sensor in subjects with bronchiolitis, revealed that many peaks were observable that could possibly be caused by sneezing, coughing, drinking or moving [39,44]. In vitro experiments also showed an influence of the insertion length of the nasal prongs [10]. In addition, the measurement of the ECT take up to 15 minutes which makes it very likely that manipulations to the signal occur. To investigate these manipulations to the pressure measurements, pilot measurements were conducted. Four healthy volunteers were asked to wear the nasal cannula and perform lung function measurements, instructed to swallow, clear the throat, cough, itch the nose and reposition the prongs. Those were manipulations were chosen as these are regularly seen by the ECT.

Lung function measurement

During lung function measurements, the subject breaths through his mouth and therefore there is almost no change in the pressure signal which can be observed in figure 51. As a spirometry measurement uses a forced manoeuvre, some little change could arise. The nose clip closes the nose off, however, the position of the nose clip determines the amount nose breathing during a lung function measurement.

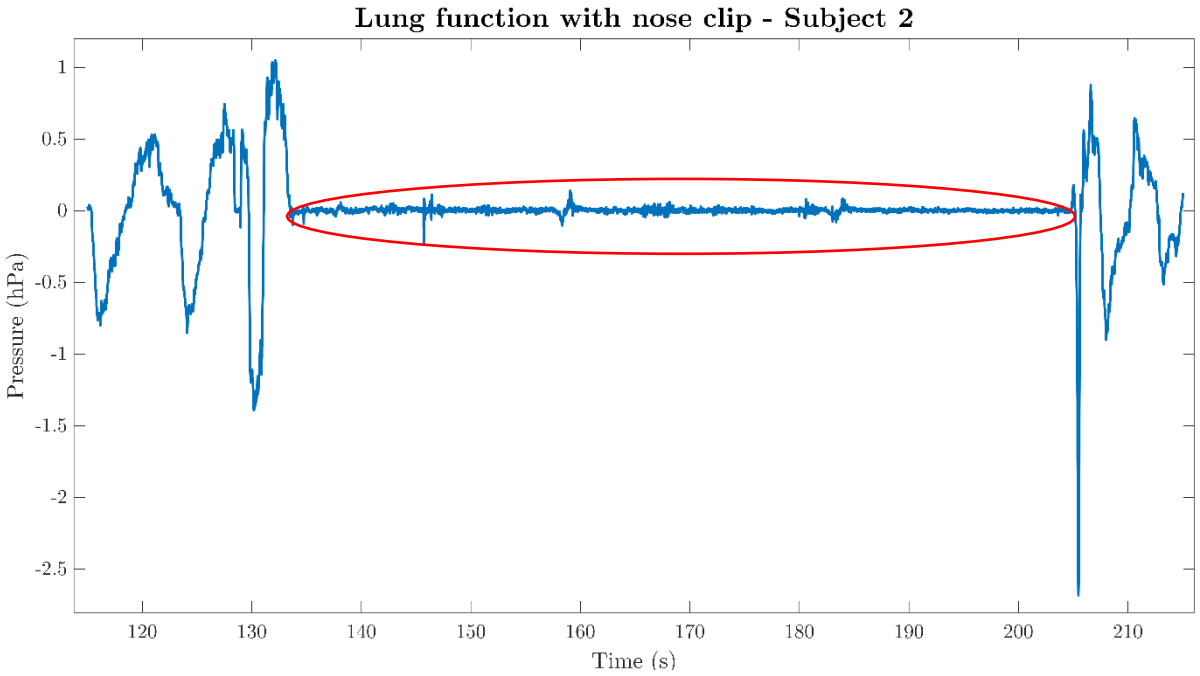

Figure 51: Pressure signal with lung function measurement in the red circle.

Repositioning of the nasal cannula

If the nasal cannula is repositioned, often the volunteers held their breath for the duration of that moment or breathing was shifted from nose to mouth. See figure 52 for the result of the manipulation in the pressure signal.

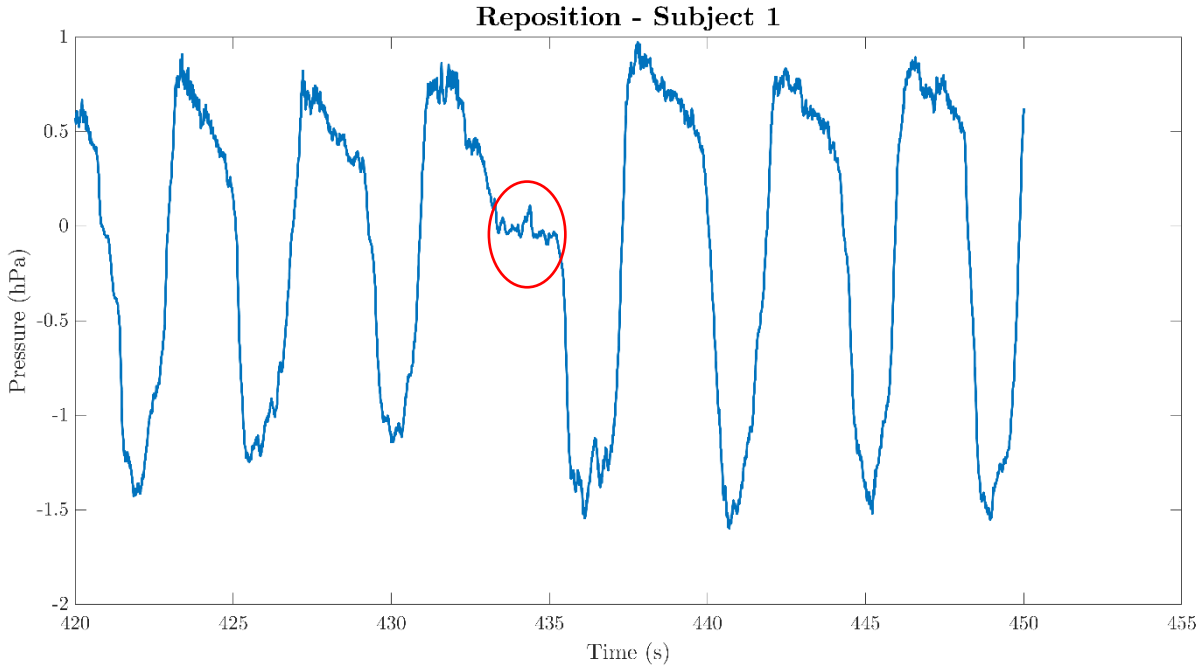

Figure 52: Repositioning of the nasal cannula.

Swallowing

When a subject swallows, a negative peak is generated with a higher amplitude compared to normal breathing. Figure 53 shows the negative peak generated by swallowing.

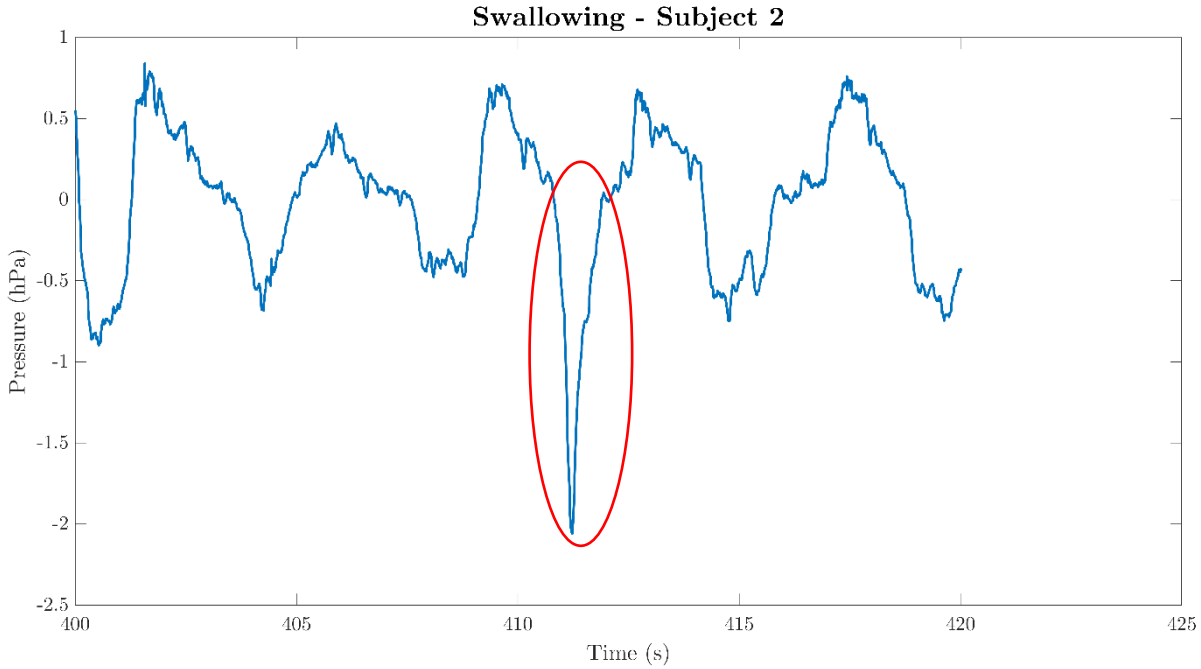

Figure 53: Pressure signal, the subject swallowed in the red circle.

Nose itching

During itching the nose, the pressure stabilizes around 0 Pa and shows spikes, observable in figure 54.

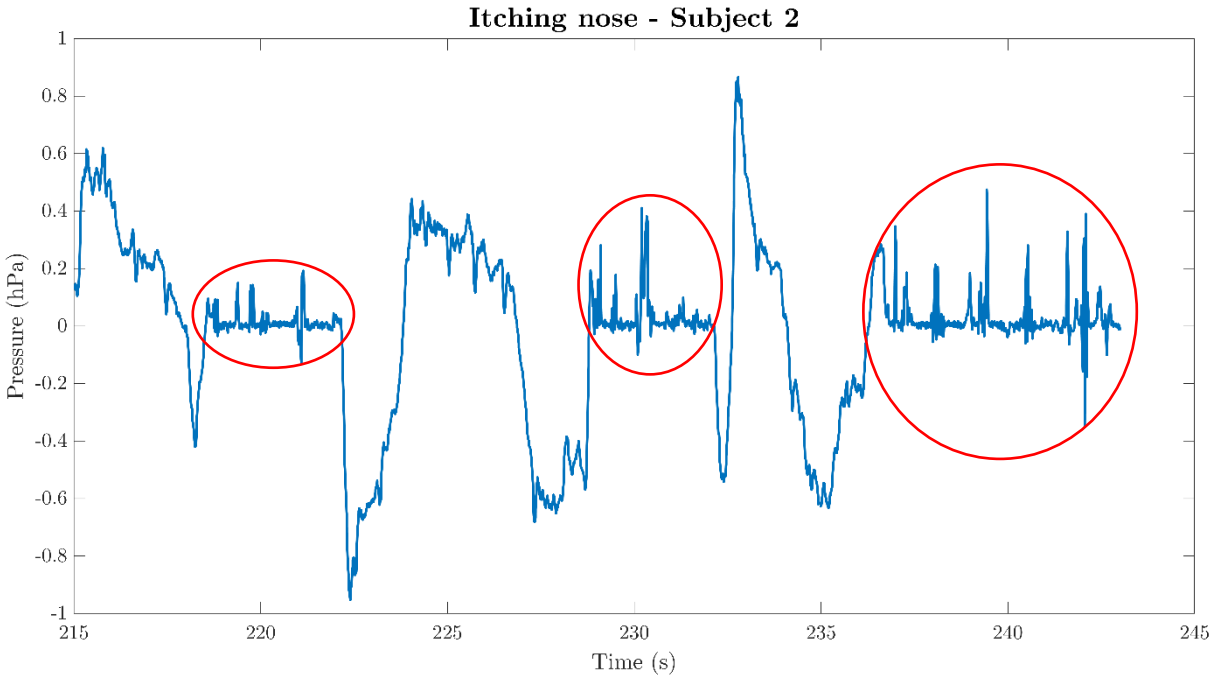

Figure 54: Periods of nose itching are observable in the red circles.

Clearing throat

Clearing the throat results in smaller peaks with a higher amplitude compared to normal breathing. The degree of clearing the throat influences the amplitude, see figure 55.

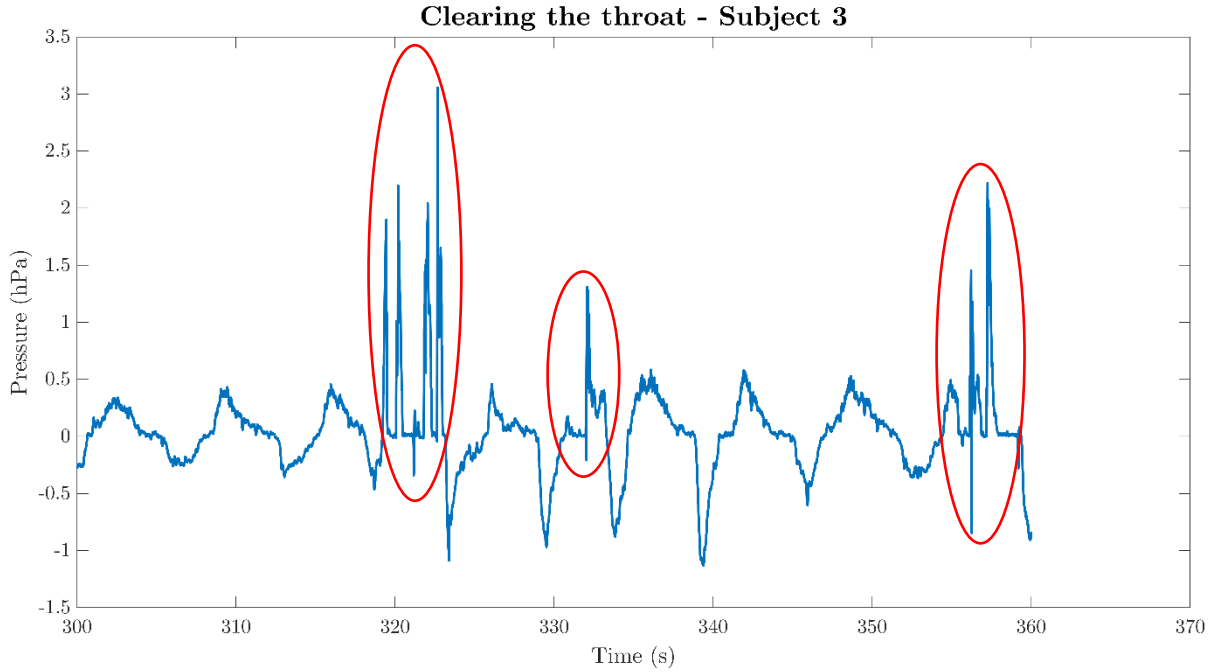

Figure 55: Periods of clearing the throat are observable in the red circles.

Coughing

Coughing appears with the same characteristics as clearing the throat, which consist of small spikes. The influence of coughing on the pressure signal is observable in figure 56.

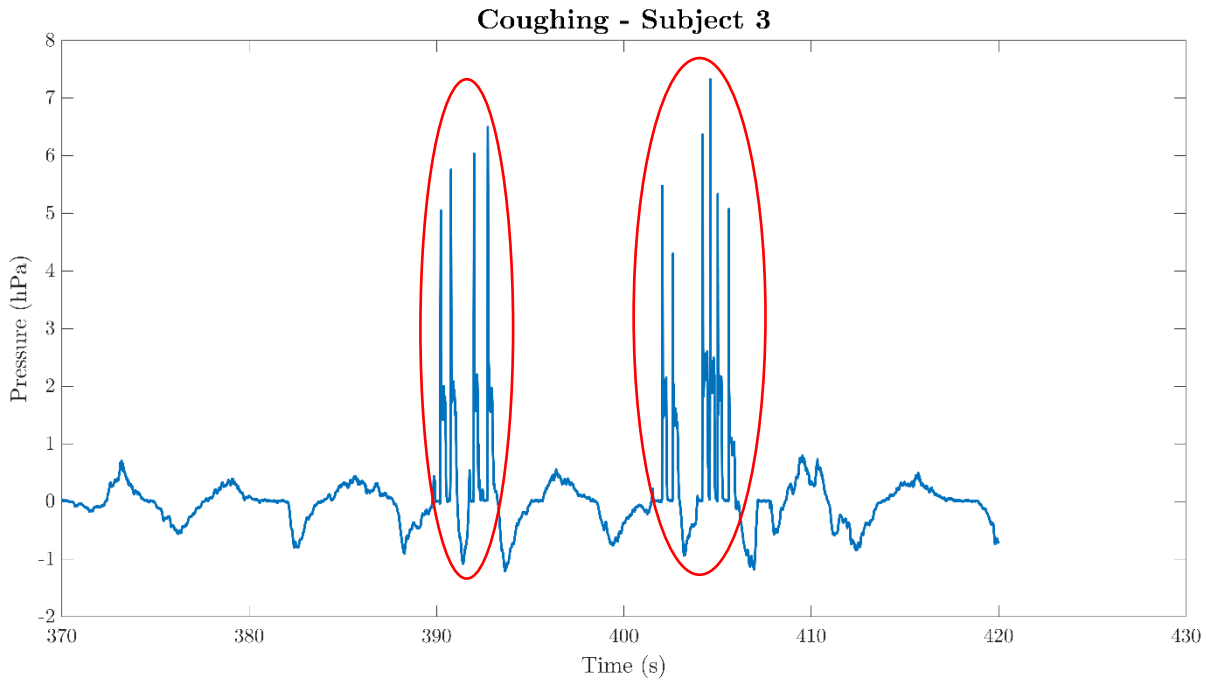

Figure 56: Three periods of coughing are observable in the red circles.

Movement

Different variations in movement of the head and parts of the measurement setup all appear to have no effect on the pressure signal. In figure 57, the influence of horizontal movement of the head can be observed.

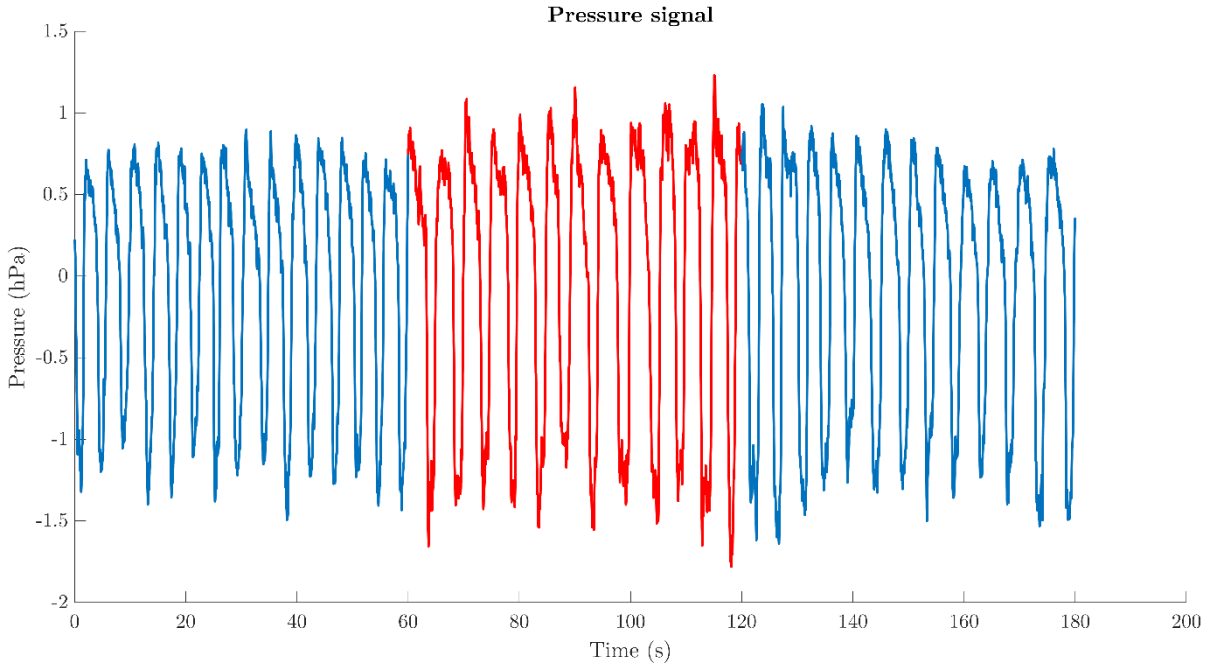

Figure 57: Pressure signal with horizontal movement of the head in red.

Failure of LabVIEW 2017 application

Using the LabVIEW 2017 application, the phase diagram can be viewed in real-time. However, during the pilot measurements errors appeared resulting in a default value, see figure 58. Therefore, the application of the device itself (OMEGA) is used during further measurements. This application is only able to show the current measurement value and data can be obtained after a measurement.

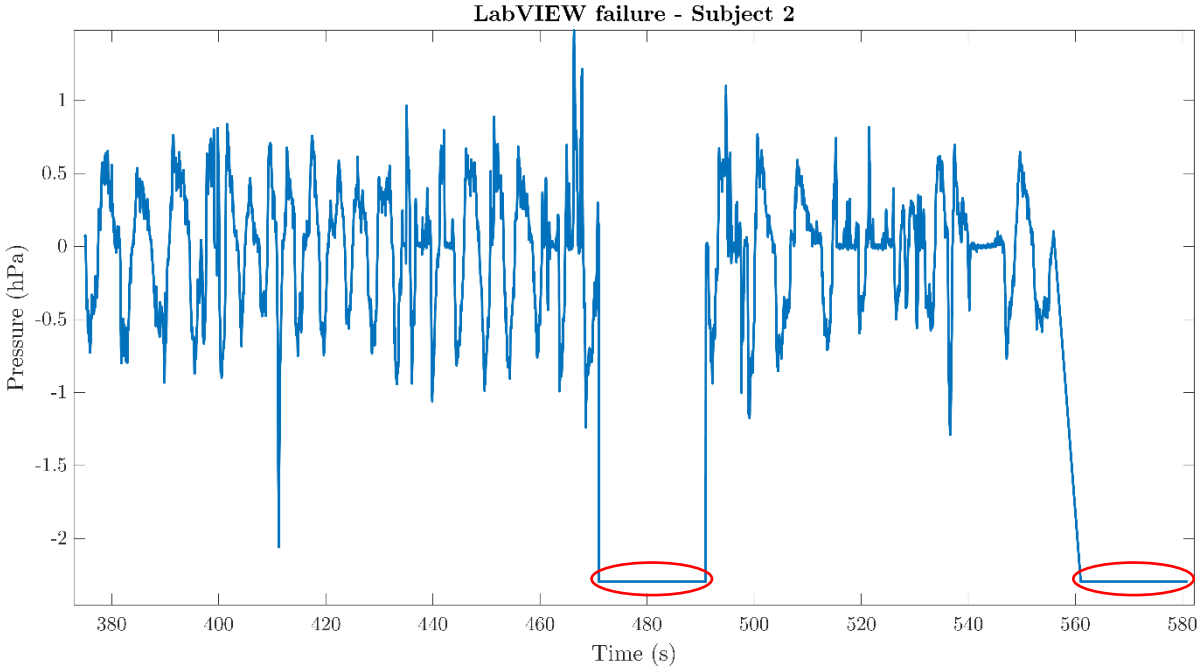

Figure 58: Failure of LabVIEW 2017 results in a constant default value until the program is reset.

Data pre-processing

Concluding, the effect of the manipulations described above, spikes and segments around zero are observed. Filtering the data with for example a bandpass filter around the breathing frequency only smoothens the signal but is not able to remove the effect of manipulations. Therefore, the characteristics of the manipulations are used to determine suitable functions to localize these manipulations. After localization, the manipulations can be removed by locating the minimum and remove the segment in between. The minimum are used instead of the minimal segment or the maximum as the minima are used for the division into breaths by the function 'FUN_periodic_cutter', see Appendix D.3 for explanation of the function.

Zero segments

In order to locate the segment in which manipulations occur that result in pressures around zero the Matlab functions movmean, movmedian, movsum, movstd, movvar, and movmad were investigated. Movmean, movmedian, and movsum calculate respectively the mean, median, and sum over a sliding window of length k. When k is odd, the window is centered about the element in the current position, therefore, odd k's have been investigated. This is also applicable for the other Matlab functions mentioned. Regarding the movstd, the standard deviation is calculated over a sliding window of length k. For the movvar this is achieved using the variance. The function movmad computes the median absolute deviation over a sliding window with length k. For the above mentioned functions, k's of 5, 11, and 15 samples were computed and compared to the pressure signal in which manipulations occur. The movmean, movmedian, and movsum only smoothen the signal and are therefore not suitable to locate or remove segments

with zero pressure due to the occurrence of manipulations. The movstd, movvar, and movmad are all around zero if for example a lung function is performed. The movstd has been chosen as the value during the manipulation is closer to zero and had less outliers to higher values compared to movvar and movmad. The movstd for 5, 11, and 15 samples is observable in figure 59. A window length of 11 samples is chosen as the amplitude is higher if the pressure is nonzero in comparison to 5 samples. Regarding using a window length of 15 samples, there is no further improvement in the distinction between zero and nonzero segment compared to 11 samples.

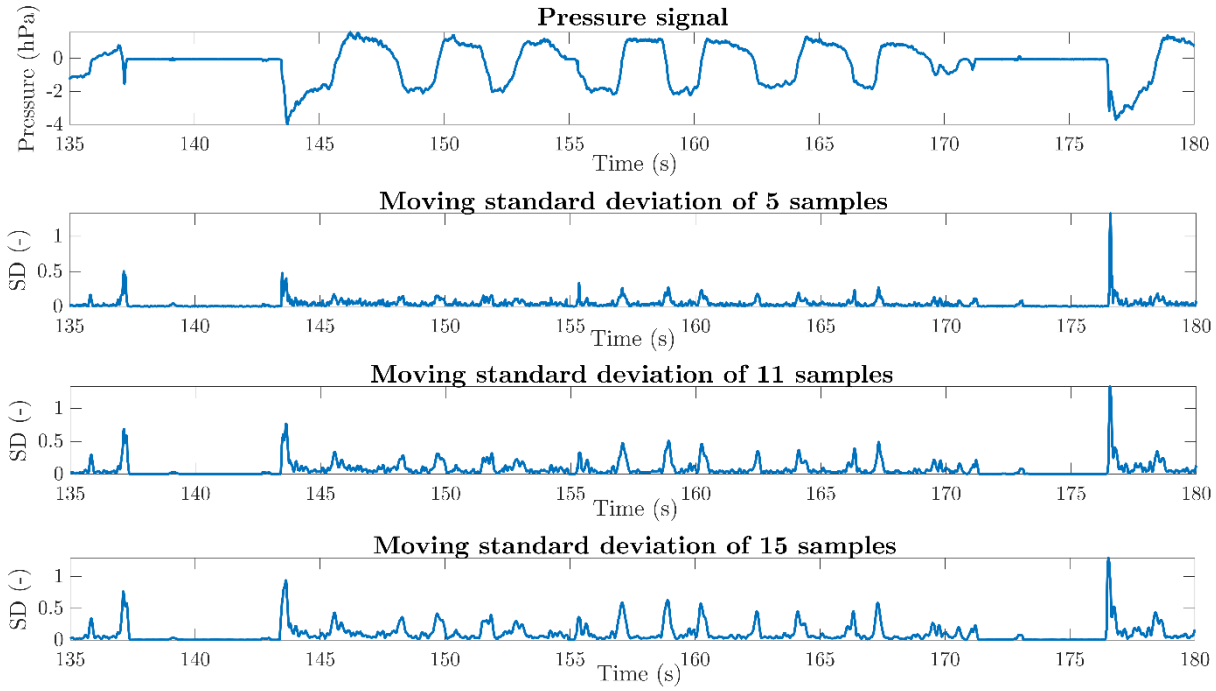

Figure 59: Pressure signal and movstd of the pressure signal using window lengths of 5, 11, and 15 samples.

Artefact segments

In order to locate the segments in which manipulations occur that result in spikes in the pressure signal, the Matlab function diff is used. This function is chosen as spikes can be seen as sudden changes in the signal. The diff calculates the difference between adjacent elements of the pressure signal. In comparison to the mov functions, the diff cannot be calculated using a sliding window only the order is changeable. For the purpose of detecting sudden changes, the first order will suffice.

D. Matlab scripts

Figure 60 gives an overview of the Matlab scripts used to compute the parameters.

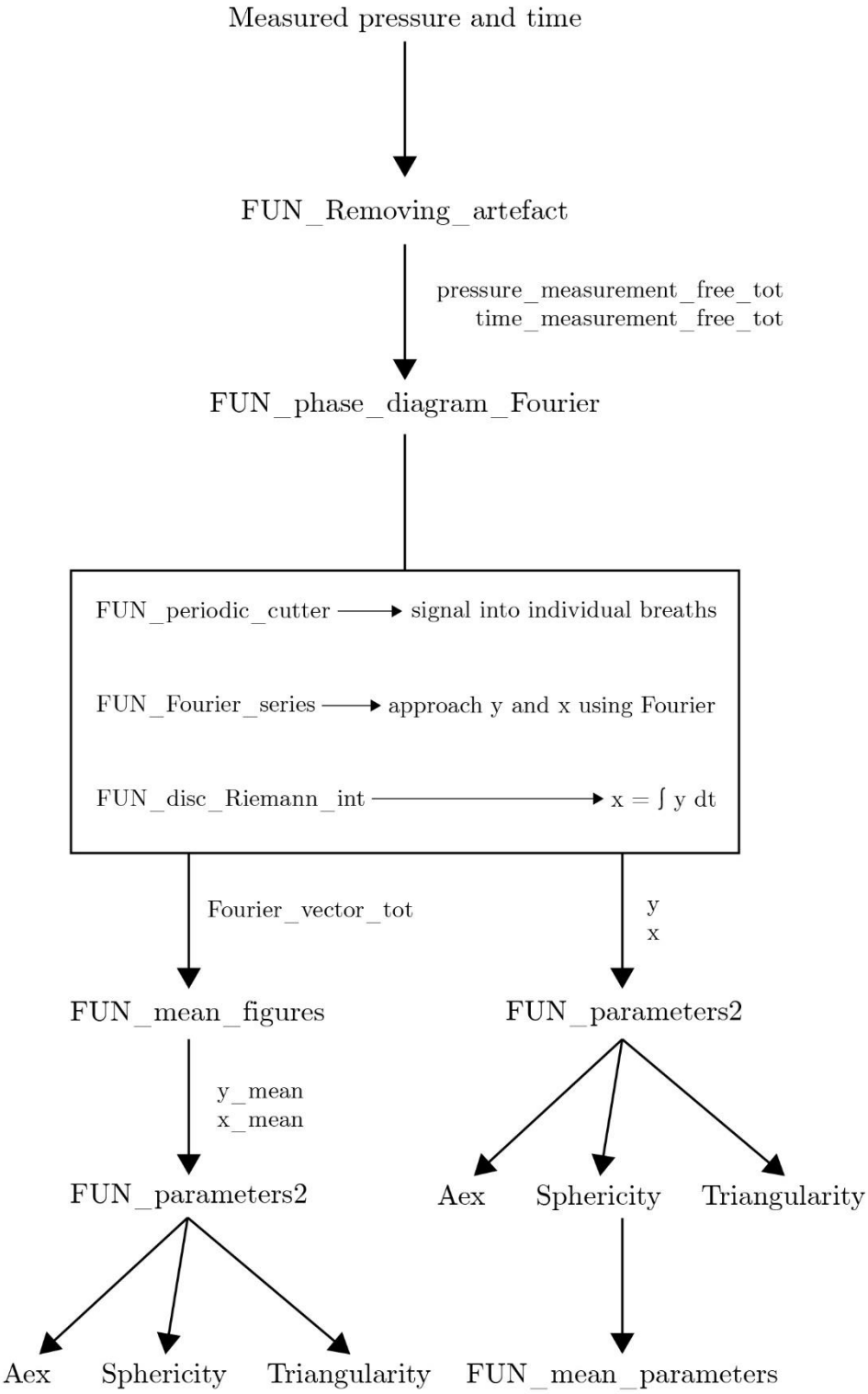

Figure 60: Overview of the used Matlab scripts

D.1. FUN_phase_diagram_Fourier

This is the main script. Phase_diagram_Fourier makes the phase diagram from the device pressure signal and the corresponding time vector. The FUN_Removing_artefact script first determines if there are other characteristics in the signal than breathing, which should be removed. The script determines the number of full breathing periods by finding the "zeros" (crossing of the equilibrium position). The pressure and time of each phase diagram are translated in such a way that the expiration is the start of the phase diagram. Hereafter, the pressure signal is expanded in sines and cosines up to the 25^{th} component during 1 period (one breath from the maximum of the previous inspiration to the next inspiration). The x and y of the phase diagram are computed using the Fourier approached signal. Inputs are the measured pressure and the corresponding time vector

```
function [x,y,N,t,p] = FUN_phase_diagram_Fourier(pressure_measurement,
time_measurement,N_Fourier)
[~,~,N,indices_periods] =FUN_periodic_cutter(pressure_measurement,time_measurement);
% Cut the signal into full cycles
x = cell(N,1);  % initialise a vector for x (normalised integral of pressures)
y = cell(N,1); % initialise a vector for y (normalised pressure)
t = cell(N,1);
p = cell(N,1);
N_Fourier=25;
% ind_period_start = 1;
for k = 1:N
    ind_start = indices_periods(k); % Determine the start index of the breathing cycle
    ind_end = indices_periods(k+1); % Determine the end index of the breathing cycle
    p_period = pressure_measurement(ind_start:ind_end); % Take the pressures of the
    considered breathing cycle
    t_period_translated = time_measurement(ind_start:ind_end)
        time_measurement(ind_start); % Translate the time such that the start is at t=0
    Tm = t_period_translated(end)-t_period_translated(1);
    %Makes sure the p_period and t_period_translated always start at the first sample of the
    expiration
    t_start_exp=find(p_period>0);
    t_start_exp= t_period_translated(t_start_exp(1)); %-1 gaf foutmelding bij subject2_b2_tot_fot
  dus maar weggehaald. Betekend dat nu eerste positieve drukwaarde als begin expiratie gezien wordt
    t_shifted=t_period_translated-t_start_exp;
    t_normalized=t_shifted./(t_shifted(end)-t_shifted(1));
    p_fourier_period = FUN_Fourier_series(p_period,t_period_translated,N_Fourier);

    [Fourier_vector,p_fourier_period,factors]= FUN_Fourier_series(p_period,t_normalized,
    N_Fourier);

    t_normalized_shifted = linspace(0,1,1000)';
    Tm_norm = 1;
    p_normalized_shifted = factors.a0/2 + sum(factors.a .* cos(2*pi*(1:N_Fourier).*
    t_normalized_shifted./Tm_norm) + factors.b.*sin(2*pi*(1:N_Fourier).*
    t_normalized_shifted./Tm_norm),2);
```

```
    a = -FUN_disc_Riemann_int((p_period>=0).*p_fourier_period,t_period_translated)./
        (FUN_disc_Riemann_int((p_fourier_period<=0).*p_fourier_period,
        t_period_translated));
    y_period = p_normalized_shifted./max(p_normalized_shifted);
    [~,integral_pos] = FUN_disc_Riemann_int(1/Tm.*(p_normalized_shifted>=0).
    *y_period,t_normalized_shifted);
    [~,integral_neg] = FUN_disc_Riemann_int(a/Tm.*(p_normalized_shifted<=0).
    *y_period,t_normalized_shifted);
    x_period = integral_pos + integral_neg;

    x{k} = x_period-max(x_period);
    y{k} = y_period;
    t{k} = t_normalized;
    p{k} = p_fourier_period;
    Fourier_vector_tot(k,:)=Fourier_vector;
end
end
```

D.2. FUN_Removing_artefact

This script has been written based on the test data. As the sampling frequency (fs) of the test data was only 80 Hz (compared to 320 for the measurements at OCON), the characteristics used to determine the segment which contain breaths could not be used in the same way for a fs of 320 Hz. Therefore, the inputs were down sampled to 80 Hz and the locations which indicate a change from breathing to other characteristics were used to remove the characteristics other than breathing the signal with fs = 320 Hz.

To locate the segment which likely contain other characteristics than breaths, the movstd is used for segments around zero and diff indicates sudden changes in the signal. Appendix C described the other characteristics than breaths and why the movstd and diff were chosen.

```
function [pressure_measurement_free,time_measurement_free] =
FUN_Removing_artefact(pressure_measurement,time_measurement)

!!druk=pressure_measurement; %segment selection per subject of the down sampled signal
!!tijd=time_measurement; %segment selection per subject down sampled signal

%% Dependent on the signal of the subject, the demands regarding the peak detection should
be adapted slightly.
%findpeaks
h=0.30; %Minimal height of the peaks
d=110; %Minimal distance between peaks
[pks,locs,w,p] = findpeaks(druk, 'MinPeakHeight', h, 'MinPeakDistance', d);
minValue = -1*(druk);
[pks2,locs2,w2,p2] = findpeaks(minValue, 'MinPeakHeight', h, 'MinPeakDistance', d);
figure %Plotted in order to determine of the peaks were selected appropriately.
plot(tijd,druk)
hold on
plot (tijd(locs),pks,'o')
plot (tijd(locs2),-pks2,'+')
hold off

%Determining the mean distance between the peaks as the breathing frequency is variable
due to age and for example exercise.
locs_diff=zeros(length(locs),1);
for i=2:length(locs);
    locs_diff(i)=locs(i)-locs(i-1);
end
locs_diff2=zeros(length(locs2),1);
for j=2:length(locs2);
    locs_diff2(j)=locs2(j)-locs2(j-1);
end
```

```
%Adapting the height of the peaks and distance between the peaks to the signal of the
subject.
determined=median(locs_diff(2:end)); %median is less influenced by outliers compared to the
mean of the signal.
d2=0.7*determined; %adaptable per subject
heigth=median(pks); %median is less influenced by outliers compared to the mean of the
signal.
h2=0.4*heigth; % adaptable per subject
determined1=median(locs_diff2(2:end)); %median is less influenced by outliers compared to
the mean of the signal.
d3=0.5*determined1; %adaptable per subject
heigth1=median(pks2); %median is less influenced by outliers compared to the mean of the
signal.
h4=0.3*heigth1; %adaptable per subject
[pks,locs,w,p] = findpeaks(druk, 'MinPeakHeight', h2, 'MinPeakDistance', d2);
minValue = -1*(druk);
[pks2,locs2,w2,p2] = findpeaks(minValue, 'MinPeakHeight', h4, 'MinPeakDistance', d3);
figure
plot(tijd,druk)
hold on
plot (tijd(locs),pks,'o')
plot (tijd(locs2),-pks2,'+')
hold off

%% Removing segments with a value around zero and a minimal duration.
%Using the moving standard deviation to determine the constant value.
N=movstd(druk,11);
c_m=nanmean(N);
c_md=nanmedian(N);
c_v=nanvar(N);
c_std=nanstd(N);
%% Determination of the length of the segments with a value of around zero and a maximal
value of Nupper.
Nupper=5*c_v;
[row]=find(N<Nupper);
zero_row=nan(length(row),length(row));
zero_row(1,1)=row(1);
y=1;
a=1;
% Each row represents a next segment with a value around zero. This is achieved by
comparison of the sample number and a new row is created is there is a difference in sample
number more than 1.
for x=2:length(row);
    if row(x)==row(x-1)+1;
       a=a+1;
       zero_row(y,a)=row(x);
    else y=y+1;
        a=1;
```

```
        zero_row(y,a)=row(x);
    end
end
zero_row1a=zero_row;

zero_row1 = zero_row(:,~all(isnan(zero_row1a))); % for nan - columns
joo=find(isnan(zero_row1(:,1)));
zero_row2 = zero_row1((1:joo(end)),:); % Selecting the rows that contain segment with a
                                          value around zero.

[m,n]=size(zero_row2);
m1=find(isnan(zero_row1(:,1)));
segment_length=zeros((m1(1)-1),1);
for z=1:(m1(1)-1);
    a=find(isnan(zero_row1(z,:)));
    segment_length(z,1)=n-length(a);
end
sort_segment=sort(segment_length,'ascend') % To inspect the length of the found segments.

afkap=5*median(segment_length); % The minimal length of the zero segment which are
                                   considered for removal.
segment_select=find(segment_length>afkap); % Selecting only the segments with a minimal
                                   duration. 5 is variable and dependents on the found segments.


zero_row3=zero_row2(segment_select,:); % Contain the first sample number of each
segment who met the criteria of Nupper and the minimal length
sample_select=reshape(zero_row3,[],1); % convert matrix to column vector, reshape(A,1,[]) -
→ convert matrix to row vector. Every column will be set after the previous one.
sample_select_order=sort(sample_select,'ascend'); % All sample numbers are ascending
sample_Nan=find(isnan(sample_select_order(:,1)));

%% Control if the found segments are truely around zero or around another constant value.
pressure_value=zeros(size(zero_row3));
[m,n]=size(zero_row3);
for a=1:m;
    x=find(isnan(zero_row3(a,:)));
    last_value=n-length(x);
    pressure_value(a,1:last_value)=druk(zero_row3(a,1):zero_row3(a,last_value));
end

%mean/median per row to determine the 'constant' value of the segment.
for a=1:m;
    x=find(pressure_value(a,:)==0);
    last_value2=n-length(x);
    pressure_value_mean(a,1)=mean(pressure_value(a,1:last_value2));
    pressure_value_median(a,1)=median(pressure_value(a,1:last_value2));
end
```

```
afkap_exclusie=4.3*abs(median(pressure_value_median(:,1))); % Criteria of the values that are considered to be around zero. This is variable per subject and is influenced by outliers.
excl=find(abs(pressure_value_mean(:,1))>afkap_exclusie); % Excluding the segments that are not around zero.

% Removing the segments with a higher median than considerd acceptable around zero.
excl=find(abs(pressure_value_median(:,1))>afkap_exclusie);
for exclusie=1:length(excl)
    zero_row3(excl(exclusie),:)=nan;
end

%% Plotting the segment that are considered for removal in green to be visually inspected if these segments contain breaths and therefore exclusion is not acceptable.
[rows1]=size(zero_row3);

figure
plot(tijd,druk, 'b')
title('Pressure measurement, zero segments in green')
hold on
for def=1:rows1(1);
    a=find(isnan(zero_row3(def,:)));
    last_value3=rows1(1,2)-length(a);
    plot(tijd(zero_row3(def,1:last_value3)),druk(zero_row3(def,1:last_value3)), 'g')
end
plot (tijd(locs),pks,'o')
plot (tijd(locs2),-pks2,'+')
hold off
% Removing the segments that met the criteria
for exclusie=1:length(excl)
    zero_row3(excl(exclusie),:)=nan;
end

%% Searching the closest peaks that are located on the inspiration.
zero_row4=zero_row3;
a=0;
for exclusie=1:length(excl)
    zero_row4 = zero_row4(setdiff(1:size(zero_row4,1),[excl(exclusie)-a]),:);
    a=a+1;
end

%minimal value of the segment
min_segment=zero_row4(:,1);
min_segment=min_segment'; %row with te first values of the segment

[rows2]=size(zero_row4);
max_segment=zeros(1,rows2(1));
for i=1:rows2(1)
    a=find(isnan(zero_row4(i,:)));
```

```
    last_value3=rows1(1,2)-length(a);
    max_segment(1,i)=zero_row4(i,last_value3);
end

%For peaks of the inspiration = locs2
for dal=1:length(min_segment)
    [~,index_min]=min(abs(min_segment(1,dal)-locs2));
    [~,index_max]=min(abs(max_segment(1,dal)-locs2));
    if index_min==index_max && min_segment(1,dal)>locs2(index_min); %If the closest
peak of the end of the previous segment is equal to the closest peak of the begin of the next
segment AND this peak is located for the first value of the 'second = next' segment:
       minVal_segment=locs2(index_min);
       maxVal_segment=locs2(index_min+1);
    else if index_min==index_max && locs2(index_min)>max_segment(1,dal); %If the
closest peak of the end of the previous segment is equal to the closest peak of the begin of the
next segment AND this peak is located after the first value of the 'second = next' segment:
              minVal_segment=locs2(index_min-1);
              maxVal_segment=locs2(index_min);
         else minVal_segment=locs2(index_min-1);
             maxVal_segment=locs2(index_min+1);
         end
    end

    if locs2(index_min)<min_segment(1,dal);
        minVal_segment=locs2(index_min);
    else if locs2(index_min)>min_segment(1,dal);
            minVal_segment=locs2(index_min-1);
        end
    end
    if locs2(index_max)>max_segment(1,dal);
        maxVal_segment=locs2(index_max);
            else if locs2(index_max)<max_segment(1,dal);
            maxVal_segment=locs2(index_max+1);
                end
    end
    interval_dal(dal,1)=minVal_segment;
    interval_dal(dal,2)=maxVal_segment;
end

% Compare if the intervals differ per row
[~,idx] = unique(interval_dal(:,1));   %which rows have a unique first value?
interval_dal = interval_dal(idx,:);              %only use those

lengte=min(length(interval_dal));
lengte2=max(length(interval_dal));
```

```
%findpeaks
!!druk2=pressure_b2_spiro_5min_tot_eind; % segment containing the original data
!!tijd2=time_b2_spiro_5min_tot_eind; %segment containing the original data
h=0.30; %Minimal height of the peaks
d=320; %Minimal distance between peaks, 110*4 as the fs is now 320 instead of 80 Hz.
minValue = -1*(druk2);
[pks23,locs23,w2,p2] = findpeaks(minValue, 'MinPeakHeight', h, 'MinPeakDistance', d);

%correcte sample numbers of the interval_dal
interval_dal_trans=interval_dal*4; %(column 1 correspond to start and column 2 to end of
                                    the interval.)
for i=1:length(interval_dal_trans(:,1))
    [~,ix] = min(abs(locs23-interval_dal_trans(i,1)));
    interval_dal_translated_min(1,i)=locs23(ix);
end
for i=1:length(interval_dal_trans(:,2))
    [~,ix] = min(abs(locs23-interval_dal_trans(i,2)));
    interval_dal_translated_max(1,i)=locs23(ix);
end

druk_down=druk;
for i=1:length(interval_dal_translated_min)
    druk2(interval_dal_translated_min(1,i):interval_dal_translated_max(1,i))=nan;
    druk_down(interval_dal(i,1):interval_dal(i,2))=nan;
end

pressure_measurement_free = druk2(~isnan(druk2)); % removal of the Nans
time_measurement_free = tijd2(1:length(pressure_measurement_free));
druk_down = druk_down(~isnan(druk_down)); % removal of the Nans
tijd_down=tijd(1:length(druk_down));

%% In order to remove the artefact, the peaks have to be selected again as parts of the signal
could be removed if they are considered to be around zero.
%findpeaks
tijd=tijd_down; druk=druk_down;
h=0.30; %Minimal height of the peaks
d=320; %Minimal distance between peaks, 110*4 as the fs is now 320 instead of 80 Hz.
[pks,locs,w,p] = findpeaks(druk, 'MinPeakHeight', h, 'MinPeakDistance', d);
minValue = -1*(druk);
[pks2,locs2,w2,p2] = findpeaks(minValue, 'MinPeakHeight', h, 'MinPeakDistance', d);
figure
plot(tijd,druk)
hold on
plot (tijd(locs),pks,'o')
plot (tijd(locs2),-pks2,'+')
hold off
```

```
%Determining the mean distance between the peaks as the breathing frequency is variable
due to age and for example exercise.
locs_diff=zeros(length(locs),1);
for i=2:length(locs);
    locs_diff(i)=locs(i)-locs(i-1);
end
locs_diff2=zeros(length(locs2),1);
for j=2:length(locs2);
    locs_diff2(j)=locs2(j)-locs2(j-1);
end

%Adapting the height of the peaks and distance between the peaks to the patient's signal.
determined=median(locs_diff(2:end)); %median is less influenced by outliers compared to the
mean of the signal.
d2=0.6*determined; %adaptable per subject
heigth=median(pks); %median is less influenced by outliers compared to the mean of the
signal.
h2=0.49*heigth; %adaptable per subject
determined1=median(locs_diff2(2:end)); %median is less influenced by outliers compared to
the mean of the signal.
d3=0.6*determined1; %adaptable per subject
heigth1=median(pks2); %median is less influenced by outliers compared to the mean of the
signal.
h4=0.6*heigth1; %adaptable per subject
[pks,locs,w,p] = findpeaks(druk, 'MinPeakHeight', h2, 'MinPeakDistance', d2);
minValue = -1*(druk);
[pks2,locs2,w2,p2] = findpeaks(minValue, 'MinPeakHeight', h4, 'MinPeakDistance', d3);
figure %Plotted in order to determine of the peaks were selected appropriately.
plot(tijd,druk)
hold on
plot (tijd(locs),pks,'o')
plot (tijd(locs2),-pks2,'+')
hold off

%% To localise and remove the artefacts
pressure5=druk;

% Using the diff, which is the difference between 2 adjacent sample numbers, to localise
outliers.
dif=diff(pressure5);
thr=5*std(dif); % Threshold of the peaks considered to be localise artefacts
thr2=5*std(dif); % Threshold of the peaks considered to be localise artefacts
[peaks,loci]=findpeaks(dif, 'MinPeakHeight',thr, 'MinPeakDistance', 100);
[peaks2,loci2]=findpeaks((-1*dif), 'MinPeakHeight',thr2, 'MinPeakDistance', 100);
```

```
%% locs2
% If there is no peak after the last value of loci, the for loop will give an error. Therefore, it
is first coded to resolve this issue. Thereafter, it is determined if there what the closest locs2
before and after each segment is to remove as minimal as possible.
if loci(end)==locs2(end)
    pressure5(loci(end):end)=nan;
end
B=(length(loci)-1);

if loci(end)>locs2(end) && loci(end-1)==locs2(end)
    pressure5(loci(end-1):end)=nan;
    B=(length(loci)-2);
else if loci(end)>locs2(end)
        pressure5(locs2(end):end)=nan;
    end
end

b1=length(loci2);
if loci2(end)==locs2(end)
    pressure5(loci2(end):end)=nan;
    b1=b1-1;
end

if loci2(end)>locs2(end)
    pressure5(locs2(end):end)=nan;
    b1=b1-1;
end

a=1;
if loci(1)<locs2(1)
    minVal=1;
    max2=locs2(1);
    a=2;
    pressure5(minVal:max2)=nan;
end

for i=a:B;
    [~,ix] = min(abs(locs2-loci(i)));
if locs2(ix)==loci(i);
    minVal=locs2(ix-1);
    max2=locs2(ix+1);
end
if locs2(ix)>loci(i)
    minVal=locs2(ix-1);
    max2=locs2(ix);
else if locs2(ix)<loci(i)
    max2=locs2(ix+1);
    minVal=locs2(ix);
```

```
    end
end
pressure5(minVal:max2)=nan;
end

if loci2(1)<locs2(1)
    minVal1=1;
    max1=locs2(1);
    a1=2;
    pressure5(minVal1:max1)=nan;
end

for i=1:b1
    [~,ix2] = min(abs(locs2-loci2(i)));
if locs2(ix2)==loci2(i);
    minVal1=locs2(ix2-1);
    max1=locs2(ix2+1);
end
if locs2(ix2)>loci2(i)
    minVal1=locs2(ix2-1);
    max1=locs2(ix2);
else if locs2(ix2)<loci2(i)0
    max1=locs2(ix2+1);
    minVal1=locs2(ix2);
    end
end
pressure5(minVal1:max1)=nan;
end

pressure6=pressure5;
indices=find(isnan(pressure6));
y=1;
a=1;
segment_indices=nan(length(indices),length(indices));
segment_indices(1,1)=indices(1);
for x=2:length(indices);
    if indices(x)==indices(x-1)+1;
       a=a+1;
       segment_indices(y,a)=indices(x);
    else y=y+1;
        a=1;
        segment_indices(y,a)=indices(x);
    end
end
segment_indices = segment_indices(:,~all(isnan(segment_indices))); % for nan - columns
joo=find(isnan(segment_indices(:,1)));
segment_indices = segment_indices((1:joo(1)-1),:);
```

```
segment_min=segment_indices(:,1)';
max_duration_segment=size(segment_indices);
for i=1:length(segment_min)
    a=find(isnan(segment_indices(i,:)));
    last_value4=max_duration_segment(1,2)-length(a);
    segment_max(1,i)=segment_indices(i,last_value4);
end

%% Find the corresponding segments in the original signal.
segment_max=segment_max*4;
segment_min=segment_min*4;

if segment_min(1,1)==4
    segment_min(1,1)=1;
end

h=0.30; %Minimal height of the peaks
d=320; %Minimal distance between peaks, 110*4 as the fs is now 320 instead of 80 Hz
minValue = -1*(pressure_measurement_free);
[pks23,locs23,w2,p2] = findpeaks(minValue, 'MinPeakHeight', h, 'MinPeakDistance', d);

%correct sample numbers for segment_max
for i=1:length(segment_max)
    [~,ix] = min(abs(locs23-segment_max(i)));
    segment_max_translated(1,i)=locs23(ix);
    [~,ix2] = min(abs(locs23-segment_min(i)));
    segment_min_translated(1,i)=locs23(ix2);
    if segment_min(1)==1
    segment_min_translated(1,1)=1;
    end
end

for i=1:length(segment_min_translated)
    pressure_measurement_free(segment_min_translated(1,i):segment_max_translated(1,i))
    =nan;
end

pressure_measurement_free_tot = pressure_measurement_free
(~isnan(pressure_measurement_free)); %removal of the Nans
time_measurement_free_tot = time_measurement_free
(1:length(pressure_measurement_free_tot));
end
```

D.3. FUN_periodic_cutter

FUN_periodic_cutter divides the pressure signal (after removal of the artefacts) into N full periods based on minima. This results in segments starting at the maximum of the inspiration (is a minimum of the signal) up to the maximum of the next inspiration. As a result, the expiration of a breath is never divided into two phase diagrams.

```
function [f_cutted,t_cutted,N_cycles,ind_periods,eq_pos,t_minima,P_minima,
ind_minima,t_maxima,P_maxima,ind_maxima] = FUN_periodic_cutter(f,t)
dt_cyc_crit = 0.6; % [s] minimum half cycle time. If a minimum and a maximum are found
within this range, it is regarded as noise.
last_ind_crit = 40; % Amount of elements that must be there since the last minimum or
maximum
dP_crit = 1500; % [Pa] minimum difference between starting value and starting
minimum/maximum

N_minima = 0; % Number of minima found
N_maxima = 0; % Number of maxima found
minimum_found = true; % boolean to indicate that we can search for a maximum in the
cycle
maximum_found = true; % boolean to indicate that we can search for a minimum in the
cycle
t_max_prev = -1;  % set time of previous maximum to -1 (small enough to ensure that the
first maximum we find will be counted)
t_min_prev = -1; % set time of previous minimum to -1 (small enough to ensure that the
first minimum we find will be counted)
P_max_prev = -inf; % set value of previous max pressure very low (new value always
higher)
P_min_prev = inf; % set value of previous min pressure very high (new value always lower)
ind_min_prev = -1; % same for indices
ind_max_prev = -1; % same for indices
start = -1; % indicate start: 0 is minimum, 1 is maximum
optimised_start = false; % indicate if starting min/max was "optimised" or not.

% Predefine (far too large) vectors for t and P for minima and maxima
ind_minima = zeros(size(t));
t_minima = zeros(size(t));
P_minima = inf.*ones(size(f));
ind_maxima = zeros(size(t));
t_maxima = zeros(size(t));
P_maxima = inf.*ones(size(f));

for k = 2:length(f)-1
    if (f(k)>=f(k-1) && f(k)>=f(k+1) )
        % Local maximum found
        if minimum_found % A correct minimum was found since the last maximum, so look
                         for a new maximum to end cycle.
            if t(k)-t_min_prev > dt_cyc_crit % time between minimum and maximum
```

```
                                                sufficiently long
            maximum_found = true; % Indicate that we found a maximum
            minimum_found = false; % Indicate that we now need to find a minimum
            N_maxima = N_maxima+1;
            % save values of t and P as the values of the maximum we found
            t_max_prev = t(k);
            P_max_prev = f(k);
            ind_max_prev = k;
    % Save the values of the minima to the vectors containing the information of the
minima
            if N_minima>0
                t_minima(N_minima) = t_min_prev;
                P_minima(N_minima) = P_min_prev;
                ind_minima(N_minima) = ind_min_prev;
            else
                start = 1;
                if f(1) + dP_crit < f(k) % signal did increase since start, so correct maximum
                                            to start cutted signal with
                    optimised_start = true;
                end
            end
        end
    else % There has not been found a correct minimum since the last maximum, so
         optimise the maximum found
        if f(k)>P_max_prev % Maximum found now is larger than previous maximum
                            found, so a more accurate maximum is found
            t_max_prev = t(k);
            P_max_prev = f(k);
            ind_max_prev = k;
            if f(1) + dP_crit < f(k) && N_minima==0 % signal did increase since start, so
                                                    correct maximum to start cutted signal with
                optimised_start = true;
            end
        end
    end
elseif (f(k)<=f(k-1) && f(k)<=f(k+1))
    % Local minimum found if maximum_found. A correct maximum was found since the
    last minimum, so look for a new minimum to end cycle
        if t(k)-t_max_prev > dt_cyc_crit
            minimum_found = true; % Indicate that we found a minimum
            maximum_found = false; % Indicate that we now need to find a maximum
            N_minima = N_minima + 1;

            % save values of t and P as the values of the minimum we found
            t_min_prev = t(k);
            P_min_prev = f(k);
            ind_min_prev = k;
% Save the values of the maxima to the vectors containing the information of the maxima
```

```
            if N_maxima>0
                t_maxima(N_maxima) = t_max_prev;
                P_maxima(N_maxima) = P_max_prev;
                ind_maxima(N_maxima) = ind_max_prev;
            else
                start = 0;
                if f(1) - dP_crit > f(k)
                    optimised_start = true; % signal did decrease since start, so correct
                                            minimum to start with.
                end
            end
        end
    else % There has not been found a correct maximum since the last minimum, so
         optimise the maximum found
        if f(k)<P_min_prev
            t_min_prev = t(k);
            P_min_prev = f(k);
            ind_min_prev = k;
            if f(1) - dP_crit > f(k) && N_maxima==0
                optimised_start = true; % signal did decrease since start, so correct minimum
                                        to start with.
            end
        end
    end
  end
end

% after looping, save last maximum or minimum if it is sufficiently far from the side of the
domain (assumably optimised)
% And use the critical dp again
if minimum_found
    if ind_min_prev < (length(t) - last_ind_crit) &&  f(end) > P_min_prev + dP_crit
        t_minima(N_minima) = t_min_prev;
        P_minima(N_minima) = P_min_prev;
        ind_minima(N_minima) = ind_min_prev;
    else
        N_minima = N_minima -1;
    end
elseif maximum_found
    if ind_max_prev < (length(t) - last_ind_crit) && f(end) < P_max_prev - dP_crit
        t_maxima(N_maxima) = t_max_prev;
        P_maxima(N_maxima) = P_max_prev;
        ind_maxima(N_maxima) = ind_max_prev;
    else
        N_maxima = N_maxima -1;
    end
end
```

```
% Remove all zero or infinite elements
ind_minima(ind_minima==0) = [];
t_minima(t_minima==0) = [];
P_minima(P_minima==inf) = [];
ind_maxima(ind_maxima==0) = [];
t_maxima(t_maxima==0) = [];
P_maxima(P_maxima==inf) = [];

% Determine the number of cycles, and cut the signal to N_cycle full cycles.
if start == 0
    if optimised_start
        N_cycles = N_minima - 1;
        t_cutted = t(ind_minima(1):ind_minima(N_cycles+1));
        f_cutted = f(ind_minima(1):ind_minima(N_cycles+1));
        ind_periods = ind_minima(1:N_cycles+1);
    else
        N_cycles = N_maxima - 1;
        t_cutted = t(ind_minima(1):ind_minima(N_cycles+1));
        f_cutted = f(ind_minima(1):ind_minima(N_cycles+1));
        t_minima(1) = [];
        P_minima(1) = [];
        ind_periods = ind_minima(1:N_cycles+1);
    end
elseif start == 1
    if optimised_start
        N_cycles = N_maxima - 1;
        t_cutted = t(ind_minima(1):ind_minima(N_cycles+1));
        f_cutted = f(ind_minima(1):ind_minima(N_cycles+1));
        ind_periods = ind_minima(1:N_cycles+1);
    else
        N_cycles = N_minima - 1;
        t_cutted = t(ind_minima(1):ind_minima(N_cycles+1));
        f_cutted = f(ind_minima(1):ind_minima(N_cycles+1));
        t_maxima(1) = [];
        P_maxima(1) = [];
        ind_maxima(1) = [];
        ind_periods = ind_minima(1:N_cycles+1);
    end
end

[~,~,eq_pos] = FUN_disc_Riemann_int(f_cutted,t_cutted);

end
```

D.4. FUN_Fourier_series

FUN_Fourier_series expands a signal f (pressure signal) during 1 period (one breath from the maximum of the previous inspiration to the next inspiration) in sines and cosines up to the Nth component.

```
function [fn,factors] = FUN_Fourier_series(f,t,N)
% We need column vectors for f and t
if size(t,1) == 1
        t = t';
end
if size(f,1) == 1
        f = f';
        f_transposed = true;
else
        f_transposed = false;
end

% Determine the period Tm
Tm = t(end) - t(1);
% Vectors to save the components a_n and b_n
a = zeros(1,N);
b = zeros(1,N);
% Determine a0
a0 = 2/Tm * FUN_disc_Riemann_int(f,t);
% Determine the components a_n and b_n for n>0
for n = 1:N
        a(n) = 2/Tm * FUN_disc_Riemann_int(f.*cos((2*pi*n.*t)./Tm),t);
        b(n) = 2/Tm * FUN_disc_Riemann_int(f.*sin((2*pi*n.*t)./Tm),t);
end
% Determine the Fourier function f_n at every time
fn = a0/2 + sum(a.*cos(2*pi*(1:N).*t./Tm) + b.*sin(2*pi*(1:N).*t./Tm),2);

% Return the vectors with coefficients
factors.a0 = a0;
factors.a = a;
factors.b = b;
factors.N = N;

% Make sure that the output is in the same format as the input
if f_transposed
        fn = fn';
end

end
```

D.5. FUN_disc_Riemann_int

FUN_disc_Riemann_int computes the discrete (centre) Riemann integral. It returns the integral and the average of the function in the domain. The input will be integrated over the column vectors. This function is used for the calculation of x which represents the ∫ in a flow volume curve.

```
function [solution,integral,average_vec,average_val] = FUN_disc_Riemann_int
        (integrand_vec,variable_vec,bool_areacalc)
    % Check input
    if size(integrand_vec,1) == 1
        integrand_vec = integrand_vec';
        transposed = true;
    else
        transposed = false;
    end

    if nargin == 2
        bool_areacalc = false;
    end

    % Another check on the input, and then the actual computations
    if ~isempty(integrand_vec)
        integral = zeros(size(integrand_vec)); % initial value of integral
        for k = 2:(length(variable_vec)) % loop over all intervals (one interval less
                                            than items in vectors)
            integrand_avg_interval = (integrand_vec(k-1,:)+integrand_vec
            (k,:))./2; % Compute the average of the integrand in the integral
            if bool_areacalc
                dx = abs(variable_vec(k)-variable_vec(k-1)); % Compute the
                                                length of the variable in the interval
            else
                dx = variable_vec(k)-variable_vec(k-1); % Compute the length
                                                    of the variable in the interval
            end
            integral(k,:) = integral(k-1,:)+integrand_avg_interval.*dx;
            % Compute the new value of the integral as the old value
        end
        average_vec = integral./(variable_vec(end)-variable_vec(1));
        average_val = average_vec(end,:);

        if transposed
            integral = integral';
            average_vec = average_vec';
        end
        solution = integral(end);
    else
        solution = 0;
```

```
                integral = [];
                average_vec = [];
                average_val = 0;
        end
end
```

D.6. FUN_mean_figures

FUN_mean_figures first determines the Fourier coefficients which results in a vector length of 1 to be able to mean these Fourier vectors. Thereafter, the factors of the Fourier vector of the phase diagrams are averaged using the mean of all considered phase diagrams for each factor. The number of phase diagrams taken into consideration start from the closest phase diagram of that segment up to N_figures. Subsequently, the factors of the Fourier vector are used to compute the x_mean and y_mean of the phase diagram averaged at the start and/or end of the segment. The parameters are calculated from an averages phase diagram which is the mean of one up to N_figures phase diagrams.

```
function [x_mean_start,y_mean_start,x_mean_end,y_mean_end]=
FUN_mean_figures(Fourier_vector_tot,N_figures);
%Scaling the length of the vector by dividing all factors by the norm. Therefore the length of
each Fourier vector will be 1.
for i=1:N
Fourier_vector_scaled(i,:)=(Fourier_vector_tot(i,:))/(norm(Fourier_vector_tot(i,:)));
end

%% Mean Fourier vector of N_figures
%Regarding the figures from the beginning of the segment
for i=1:N_figures
    for j=1:51
    Fourier_vector_mean_figures_start(i,j)=mean(Fourier_vector_scaled(1:i,j));
    end
end

%Regarding the figures from the end
reverse_Fourier_vector_scaled=flip(Fourier_vector_scaled);
for i=1:N_figures
    for j=1:51
    Fourier_vector_mean_figures_end(i,j)=mean(reverse_Fourier_vector_scaled(1:i,j));
    end
end

%% Compute x and y using Fourier_vector_mean_figures_start/end
%Regarding the figures from the beginning of the segment
x_mean_start = cell(N_figures,1);  % initialise a vector for x (normalised integral of
                                     pressures)
y_mean_start = cell(N_figures,1);
for k=1:N_figures
    factorsa0=Fourier_vector_mean_figures_start(k,1);
    factorsa=Fourier_vector_mean_figures_start(k,2:26);
    factorsb=Fourier_vector_mean_figures_start(k,27:51);
    t_normalized_shifted = linspace(0,1,1000)';
    Tm_norm = 1;
    p_normalized_shifted = factorsa0/2 + sum(factorsa .* cos(2*pi*(1:N_Fourier).*
    t_normalized_shifted./Tm_norm) + factorsb.*sin(2*pi*(1:N_Fourier).*
```

```
    t_normalized_shifted./Tm_norm),2);
    a = -FUN_disc_Riemann_int((p_normalized_shifted>=0).*p_normalized_shifted,
    t_normalized_shifted)./(FUN_disc_Riemann_int((p_normalized_shifted<=0).*
    p_normalized_shifted,t_normalized_shifted));

    y_period = p_normalized_shifted./max(p_normalized_shifted);
    [~,integral_pos] = FUN_disc_Riemann_int(1/Tm.*(p_normalized_shifted>=0).*
    y_period,t_normalized_shifted);
    [~,integral_neg] = FUN_disc_Riemann_int(a/Tm.*(p_normalized_shifted<=0).*
    y_period,t_normalized_shifted);
    x_period = integral_pos + integral_neg;
    x_mean_start{k} = x_period-max(x_period);
    y_mean_start{k} = y_period;
end

%Regarding the figures from the beginning of the segment
x_mean_end = cell(N_figures,1);  % initialise a vector for x (normalised integral of
                                   pressures)
y_mean_end= cell(N_figures,1);
for k=1:N_figures
    factorsa0=Fourier_vector_mean_figures_end(k,1);
    factorsa=Fourier_vector_mean_figures_end(k,2:26);
    factorsb=Fourier_vector_mean_figures_end(k,27:51);
    t_normalized_shifted = linspace(0,1,1000)';
    Tm_norm = 1;
    p_normalized_shifted = factorsa0/2 + sum(factorsa .* cos(2*pi*(1:N_Fourier).*
    t_normalized_shifted./Tm_norm) + factorsb.*sin(2*pi*(1:N_Fourier).*
    t_normalized_shifted./Tm_norm),2);
    a = -FUN_disc_Riemann_int((p_normalized_shifted>=0).*p_normalized_shifted,
    t_normalized_shifted)./(FUN_disc_Riemann_int((p_normalized_shifted<=0).*
    p_normalized_shifted,t_normalized_shifted));

    y_period = p_normalized_shifted./max(p_normalized_shifted);
    [~,integral_pos] = FUN_disc_Riemann_int(1/Tm.*(p_normalized_shifted>=0).*
    y_period,t_normalized_shifted);
    [~,integral_neg] = FUN_disc_Riemann_int(a/Tm.*(p_normalized_shifted<=0).*
    y_period,t_normalized_shifted);
    x_period = integral_pos + integral_neg;
    x_mean_end{k} = x_period-max(x_period);
    y_mean_end{k} = y_period;
end
end
```

D.7. FUN_parameters2

This script uses the output of the FUN_phase_diagram_Fourier, x and y, to compute the parameters Aex_1, sphericity and triangularity. The area of the Aex_1 is computed using the function trapz. Trapz integrated y with respect to the scalar spacing specified by x. The perimeter of the phase diagram is calculated by summation of the square root of the differences in x and y value of the phase diagram. The Aex_1 is computed by perimeter^2/area which is equation (11). The sphericity is calculated by dividing the inscribed circle by the circumscribed circle. The radius of both circles is determined using the Pythagorean Theorem ($a^2 + b^2 = c^2$). The triangularity is computed by dividing the area of the signal by the area of the triangle.

```
function [Aex1,sphericity,triangularity]=FUN_parameters(xcell,ycell,Ncell)
[s,d] = cellfun(@size,ycell); out = max([s,d]); l=max(out); b=length(d);
for j=1:Ncell;
    h=figure;
    plot(xcell{j},ycell{j});
    select_y=ycell{j};
    select_x=xcell{j};
    saveas(h,sprintf('FIG_fasediagram%d.png',j));
    saveas(h,sprintf('FIG_fasediagram%d.fig',j));
    [x1(1,j),y1(1,j)]=max(ycell{j}); %PTEF
    [x2(1,j),y2(1,j)]=min(select_x(1:10)); %start of expiration
    [x3(1,j),y3(1,j)]=max(x); %end of expiration
end

%% parameter determination
%area under the expiratory TBFV-curve, unitless: perimeter^2/auc
for j=1:Ncell;
    select_y=ycell{j};
    select_x=xcell{j};

    %For the total phase diagram
    select_x_tot=[select_x;select_x(1)];
    select_y_tot=[select_y;select_y(1)];
    x_diff_tot=diff(select_x_tot);
    y_diff_tot=diff(select_y_tot);
    segment_lengths_tot=sqrt(x_diff_tot.^2+y_diff_tot.^2);
    perimeter_tot(j,1)=sum(segment_lengths_tot);
    auc_corr_tot(j,1)=trapz(select_x,select_y); %for every individual phase diagram
    Aex1 (j,1)=(perimeter_tot(j,1)*perimeter_tot(j,1))/auc_corr_tot(j,1);
end
```

```
%% Determination of the sphericity by the minima land maximal radius of the circle using
pythagoras
expiratie_x=zeros(l,b); expiratie_x_ad=zeros(l,b); x_adapted=zeros(l,b);
expiratie_y=zeros(l,b); straal=zeros(l,b);
y_inscribed_circle=zeros(l,b); x_inscribed_circle=zeros(l,b);
y_circumscribed_circle=zeros(l,b); x_circumscribed_circle=zeros(l,b);
for j=1:Ncell;
    lengte=length(y2(1,j):y3(1,j));
    select_x=xcell{j};
    expiratie_x(1:lengte,j)=select_x(y2(1,j):y3(1,j)); % taking only the expiration into
    consideration regarding the x-axis
    factor=abs(2/min(expiratie_x(:,j)));
    expiratie_x_ad(1:lengte,j)=expiratie_x(1:lengte,j)*factor;
    x_adapted(1:lengte,j)=expiratie_x_ad(1:lengte,j)+1; %normalisation of x-axis
    select_y=ycell{j};
    expiratie_y(1:lengte,j)=select_y(y2(1,j):y3(1,j)); % taking only the expiration into
    consideration regarding the y-axis
    size1(1,j)=length(x_adapted(1:lengte,j));
    th=linspace(-pi/2,pi/2,size1(1,j));
    for i=1:size1(1,j);
    straal(i,j)=sqrt(x_adapted(i,j)*x_adapted(i,j)+expiratie_y(i,j)*expiratie_y(i,j));
    end
    r_inscribed(1,j)=min(straal(1:lengte,j));
    r_circumscribed(1,j)=max(straal(1:lengte,j));
    y_inscribed_circle(1:lengte,j)=r_inscribed(1,j)*cos(th)';
    x_inscribed_circle(1:lengte,j)=r_inscribed(1,j)*sin(th)';
    y_circumscribed_circle(1:lengte,j)=r_circumscribed(1,j)*cos(th)';
    x_circumscribed_circle(1:lengte,j)=r_circumscribed(1,j)*sin(th)';
    sphericity(j,1)=r_inscribed(1,j)/r_circumscribed(1,j);
end

%% Determination of triangularity
expiratie_x=zeros(l,b); expiratie_x_ad=zeros(l,b); x_adapted=zeros(l,b);
expiratie_y=zeros(l,b);
for j=1:Ncell;
    lengte=length(y2(1,j):y3(1,j));
    select_x=xcell{j};
    expiratie_x(1:lengte,j)=select_x(y2(1,j):y3(1,j)); % taking only the expiration into
    consideration regarding the x-axis
    factor=abs(2/min(expiratie_x(:,j)));
    expiratie_x_ad(1:lengte,j)=expiratie_x(1:lengte,j)*factor;
    x_adapted(1:lengte,j)=expiratie_x_ad(1:lengte,j)+1; %normalisation of x-axis
    select_y=ycell{j};
    expiratie_y(1:lengte,j)=select_y(y2(1,j):y3(1,j)); % taking only the expiration into
                                                        consideration regarding the y-axis
    [~,y_1(1,j)]=max(expiratie_y(:,j)); %PTEF
    [~,y_2(1,j)]=min(x_adapted(:,j)); %start of expiration
    [~,y_3(1,j)]=max(x_adapted(:,j)); %end of expiration
```

```
    x_11(1,j)=x_adapted(y_1(1,j),j); y_11(1,j)=expiratie_y(y_1(1,j),j);
    x_22(1,j)=x_adapted(y_2(1,j),j); y_22(1,j)=expiratie_y(y_2(1,j),j);
    x_33(1,j)=x_adapted(y_3(1,j),j); y_33(1,j)=expiratie_y(y_3(1,j),j);
    x_triang(1:3,j)=[x_11(1,j);x_22(1,j);x_33(1,j)];
    y_triang(1:3,j)=[y_11(1,j);y_22(1,j);y_33(1,j)];
end

%% First control y_triang to determine if the lower corners of the triangle are located closely
enough (<0.01) to zero.
for j=1:Ncell;
    lengte=length(y2(1,j):y3(1,j));
    y_triang(2:3,:)=zeros(2,N); %the lower corners of the triangle are plotted at (-1,0) and
                                (1,0) in this way
    area_triang(1,j)= polyarea(x_triang(1:3,j),y_triang(1:3,j)); %area of the triangle
    auc_corr_trian(1,j)=trapz(x_adapted(:,j),expiratie_y(:,j)); %area of the signal
    triangularity(j,1)=(auc_corr_trian(1,j)/area_triang(1,j))-1;
end

%% Loading the values into an excel sheet.
T = table(Aex1,sphericity,triangularity); filename = 'fourrierreeks.xlsx';
writetable(T,filename,'Sheet',1,'Range','A:C')

end
```

D.8. FUN_mean_parameters

FUN_mean_parameters averages every parameter using the mean of all considered parameters. The number of parameters taken into consideration start from the closest phase diagram of that segment up to N_figures as the number must be equal to be able to compare both methods.

```
function [Aex1_start,sphericity_start,triangularity_start,Aex1_end,sphericity_end,
triangularity_end]=FUN_mean_parameters(Fourier_vector_tot,N_figures,
auc_exp_unitless,auc_tot_unitless,sphericity,triangularity);
%Scaling the length of the vector by dividing all factors by the norm. Therefore the length of
each Fourier vector will be 1.
for i=1:N
    Fourier_vector_scaled(i,:)=(Fourier_vector_tot(i,:))/(norm(Fourier_vector_tot(i,:)));
end

%% Mean Fourier vector of N_figures
%Regarding the parameters from the beginning of the segment
for i=1:N_figures
    Aex1_start(i,1)=mean(Aex1(1:i,1));
    sphericity_start(i,1)=mean(sphericity(1:i,1));
    triangularity_start(i,1)=mean(triangularity(1:i,1));
end

%Regarding the parameters from the end
reverse_Aex1=flip(Aex1);
reverse_sphericity=flip(sphericity);
reverse_triangularity=flip(triangularity);
for i=1:N_figures
    Aex1_end(i,1)=mean(Aex1(1:i,1));
    sphericity_end(i,1)=mean(reverse_sphericity(1:i,1));
    triangularity_end(i,1)=mean(reverse_triangularity(1:i,1));
end

%% In excel zetten
T = table(Aex1_start,sphericity_start,triangularity_start,Aex1_end,sphericity_end,
triangularity_end); filename = 'mean_parameters.xlsx';
writetable(T,filename,'Sheet',1,'Range','A:F')

end
```

D.9. FUN_dot_product

FUN_dot_product first determines the scaled Fourier vector to be able to calculate a mean Fourier vector. Thereafter, the mean Fourier vector is calculated using every Fourier vector of the total Fourier vector. Subsequently, the dot product is calculated by dividing the dot product by the norm of a single Fourier vector with the mean Fourier vector.

```
function [dot_product]=FUN_dot_product(Fourier_vector_tot,N,N_figures);
%Scaling the length of the vector by dividing all factors by the norm. Therefore the length of
each Fourier vector will be 1.
for i=1:N
    Fourier_vector_scaled(i,:)=(Fourier_vector_tot(i,:))/(norm(Fourier_vector_tot (i,:)));
end

%Provides one Fourier vector with the means for every phase diagram per factor (a0,a's,b's)
for i=1:N_Fourier
    Fourier_vector_mean_tot (1,i)=mean(Fourier_vector_scaled_tot (1:N,i));
end

%Difference in Fourier vector between every phase diagram and the mean of all included
phase diagrams
for k=1:N;
    teller(k,1)=dot(Fourier_vector_scaled (k,:),Fourier_vector_mean (1,:));
    noemer(k,1)=norm(Fourier_vector_scaled (k,:))*norm(Fourier_vector_mean);
    dot_product(k,1)=abs(teller_mean (k,1)/noemer_mean (k,1));
end

end
```

E. 10 healthy and unhealthy selected phase diagrams

E.1. Subject 21, 10 healthy phase diagrams

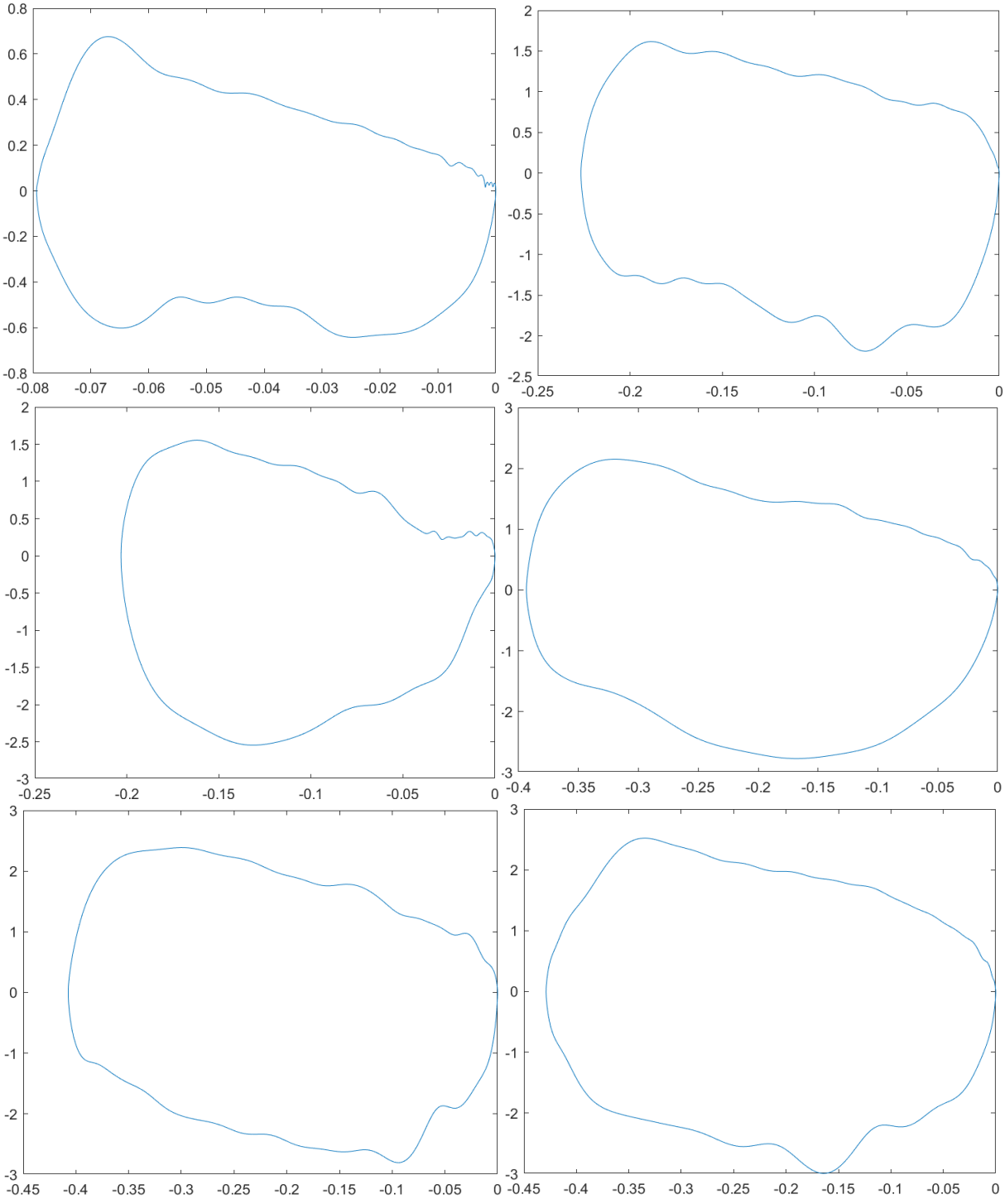

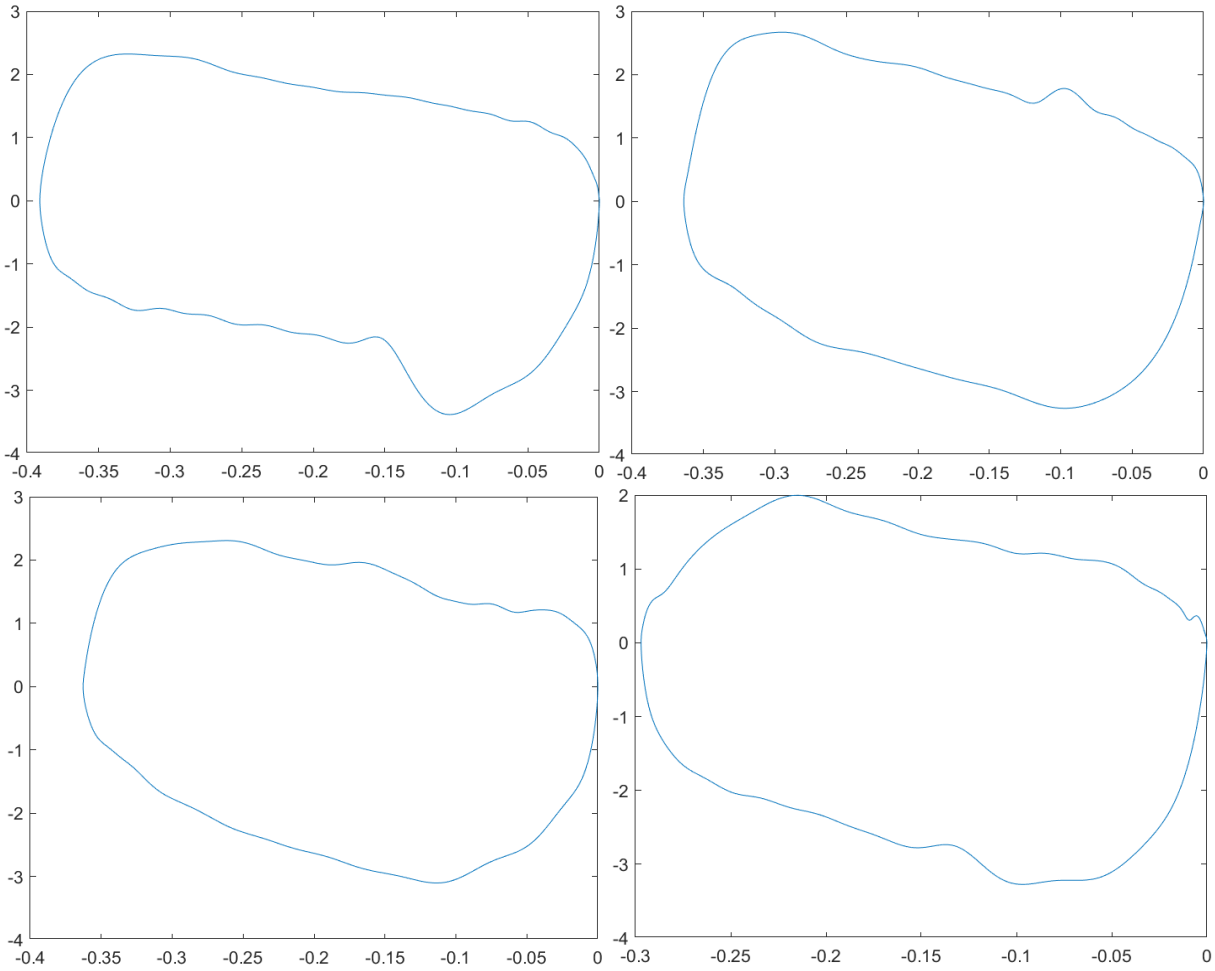
3
2
1
0
-1
-2
-3
-4
-0.4
-0.35
-0.3
-0.25
-0.2
-0.15
-0.1
-0.05
0
-0.3

E.2. Subject 7, 10 unhealthy phase diagrams

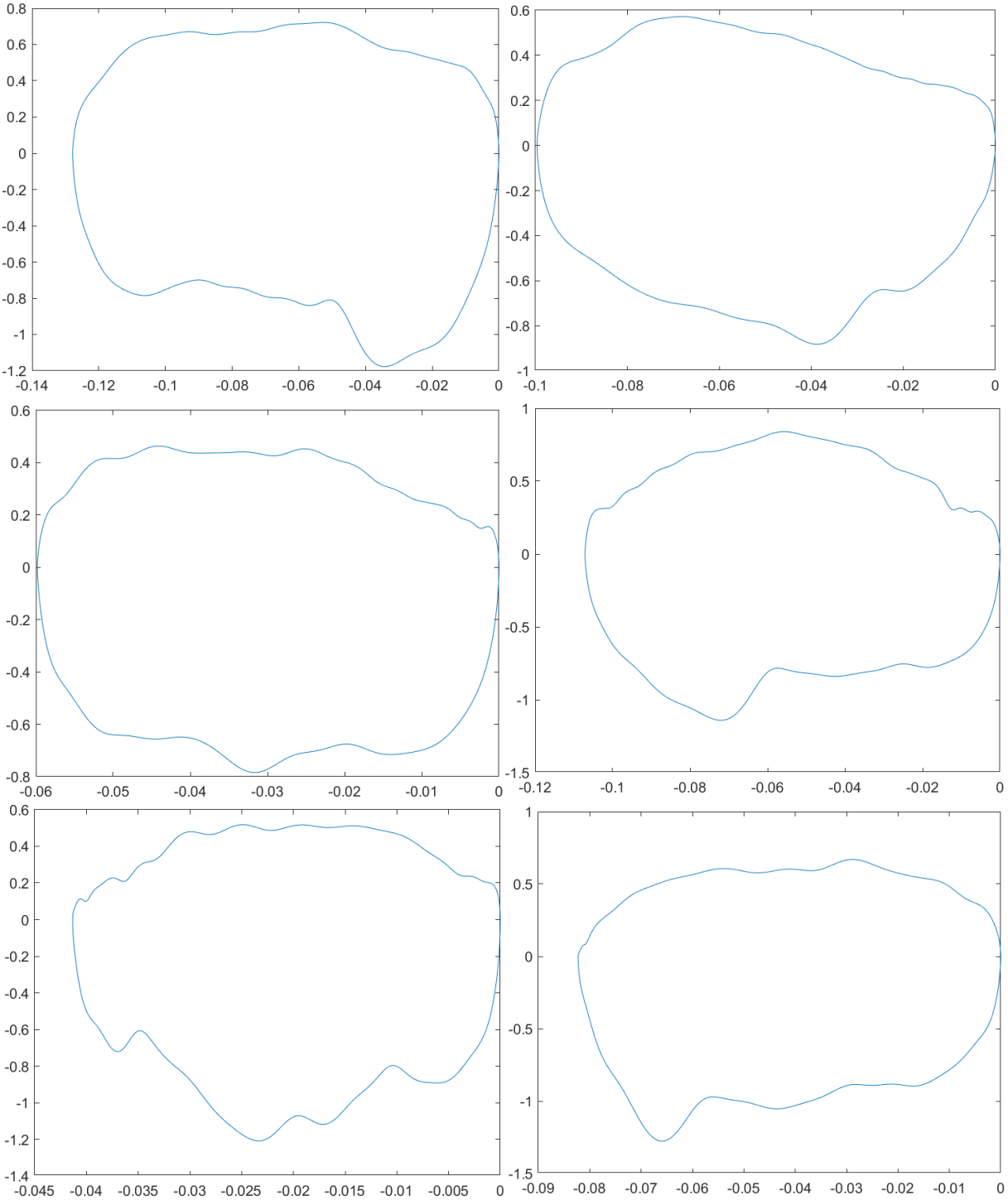

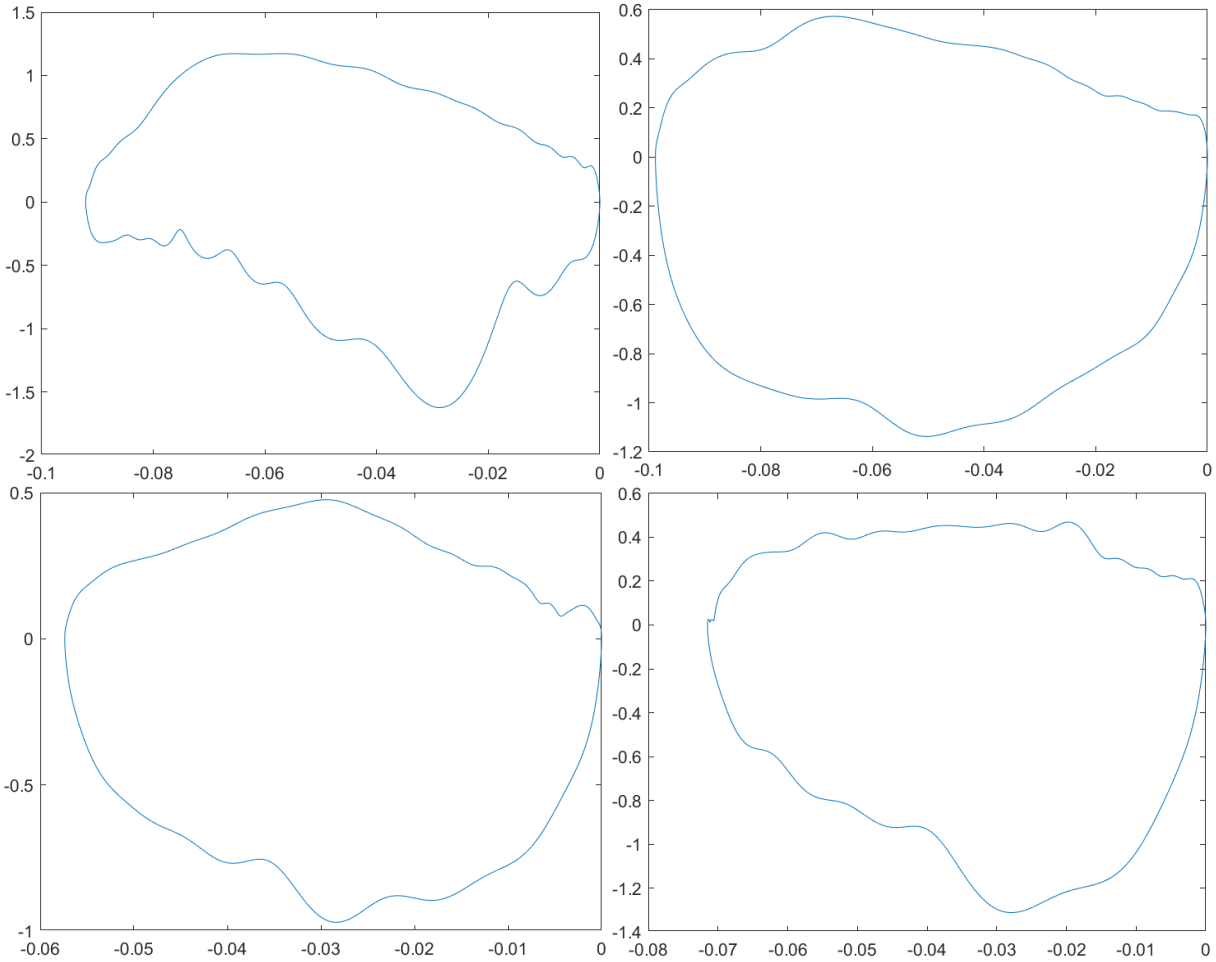
1.5
1
0.5
0
-0.5
-1
-1.5
-2
-0.1
-0.08
-0.06
-0.04
-0.02
0
0.6
0.4
0.2
0
-0.2
-0.4
-0.6
-0.8
-1
-1.2
-0.1
-0.08
-0.06
-0.04
-0.02
0
0.5
0
-0.5
-1
-0.06
-0.05
-0.04
-0.03
-0.02
-0.01
0
0.6
0.4
0.2
0
-0.2
-0.4
-0.6
-0.8
-1
-1.2
-1.4
-0.08
-0.07
-0.06
-0.05
-0.04
-0.03
-0.02
-0.01
0